

THESIS OF LICENTIATE DEGREE

Visualizations of particle-field interactions

ANDREAS JOHANSSON

Department of Physics
UNIVERSITY OF GOTHENBURG
Göteborg, Sweden 2022

ANDREAS JOHANSSON

Available at: <https://hdl.handle.net/2077/74186>

© Andreas Johansson, 20th November, 2022

Department of Physics
University of Gothenburg
SE-412 96 Göteborg, Sweden

Printed by: Stema Specialtryck AB, Borås, 2022

Typeset in X_YL^AT_EX with Times Ten and Akzidenz-Grotesk

Abstract

Visualizations within physics education are critical for learning physics and can be realized in a classroom with experiments, demonstrations, digital tools, mathematical analysis, or other representations, all with different levels of abstraction. This project aimed to determine whether the concept of field (i.e. electrical, acoustic, or optical fields) can be demonstrated, visualized, and applied in various experiments.

In the first Paper, an experimental setup for visualizing charge particles' motion in an electrical field was built. Designed learning activities were performed, and the effects on Swedish upper secondary school students' conceptual understanding were tested. This work shows that students' understanding of the interaction of charged particles with electrical fields increases more than without if a lecture includes an experiment that visualizes the phenomenon, either live or videotaped.

In Paper II a remotely operable optical trap was realized and used to levitate and investigate charged droplets remotely from a classroom. Visualizing and measuring many fundamental physical processes are described. The motion of charged particles in electric fields and the photon pressure of light is described as well as how it can be safely demonstrated for a class.

In Paper III, an optical trap is used to visualize the electron's quantization. In this work, it was shown that the effect of a single electron addition can be magnified and observed by the naked eye and measured with a ruler analogous to Millikan's experiment. The droplet is optically trapped and uncharged in an alternate electric field by an alpha radiation source. A strong electrical field was applied and as the uncharged droplet gained charges from the ionized air it jumped a well-defined step depending on how many electrons were added. The smallest jump corresponds to the addition of one electron, i.e. one elementary charge, and longer jumps are multiples of this.

Finally, in Paper IV, a new type of experimental method to determine the volume of microliter-sized droplets in acoustic fields is described. By using a simulation of the acoustic field to assist in setting the cavity length a fast and self-calibrated method is presented.

Sammanfattning

Visualiseringar inom fysikundervisning är kritiskt för inläring i fysik och kan utgöras av experiment, demonstrationer, digitala verktyg, matematisk analys och andra representationer som alla har olika abstraktionsnivå. Denna avhandling syftar till att avgöra om fysikbegreppet, fält (ex. elektriska, optiska eller akustiska fält) kan demonstreras, visualiseras och användas i olika experimentella uppställningar.

Framtagandet av en experimentell uppställning för att visualisera laddade partiklars rörelse i elektriska fält beskrivs i Paper I. Designade lärandeaktiviteter genomfördes med svenska gymnasieelever och effekterna på deras begreppsförståelse testades. Detta arbete visar att elevers förståelse för laddade partiklars rörelse i elektriska fält ökar mer om fenomenet under genomgången visualiseras med ett experiment antingen live eller på film.

I Paper II beskrivs uppbyggandet och användandet av fjärrstyrning av en optisk fälla för att fånga laddade droppar och hur detta kan styras och undersökas från ett klassrum. Visualisering och mätning av flera fysikaliska processer infattas i experimentet. Laddade partiklar i elektriska fält och fotontryck från ljus beskrivs samt hur det på ett säkert sätt kan demonstreras i ett klassrum.

I Paper III visualiseras kvantiseringen av elektronens laddning i en optisk fälla. Effekten av enstaka elektroners addition till en fångad droppe förstörades och kunde observeras med bara ögat och mätas med en linjal, analogt med Millikans experiment. Den laddade droppen fångades och laddades ur, i ett växlande elektriskt fält, genom alfastrålning. Ett starkt elektriskt fält användes och addition av elektroner till den oladdade droppen från den joniserade luften gav upphov till diskreta hopp vars storlek berodde på hur många elektroner som adderades. Det minsta hoppet motsvarade tillägget av en enda elektron, d.v.s. en elementarladdning, och större hopp var multiplar av detta.

Slutligen beskrivs i Paper IV en ny metod att använda för att bestämma akustiskt fångade droppars volym. Genom en simulering av det akustiska fältet kan rätt längd på fällan ställas in och därigenom kan en självkalibrerande mätmetod presenteras.

Keywords: Physics Education Research, Variation theory, Upper secondary school, Particle-field interaction, Visualization, Electric field, Optical levitation, Acoustic levitation, Remote labs

Preface

Foreword

I am a secondary school teacher in physics and mathematics at Klara gymnasium (formerly Hermods gymnasium in Gothenburg) since 2013. In 2017, I was accepted to the interdisciplinary research school Center for Educational Science and Teacher Research (CUL), a research school for already working teachers. Since then, I have worked about half-time at each workplace and about a year of parental leave. I am grateful for this arrangement as it provides, me, with a perfect balance between professional development, theoretical input, and practical work. CUL aims to develop us, students, into independent and analytical researchers with the ability to plan, implement and present scientific projects that investigate the fields of knowledge development, teaching, and education. In addition, we will develop expertise in scientific methods in science and education and an awareness of their respective theoretical frameworks. CUL is also a community of graduate students who meet, truly interdisciplinary, at gatherings, conferences, and in the compulsory courses.

This thesis is therefore an interdisciplinary work, in which I have tried to give my subjective theoretical position as a researcher in pedagogy and the scientific objective language in science. Experimental setups for visualization of phenomena in physics as a research subject have provided excellent and interdisciplinary collaboration with researchers from many different fields. However, due to Covid-19, classroom studies have been out of the scope in recent years, and my research during this time has been weighted in favor of more classical experimental physics. It's my goal in the second half of my research to bring the experiments into the classroom and investigate how they can contribute to and improve learning and teaching. Enjoy your reading!

Regards, Andreas

Acknowledgements

First, I would like to thank you for taking the time and effort to read my thesis. I feel there should be more names than mine on this thesis, as I could never have done it alone. Therefore, I would like to thank:

- Jonas for being a true inspiration as a human being and as a supervisor, letting me explore and follow my interests while providing resources, regular support, and direction when needed.
- Dag for being an inspiring and caring leader and a good supervisor providing valuable knowledge and wise perspectives in every discussion.
- Ann-Marie Pendrill for kindly giving critical and valuable input on this text and for contributing to planning my first empirical study.
- Suah for all the care, support, and flexibility in making graduate school an option for me while still being a teacher.
- Rich for the inspiring and fun work, oscillating back and forth from my experiments to your simulations when working on the acoustic trap.
- Sebastian for all the fun and intellectual discussions on variation theory, the attributes of good teaching, emergence, and critical eyes and input on this text.
- Javier for the fun collaborations on the optical trap and all the laughing lunches.
- Oskar for introducing me to the optical levitation experiment and for all the pleasant collaboration.
- Johan for kindly introducing me to acoustic levitation.
- Mitzi for the fun collaboration on the optical trap.
- Ingela Bursjö for theoretical and text input on the project with charged droplets in electric fields.
- Ludi for all the help with finding stuff in the lab and for all the cooking tips.
- Jacob for being truly helpful and sharing with time and resources, and for the fun teaching together.

-
- Annie for the fun teaching together.
 - Ademir for your helpfulness and support in the lab.
 - Constanza for a fun collaboration.
 - David and Chaitanya for the good games of table tennis.
 - Jessica, Pablo, Julia, Miranda, Kelken, Benjamin, Raymundo, Yogeshwar, Rachel, Veena, Megha, Andrea, Hinduja, Henny, Naemi and the rest for being an awesome research group.
 - Mats for technical help and support.
 - Richard for help with chemicals.
 - CUL graduate school for providing very good conferences and other meeting arenas for us graduate students.
 - CUL-temat MaNa for providing opportunities to meet and collaborate on our texts.
 - My colleagues at Klara gymnasium (previously Hermods Göteborg) for being an amazing resource of positive energy.
 - My brothers, their families, my friends, and my teammates for making my life richer, and more than just work.
 - Helene, Jan, Elin and Niclas for all help and support.
 - My mom and my dad for your love and that you made me believe I can do anything.
 - My daughters, Astrid and Ida, for forcing my mind to reality, changing my perspective on the world, and making me happier.
 - My wife, Linnéa, for all the love, for being an inspiring human being, and a caring mother to our kids, and for your everyday support and help in keeping order in our life. Without you, this thesis wouldn't exist.

Andreas Johansson
Göteborg
2022

List of publications and conference contributions

This licentiate thesis revolves around these papers and conference contributions:

- I **Charged liquid droplets in electromagnetic fields - An experiment for developing conceptual understanding during student activity**
A. Johansson¹, D. Hanstorp¹, I. Bursjö¹, J. Enger¹. ¹Department of Physics, University of Gothenburg, Gothenburg, Sweden
Presented at ICPE-SAIP-WITS 2018: https://events.saip.org.za/event/93/images/590-ICPE-SAIP-WITS_2018_-_Book_of_abstracts-v5.pdf.
- II **Safe experimentation in optical levitation of charged droplets using remote labs**
Galán, D.¹, Isaksson, O.², Enger, J.², Rostedt, M.², **Johansson, A.**², Hanstorp, D.², de la Torre, L.¹.
¹Departamento de Informática y Automática, UNED, Madrid, Spain
²Department of Physics, University of Gothenburg, Gothenburg, Sweden
Published by: *JoVE (Journal of Visualized Experiments)*, 143, e58699, doi:10.3791/58699, 2019,
- III **Visualizing the electron's quantization with a ruler**
Javier Tello Marmolejo¹, Mitzi Urquiza-González^{1,2}, Oscar Isaksson¹, **Andreas Johansson**¹, Ricardo Méndez-Fragoso², Dag Hanstorp¹.
¹Department of Physics, University of Gothenburg, Gothenburg, Sweden
²Facultad de Ciencias, Universidad Nacional Autónoma de México, Ciudad de México, México
Published by: *Scientific reports*, **11**, 1–5, 2021, doi:10.1038/s41598-021-89714-2.
- IV **Self-calibrated droplet volume measurements in acoustic levitation**
Andreas Johansson¹, Ricardo Méndez-Fragoso², Jonas Enger¹.
¹Department of Physics, University of Gothenburg, Gothenburg, Sweden
²Facultad de Ciencias, Universidad Nacional Autónoma de México, Ciudad de México, México
In manuscript for: *Review of Scientific Instruments*

Specification of my contributions

I Charged liquid droplets in electromagnetic fields - An experiment for developing conceptual understanding during student activity

Responsible for the experimental design. Responsible for arranging all classes and lessons and collecting and analyzing data. Wrote the manuscript and conducted the oral presentation.

II Safe experimentation in optical levitation of charged droplets using remote labs

Experimental work, testing the system, and maintenance for the remote control to work. Contributed to finalizing the manuscript.

III Visualizing the electron's quantization with a ruler

Conceived and implemented the crucial motorized control of the alpha source. Conducted experiments and contributed to finalizing figures and text of the manuscript.

IV Self-calibrated droplet volume measurements in acoustic levitation

Mainly responsible for the research question and experimental design. Conducted the majority of data collection and data analysis. Drafted the manuscript and wrote the main revisions during the review process.

Contents

| | |
|--|-----------|
| Preface | v |
| 1 Introduction | 1 |
| 1.1 Aim and specific objectives | 4 |
| 2 Theoretical framework in education research | 5 |
| 2.1 Variation theory | 5 |
| 2.1.1 Intended, enacted and lived object of learning | 8 |
| 2.2 Context and construction of conceptual understanding | 8 |
| 2.2.1 Visual information, declarative memory and variation theory | 10 |
| 2.3 A model for learning and teaching | 11 |
| 2.4 Another learning and teaching framework | 14 |
| 2.5 Developing experiments for educational purposes | 15 |
| 3 Theory | 17 |
| 3.1 Electrical fields | 17 |
| 3.2 Particle traps | 19 |
| 3.2.1 Optical traps | 21 |
| 3.2.2 Acoustic traps | 24 |
| 4 Method | 27 |
| 4.1 Experimental setups | 27 |
| 4.1.1 Electrical field (Paper I) | 27 |
| 4.1.2 Optical trap (Paper II and Paper III) | 29 |
| 4.1.3 Acoustic trap (Paper IV) | 30 |
| 4.2 Method Paper I | 31 |
| 4.2.1 Educational data collection and analysis | 32 |
| 4.3 Method Paper II | 35 |
| 4.4 Method Paper III | 35 |
| 4.5 Method Paper IV | 36 |

| | | |
|------------|--|-----------|
| 5 | Results and Discussions | 39 |
| 5.1 | Experiments increases understanding of particles in electric fields (Paper I) | 39 |
| 5.2 | Optical trapping and investigation of a particle remotely from a school (Paper II) | 42 |
| 5.3 | Visualizing the electron's quantization with a ruler (Paper III) | 43 |
| 5.4 | Zoom-independent volume measurements calibrated by acoustic field (Paper IV) | 45 |
| 6 | Conclusion and Outlook | 49 |
| | Bibliography | 53 |
| | Appended Papers | 59 |
| I | Charged liquid droplets in electromagnetic fields - An experiment for developing conceptual understanding during student activity | 61 |
| II | Safe experimentation in optical levitation of charged droplets using remote labs | 65 |
| III | Visualizing the electron's quantization with a ruler | 77 |
| IV | Self-calibrated droplet volume measurements in acoustic levitation | 85 |

Introduction

Much focus within physics education research (PER) directs toward investigations of how to teach conceptual understanding of physics with methods that allow replication [1]. Successful interventions to enhance students' development of conceptual understanding combine PER results with cognitive psychology and knowledge about the brain [1–6].

In the physical world, many things are too small to be seen by the human eye. Visualizations are needed for them to be well understood. Observation of physical phenomena has together with other visualizations been found critical for learning physics and learning to do physics [6, 7]. Visualizations are helpful to understand particle-field interactions and small-scale phenomena such as quantization.

The idea of quantization is central to our understanding of the microscopic world. Some examples exist of visualized quantized phenomena, including quantized vortices [8], collisions of ultracold ground-state molecules [9], and the quantum ground state [10], but still more experiments to visualize quantization and other quantum phenomena are needed.

Visualizations can be realized with digital tools and mathematical analysis but at the cost of introducing a higher level of abstraction than direct observation. Examples within PER include Phet simulations used for active learning [4] and experimental setups or videos thereof [11]. The visualizations could also be made by observing and experimenting with an analog macroscopic object that behaves similarly to the object of study or by enhancing the microscopic effects on macroscopic objects. Experimental setups with electrical fields, optical fields, or acoustic fields in the presence of gravitational fields offer opportunities to visualize and study many concepts from the core content of the Swedish upper secondary physics curriculum [12] enlisted in Tab. 1.1. The motion of particles in electric fields is part of

Table 1.1: Core content in the subject of physics in Swedish upper secondary school [12].

| Core content |
|--|
| Equilibrium and linear motion in homogeneous gravitational fields and electrical fields Two-dimensional motion in gravitational fields and electrical fields. |
| Work, force, potential energy and kinetic energy to describe different forms of energy: mechanical, thermal, electrical and chemical energy, and also radiation and nuclear energy. Electrical energy: Electrical charging, field strength, potential, voltage, current and resistance. |
| Reflection, refraction and interference of light, sound and other wave motion. Harmonic oscillation and resonance with applications in everyday life and technology. |
| Orientation to electromagnetic radiation and the particle properties of light Wave and particle descriptions of electromagnetic radiation. Orientation to propagation of electromagnetic waves. Photoelectric effects and the concept of photons. |

the curriculum, but few experiments straightforwardly visualize the phenomenon. For charged particles, there is a classical experiment based on electrons accelerated in a cathode ray tube into an approximately homogeneous magnetic field, produced by Helmholtz coils. The magnetic field exerts a magnetic force on electrons moving into the field of the cathode ray tube filled with noble gas at low pressure. When electrons collide with the noble gas, fluorescence is produced in the visible spectrum. The experiment was first used by J.J. Thomson when the electron (corpuscles) was discovered, in 1897, and is often used in physics education to measure the specific charge of electrons (e/m) [13, 14]. Other demonstrations than cathode ray tubes to visualize charged particle interaction with electrical fields are lacking.

The use of a laser to move and trap macroscopic objects, due to the fact that light (photons) carries momentum, was first reported by Nobel laureate A. Ashkin and J. M. Dziedzic in 1971 [15]. Many of the mentioned physical phenomena can be studied using optically levitated droplets, since they can be optically trapped and controlled, making experiments using optical levitation interesting for school applications. However, many schools and institutions cannot afford the required equipment and since there are specific risks in the hands-on operation of the powerful lasers and high-voltage supplies needed, it is inappropriate to handle in a classroom.

Acoustic traps use the interference of sound waves to produce pressure differences in a media that give rise to acoustic forces strong enough to counteract grav-

ity and keep a small object such as a droplet stable. Droplets have a dynamic shape that changes with differences in the surrounding pressure and these droplet deformations and positions can be used to gain information on the acoustic field as well as droplet sample properties [16]. This fact enables the study of droplet resonances driven by the acoustic field [17]. Vice versa, a known acoustic field can also be used to gain information about the shape of droplets.

Measurements of droplet volume in an acoustic trap are often performed using diffraction patterns from an external laser or via image analysis calibrated by a precision-produced spherical bead but few or none use a known acoustic field to measure droplet volumes which could get rid of the limiting need to re-calibrate if equipment positions are altered. Versatile measurements of droplet shape dimensions could be useful for various student labs as well as for research within chemical microanalysis, spectroscopy studies, and evaporation studies [18, 19].

Acoustic traps can nowadays be 3D-printed and assembled locally at a school and driven using ordinary school lab equipment, piezo-disks or Arduino equipment [20, 21]. Videos of experiments for demonstration of physical phenomena during learning activities are used within PER as another way to easily make observations possible in the classroom [6]. Comparisons of live and video demonstrations of physical phenomena and the effects of learning are lacking in the literature with some exceptions [22, 23].

Remote laboratories have since the advent of the Internet in the 90s offered online remote access to real laboratory equipment. These laboratories offer experimental activities without exposing users to the risks of operating the equipment manually [24]. Students get training in operating computer-controlled systems, important to participate in research, development, and industry. Remote laboratories offer a solution to both the financial and safety issues that traditional labs present and can provide many interesting experimental opportunities otherwise out of reach for schools [24].

1.1 Aim and specific objectives

This thesis aims to develop research equipment visualizing particle-field interaction and their applicability as teaching tools. To investigate this aim, my licentiate thesis revolves around the following specific objectives:

1. Are students' conceptual knowledge increased as the teacher uses an experimental setup to visualize particle movement in electrical fields directly or via a movie clip, compared to a classical lesson without any experiment available?
2. How can experiments to visualize important physical phenomena, but with expensive or inappropriate equipment, be made available to use in a classroom?
3. Can the quantization of the elementary charge be visualized directly to the students?
4. Can self-calibration of volume measurements of acoustically trapped liquid droplets be realized using low cost equipment?

Theoretical framework in education research

In this chapter, variation theory is described with key concepts. Then, the conditions necessary for students to develop conceptual understanding and some of the mechanisms in the brain that contribute to this are described. This leads to a model for thinking about how pupils develop their conceptual understanding. Finally, this synthetic model is contrasted with an established teaching framework as a motivation for lessons with experimental setups that can contribute to the development of students' conceptual understanding concerning the observed physical phenomena.

2.1 Variation theory

What if, you had no previous experience with whiteboard pens or any similar objects? You simply lacked any previous experience to draw upon, to construct guesses about what might be important about these things occupying your field of view.



Figure 2.1: Unidentified objects with unknown attributes.

Then the question of what the objects in Fig. 2.1 are, and the description of them, would be rather poor.

To notice important attributes of objects we can make comparisons, where one attribute is varied at a time. As we do this, we change the way we see objects. In Fig. 2.2 such a comparison is made possible. Our description of the objects can now be a little richer.

We now know the thing on the left (top) can change color because the contrast made us able to discern it.



Figure 2.2: Contrast of the two objects' attributes makes the left (top) of the unidentified object discernible.

In *Variation theory* learning has happened, when students have changed their way of seeing something [25]. In the case of the whiteboard markers, it was possible to discern that there can be a variation in the colors of the caps. The property *cap color*, can via further examination be linked to the markers' writing color and be discovered to be an important attribute. This example is chosen to demonstrate *contrast* (described more below), a central principle within variation theory.

Variation theory was developed by Ference Marton, building on ideas from phenomenography [26, 27]. The framework has been widely used in Learning studies, a combination of the two educational research methodologies Lesson study and Design Based Research (DBR) [28]. In variation theory, the focus is on the what question. What should the student learn, to reach the objectives of the course? This "what" is called the *object of learning* [25]. Any phenomenon has its distinguishing and defining attributes, that need to be discerned to understand it in a certain way. Different learners can often already discern some of these attributes, but not all. Trivial phenomena such as triangles can easily be defined by their angles and sides, whereas their translation or rotation does not matter.

To understand the object of learning, its *critical aspects* need to come into our awareness at the same time. Then, we can perceive (discern and attend) the whole and all its parts at once [25, 28, 29]. This is achieved through the process of *fusion* when variation in all critical aspects is experienced simultaneously. First, however, two other processes need to take place; the already mentioned contrast and then what's called *generalization* (explained below). These processes are subjective in

the sense that they happen between the learner and the object of learning [28], and thus how the critical aspects are made visible for each student have to be investigated. Indications of what the critical aspects are can also be found via literature reviews [30]. Research on previously shown learning difficulties concerning the object of learning can inform the initial investigation of its critical aspects [30].

When a feature (blue cap on whiteboard pen) is contrasted with one or more other objects or events, where only this feature is varied, it is possible to discern that feature [25, 28]. A *dimension of variation* has then opened up (if the feature values are variations within a critical aspect) and this is argued to be essential to make the learner aware of aspects (cap color indicates marker color) of the object of learning. Via the principle of contrast, the experience of seeing critical aspects one after the other can make us aware of their existence. However, this is not enough, but also generalization is needed.

Generalization means refining the boundaries of the object of learning, such as contrasting whiteboard markers with permanent markers. They will, as experience taught many teachers, look the same, but the effort to erase their marks differ a lot! Generalization means also paying attention to those aspects, that has been invariant through all observations. To do this, they must first be discernible for the student. Even the non-critical aspects must then, first be visualized through contrast [28]. If we would compare even more whiteboard pens from different manufacturers, for example, this would be possible, as we would find out that shape, manufacturer, information text color, and other attributes might be non-critical to understand how to use them. Then, as all these other variations occur it is possible to experience what is critical and what is not, and separate the object of learning from its environment in our awareness [25].

Using a *pattern of variation and invariance*, as students observe physical phenomena, the critical aspects can be made visible through the principles of contrast (separating critical aspects of the object of learning), generalization (separating critical aspects from non-critical aspects and the object from its surroundings) and fusion (experiencing the whole and its' parts simultaneously).

The differences in learning outcomes observed in most classes are according to variation theory, due to students' ability or habits to contrast their observations with their current understanding. Thus, to improve the overall understanding in the class, it is up to the teacher to explicitly show the contrasting examples needed to make the critical aspects, of the object of learning, discernible for the students [25]. Lo emphasizes, that even this is not enough as "teaching is an integrative act and not simply the application of patterns of variation, and thus whether the intended effects of patterns of variation are brought about also depends on the choice of appropriate teaching strategies and teaching approaches" [25].

2.1.1 Intended, enacted and lived object of learning

To analyze a lesson or a sequence of lessons, using variation theory, one focuses on how the object of learning was handled with respect to the student group before, under, and after an intervention [31]. The ability students should develop and the relevant conceptual knowledge needed, as well as the variation patterns needed to bring these about are altogether considered as the *intended object of learning*. The pattern of variation and invariance, realized by the teachers' and students' activities during the lesson is called the *enacted object of learning* [31]. The learning outcome after the lesson can be gauged e.g. by students' answers to pre- and post-test questions, and is called the *lived object of learning* [31]. Student answers on the pre-test questions can contribute to the intended object of learning, as it gives insight into student pre-knowledge and can thus be considered in the design of the lessons' pattern of variation and invariance [31]. If the pre-test instead is conducted during the lesson it will be part of the enacted object of learning as it will not inform the planning but rather the lessons enacted pattern of variation and invariance.

2.2 Context and construction of conceptual understanding

Understanding how concepts form in memory and how they are used to reason provide useful insights in devising instructional interventions to help students adopt and use scientific concepts [5].

The mental work of constructing conceptual understanding and abstractions is carried out in the front cortex (see Fig. 2.3) by the executive functions and primarily the working memory [32–35]. The function and effectiveness of the working memory and other executive functions of the front cortex are regulated by neurotransmitters. Dopamine is the key regulator for this type of learning [36, 37].

Dopamine is released from the ventral tegmental area in response to our perception of our ability to perform rewarding in the current situation [38, 39], triggering goal-directed behavior guided by our conceptual understanding in simulating action effects and making decisions [40]. But this release is impaired as we perceive too much stress or pressure. Then the amygdala activates other memory mechanisms connected to punishment [41]. Memories from such situations will not contribute to conceptual understanding but instead, introduce feelings of familiarity in similar situations and cause aversive behavior [39]. In such situations, the dopamine needed to activate neurogenesis (production of new neurons) in the hippocampus

2.2. Context and construction of conceptual understanding

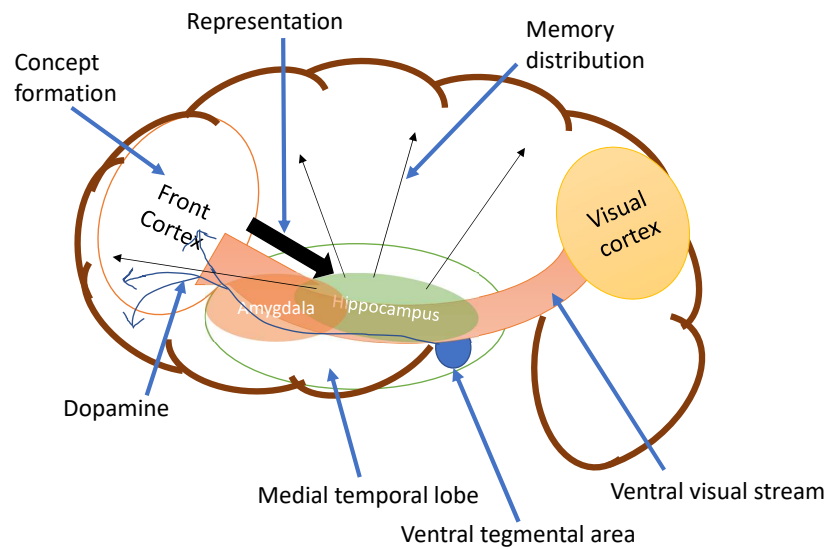


Figure 2.3: Model of the brain and some functions important to perception, concept formation, and memory formation.

and to activate the operations of the executive functions in the prefrontal cortex is impaired [39]. The executive functions have been shown necessary both to use algebra for scientific problem solving, to construct scientific concepts, and to use them to construct arguments for scientific reasoning [42–45]. The ability to use concept-dependent reasoning is a strong predictor of scientific problem-solving ability [46], which indicates the conceptual understanding is functional and fits with reality.

During concept formation, the hippocampus is vital as it mimics and represents the patterns formed by the executive functions (working memory), using the new high-plasticity neurons [39] and then distributing them to long-term (declarative) memory during slow-wave sleep, according to the prevalent model of hippocampal-neocortical memory consolidation [47]. This central function of the hippocampus function in the formation of conceptual understanding (see Section 2.3) and storing it in long-term memory, can be further enhanced by regular aerobic exercise [48].

In summary brain research suggests that students with positive emotions triggered by the expectation of reward, due to repeated experience of rewards for achievements, in co-operation with others will have increased probabilities of developing and improving the conceptual understanding needed to express the abilities of reasoning and problem solving during educational activities. Good sleep and exercise habits will further increase these probabilities.

”However, even if the teacher is very caring, the students are highly motivated to learn and the environment of the classroom is very comfortable and supported by advanced technology if students do not have the opportunity to discern the critical features of the object of learning in the classroom, then the desired learning is still unlikely to occur” [25]. This quote by Lo beautifully introduces variation theory and its capacity to inform teachers on what is important to let students experience during class to improve the probability of change in the way students see the object of learning, and thus change their conceptual understanding. But what mechanisms are at play here? How does visual information interplay with the concepts and their relations that constitutes our understanding? Since variation theory consists of methods for helping students focus their attention, and eventually recognize critical aspects as cues, this question needs some elaboration.

2.2.1 Visual information, declarative memory and variation theory

Not all critical aspects of an object of learning are discerned via inputs from sight, but many of the important cues are visual. When we use vision to scan a phenomenon, visual information gathered by the eye quickly enters several layers of hierarchically structured neural networks (the ventral visual stream, see Fig. 2.3) on the way up to the front cortex [49]. Here the executive functions informed by our neuronal networks in declarative memory send predictions back down the ventral visual stream to match against more gradually gathered information making its way up the layers [49]. If a match occurs down the stream the signal from the stimuli is attenuated (gradually damped), but if something mismatches the prediction, the executive functions receive the signal with full strength [49]. However, without attention directed at the stimuli, this won’t happen [50]. This damped signal is the effect of so-called statistical learning and tells us that our neuronal networks in declarative memory fit with reality by having categorized correctly, the perceived patterns, or correctly predicted a phenomenon [32, 49, 50]. These cognitive processes constitute one of the pillars the, within PER well-known, resources framework is based on [51]. Unexpected stimuli results in pupil dilation of the eye and more focused attention [50] letting the information pass un-attenuated to the executive functions where the situation can be remodeled as described in Section 2.2 and passed to declarative memory. In light of evidence it seems to be this communication back and forth in the ventral visual stream that is disrupted during perceived stressful situations and thus impairing the formation of declarative memories (place learning), leaving simpler stimulus-response learning unaffected [52].

The ability to discern critical features is then analog to using conceptual un-

derstanding to correctly predict attended cues on their way up the ventral visual stream. This reduces the cognitive load and more stimulus can be attended to and handled by the executive functions at the same time. When the conceptual understanding of a phenomenon involves the critical aspects, that have previously been discerned, they are perceived all at once. This is equivalent to the term fusion in variation theory [28]. Variation patterns that focus students' attention on their critical aspects of a concept or phenomenon, to incorporate in their neuronal networks of declarative memory, during low-stress situations, are thus one key to effective teaching and learning.

Although, Lo emphasizes that "teaching is an integrative act and not simply the application of patterns of variation, and thus whether the intended effects of patterns of variation are brought about also depends on the choice of appropriate teaching strategies and teaching approaches" [25].

These strategies should be informed by our current knowledge about how the brain works to design activities for the students to engage in, that will not trigger negative emotions [32] but still make available the necessary patterns of variation to make students learn.

2.3 A model for learning and teaching

In this section, I will use a philosophic approach and synthesize a model to think about teaching and conceptual learning (as opposed to stimulus-response learning), the higher level of learning needed to understand and apply physics.

As discussed above, this type of learning can happen if the executive functions of the brain are active in retrieving conceptual understanding, triggered by the sensory impressions of the situation, to perform contrasting and creative operations on them and pass the result to the hippocampus, that then represent it and distribute it to long-term memory during the night. In a model for teaching purposes, the activities that put a demand on the learner to engage their executive functions in this process should be incorporated, as well as methods to direct students' attention to their critical aspects of either physical phenomena or theoretical concepts.

Philosophy can assist in constructing theories, that later assist us in understanding. The dutch philosopher Henk W. de Regt introduces a general theory of scientific understanding and argues that understanding is a pragmatic notion and that an objective relationship between a theory T and a phenomenon P is of little use if T is not intelligible for a subject S, even if T perfectly explains P [53]. A phenomenon is understood, according to de Regt, through the process of model construction, and this process is subjective and non-deductive, he argues, since approximations and idealizations are needed to construct models. He continues to argue that a "the-

ory is intelligible to scientists if they can easily employ it to construct models to explain specific phenomena” [53]. Likewise, a theory is only intelligible to learners if they can use it to explain physical phenomena, so it is important to observe physical phenomena and try to find links between what is observed and theoretical concepts to produce such explanations.

The proposed model for teaching and learning is inspired in its form by the model-based view of physics [54]. I have used the term mental model, introduced by Johnson-Laird [55]. Informed by modern brain research the meaning of the term mental models is treated as synonymous with conceptual understanding that consists of neuronal networks and is constructed by the executive functions in the brain’s front cortex. A process that can possibly be enhanced by teaching based on variation theory and bringing attention to the front as a critical way to activate the executive functions in mental model creation during experiences of variation in the critical aspects of the object of learning.

As the learner, during observation, experiences different dimensions of variation of the object of learning, understanding can eventually be achieved if the learner engages their executive functions in the activity of constructing mental models and explanations using concepts from memory and theory. The mental models can be further developed if the learner, during activities and further observations tests them (see section 2.2 for further elaboration).

Different activities can be organized in the classroom for the students to engage, create, compare and revise their mental models. Such activities could be interacting with simulations [4] borrowed from peer-instruction [1, 56] techniques or engaging in challenging problem-solving with frequent feedback [3].

Within PER the term mental models have been used before, by E.F Redish [2]. Many similarities between the two treatments exist, especially since they build on a similar foundation from cognitive science, additions in the proposed model include more backing from cognitive and neuroscience and how mental models can be informed by teaching via variation theory. In his version of mental models, they are the resulting patterns individuals construct when organizing experiences and observations, and he connects it to constructivism and describes learning in terms, once developed by Piaget, of assimilation and accommodation [2, 57]. Later attempts to link modern brain research to the vocabularies of constructivism have been done [57]. The treatment of the term mental model here is without the vocabulary of constructivist theory.

Visualizing physical phenomena via an experimental setup with capabilities to vary physical quantities individually provides opportunities for the students to improve their models as the effects and their causes become perceptible. In Fig. 2.4, I have organized learning activities where students’ mental models are constructed as interactions with physical phenomena (physical), mental models of peers (social), theory (abstract), or memories and other e.g sociocultural mental

models, that comes from the groups and communities we participate in [51](internal/individual). Within the proposed model for learning and teaching, student mental models are constructed in such activities due to the spontaneous and sometimes, e.g. by peers, deliberate appearance of the needed patterns of variation and invariance.

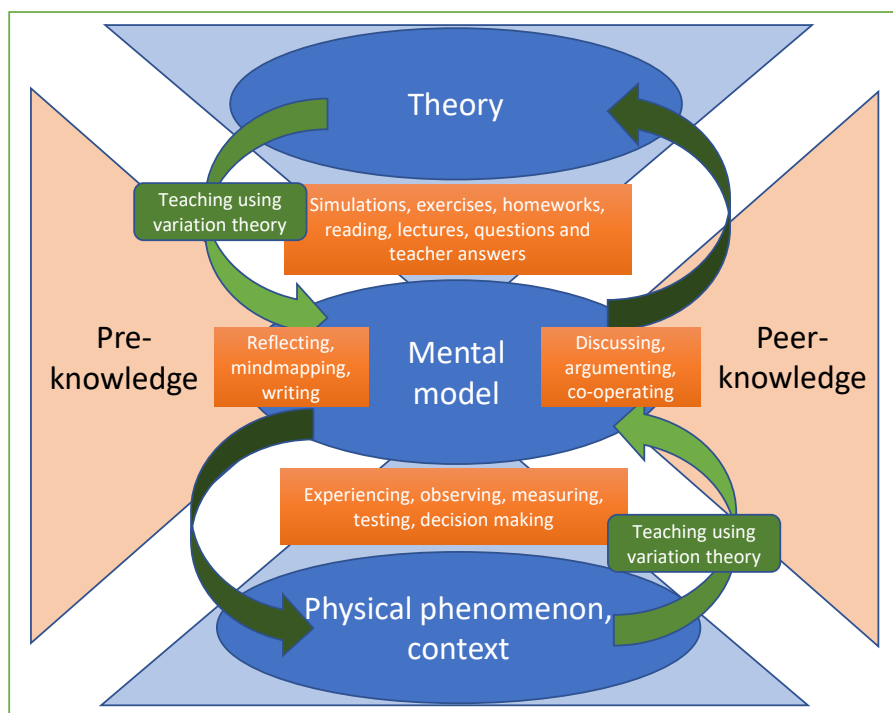


Figure 2.4: Teaching and learning. The mental model in the center is constructed by the learner when using or producing theoretical concepts to understand a physical phenomenon. The model can then be subject to changes and improvements through the learner engaging in different activities (orange) and through effective teaching via variation theory (green). The lasting changes are those reflected upon and used to form ideas or plans [32].

Students' mental models are physically represented by the many connections between neurons and the strength of these connections forms the declarative memory and is accessed by working memory to do operations on [32]. The mental models approximate both theory and physical phenomena [32], and these approximations are fundamental in mapping reality to theory and theory to reality [53]. Altering these approximations or creating new mental models for a better fit between theory and reality is one form of high-level learning, and the mental models produced in the process are what we can use to solve problems and perform pre-

dictions about the physical world.

Variation theory consists of language and methods for teachers to direct students' awareness and attention to crucial properties (students' possible critical aspects) of a phenomenon necessary in the mental model to approximate theory and physical phenomena effectively. Students have preconceptions that need to be built upon or inhibited to construct a scientifically compatible mental model [33–35, 58]. Assessing students' preconceptions provide clues for the teacher about what critical aspects the students need to attend to, in order to construct and refine these mental models. To successfully do this students need to incorporate scientific concepts as well as memories from observing cause-effect relationships of physical phenomena into their mental models [32]. This is why experimental setups for visualizing physical phenomena are a crucial part of successful physics education.

When learning physics through interaction with experimental setups as in physics laboratories the learning is more beneficial if the teacher complement student experiences with effective instruction that links what is to be learned to established scientific knowledge [7]. Such instruction could be informed by methods from variation theory (see section 2.1), as described in section 2.2.1 and visualized by the green arrows in Fig. 2.4.

The proposed model has not yet been empirically tested. It is based on an extensive literature survey.

2.4 Another learning and teaching framework

I will now introduce another framework for learning and teaching, to contrast the model described in 2.3 and highlight its domain of application.

The investigative science learning environment (ISLE) introduced by Etkina and van Heuvelen [6] incorporates several of the previously mentioned evidence from brain science (see Section 2.2), cognition science, as well as scientific epistemology and, have an overall similar theoretical stance. This means it is designed to avoid putting negative emotions in students, by letting them retry on home works and diagnoses and even avoid correcting students [11]. The general learning loop for the students consists of observation, explanations using prior knowledge, design of experiments to test these explanations, and then, performing the experiments.

In the ISLE framework, the students are not told about physics concepts before observations, but rather they should construct them, by describing observations in their own words, during the learning loop. This is, they argue, inspired by how scientific knowledge and models are generated [6]. During the crucial observation phase a demonstration of an experiment showing a physics phenomenon, ei-

ther physical or videotaped, is used to visualize it. The students are activated to produce explanations using prior knowledge [6] and non-scientific wording. The teacher's role within the ISLE framework is to introduce an observation experiment and then "scaffold" student groups in discussions to generate explanations by providing reasoning tools such as diagrams of different sorts and then, support students with materials to test predictions from their explanations [11]. The concept of scaffolding is borrowed from the social constructivist theory, developed by Jerome Bruner and founded on Lev Vygotsky's concept of Zone of Proximal Development (ZPD) [59, 60]. Scaffolding means first demonstrating, then stepping back and offering support [60] when needed while ZPD means "... the distance between the actual level of development as determined by independent problem-solving and the level of potential development as determined through problem-solving under adult guidance, or in collaboration with more capable peers" [61].

In general when compared to the learning model described in Fig. 2.4 in section 2.3 the ISLE approach try to introduce the upper "loop" where the mental models are interacting with theoretical concepts at a much later point in the learning process than suggested by the proposed model. The observations of physical phenomena constitute an important role for student learning within this framework but guiding these observations effectively with a planned pattern of variation and invariance could make it even more powerful and maybe more fit to the everyday reality for teachers and students in an upper secondary school context where the lesson time is relatively short.

The hypothesis behind the proposed model (not yet tested) in Section 2.3 was to effectively fit this type of situation and to accelerate the formation of mental models and explanations further, by explicit use of variation theory to inform teaching during student interaction with physical phenomena, theoretical concepts and during instruction and discussions.

2.5 Developing experiments for educational purposes

The act of observation has a critical role in learning physics but also in doing physics [6, 7] and since we are biologically evolved organisms, Zull argues, all learning needs to be grounded in the physical world [32], either through observations of events and the phenomena it consists of, or indirect via metaphors. This is how meaning is created even for the most abstract of concepts and theories [32]. For many physical phenomena, there's a lack of demonstration experiments that can be used as a foundation for students to build their understanding. Therefore, I have come to focus my research on identifying and developing experiments to

visualize physical phenomena with a focus on different particle-field interactions. These experiments are constructed specifically to visualize the co-variation of entities necessary to demonstrate cause-effect relationships [32] involved in understanding the relevant particle-field interaction. Using variation theory these relationships can be thought of as some, but not all, of the necessary aspects to discern and attend to when experiencing the phenomenon (object of learning, particle-field interaction), and thus they provide a set of first candidates to eventually prove to be critical aspects for a given student [29, 30]. With particle-field interaction as the object of learning the variability features within these necessary aspects have been included in the experimental design [25]. The experiments can be used to visualize physical phenomena either live or using video as Etkina and van Heuvelen have done [6]. The experiments were designed with a potential pattern of variation and invariance in mind, for a teacher to use in a class if some of the incorporated cause-effect relationships prove to be critical aspects after examining students' pre-knowledge.

A pilot study was performed to investigate the impact on student mental model formation during a lesson where a videotaped demonstration and a live demonstration, of one of my developed experiments, were used as teaching tools. In this pilot study even though a pre-test was conducted, student answers were not used to inform the lesson plan as is ordinarily done in e.g. Learning studies [29], due to time constraints during data collection. The pattern of variation and invariance was therefore designed based on the teacher's pedagogical content knowledge (PCK), including subject knowledge and usual learner difficulties and how to address them [62]. The designed variation pattern is described further in section 4.2. The successful ISLE framework [11] described in section 2.4, might not be fully applicable within for example the Swedish upper secondary school curriculum where the time and materials available for implementing such methods are too limited. Instead, instructions via variation theory can help students to discern critical aspects of physical phenomena demonstrated with experimental setups and this can be of great value as a foundation for students' mental model construction. As students construct explanations either in non-scientific terminology, in an "idea first and name afterwards" approach [63], as in ISLE [11] or by actively trying to involve the scientific concepts as in the model proposed in 2.3 their mental models are expressed. This is of great value for the teacher and the learner.

Theory

3.1 Electrical fields

A field is generated by a source in the space around it. An electrically charged particle generates an electrical field. Electrons and protons have electrical fields, and within a certain distance, they attract or repel other charged particles. In a condenser, two flat parallel conductors are connected to a voltage supply. The excess of electrons in one conductor and the deficit in the other produce a homogeneous electric field between the plates. The electric force on a charged particle in that field is obtained by

$$\vec{F}_E = q \cdot \vec{E}, \quad (3.1)$$

where \vec{F}_E , q , and \vec{E} are the electric force, droplet charge, and electric field strength respectively. The direction of the electrical force is in the direction of the electrical field for a positively charged particle and vice versa for a negative. The electric field strength in a homogenous electrical field depends on the distance between the plates (the maximal displacement of a positive particle), \vec{d} , and the voltage, U , applied between them and can be expressed as

$$\vec{E} = \frac{U}{\vec{d}}, \quad (3.2)$$

and combined with Eq. 3.1 expresses the electric force by

$$\vec{F}_E = \frac{q \cdot U}{\vec{d}}. \quad (3.3)$$

Fig. 3.1 describes a small charged particle, with mass m , falling into a homogeneous electric field. It will be affected by three forces; the gravitational, \vec{F}_g , the electric,

\vec{F}_E , and the drag force, \vec{F}_{drag} . Before entering the electric field, the particle is accelerated by the gravitational acceleration, \vec{g} , and reaches its terminal velocity, \vec{v}_y , along the y-axis when $\vec{F}_{\text{drag},y}$ balances \vec{F}_g .

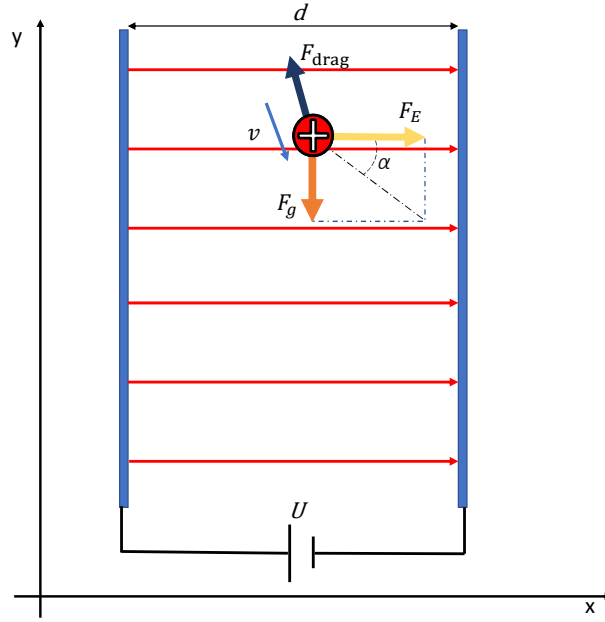


Figure 3.1: A small positively charged particle falls into a homogeneous electric field (red arrows).

Initially $\vec{F}_E > \vec{F}_{\text{drag},x}$ and the difference is a resulting force, $\vec{F}_{R,x}$. Newtons second law of motion gives the acceleration, \vec{a}_x , along the x-axis by

$$\vec{a}_x = \frac{\vec{F}_E - \vec{F}_{\text{drag},x}}{m}. \quad (3.4)$$

The acceleration, \vec{a}_x , will be zero when \vec{F}_E and $\vec{F}_{\text{drag},x}$ are equal. At this point, the droplet will move in a straight line at an angle, α , determined by the equation

$$\tan \alpha = \frac{\vec{F}_g}{\vec{F}_E} = \frac{m\vec{g}}{(qU/\vec{d})} = \frac{m\vec{g}\vec{d}}{qU}. \quad (3.5)$$

The specific charge, q/m , of a falling droplet in the homogeneous electric field can be obtained by analyzing α of its path in the field using a rewriting of Eq. 3.5 to

$$\frac{q}{m} = \frac{\vec{g}\vec{d}}{U \tan \alpha}. \quad (3.6)$$

3.2 Particle traps

Consider a ball rolling from left to right approaching a pit in the ground, see Fig. 3.2. Imagine no friction or drag forces. Can the ball be trapped in the pit, i.e. stay there?

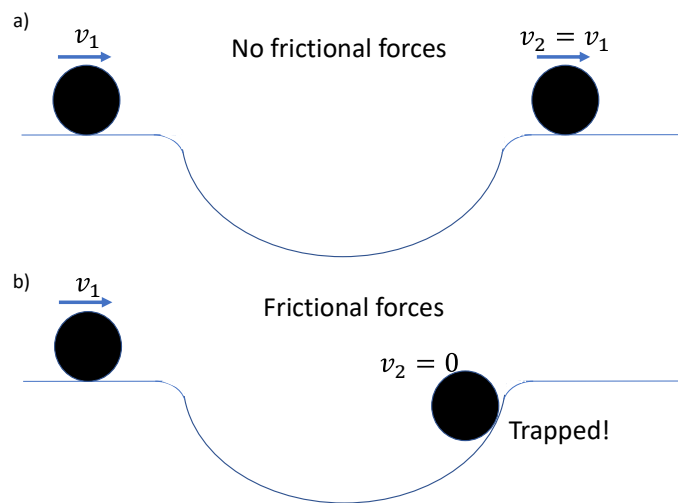


Figure 3.2: How to trap a ball using a pit in the ground. a) No frictional forces that can leak the mechanical energy from the ball. If it has any velocity, v_1 , it will go in the pit but the mechanical energy will be conserved so the ball will travel up the slope of the pit and out of it with the same velocity, $v_2 = v_1$. b) Frictional forces apply and they do work on the ball that will lose mechanical energy as it travels inside the pit (trap). This makes the ball trappable and it will end up at the bottom of the pit (center of the trap).

Conservation of mechanical energy in a gravitational field will make the ball increase in velocity until it reaches the bottom of the pit and decreases in velocity on its way up, by the same amount as potential energy transforms into kinetic energy and back again. If there are frictional forces, however, energy will leak in interaction with ground and air and hence, there is a chance for the ball to be trapped, based on its initial velocity (see Fig. 3.2). The ball is caught in a potential well, a point in space with minimal potential energy. It can only escape if some object does work on it. Analogously particle traps can be understood. In the case of the ball, there is a combination of the gravitational field pulling downwards on the object and friction that ensures the ball loses mechanical energy. A general trap can be described as a point in space, towards which a surrounding field exerts a distance-dependent force on an object. The trap center corresponds to the local

minimum of potential energy. The force, \vec{F} , will increase with the distance, $\Delta\vec{r}$, and be directed towards the center of the trap. The strength of the force will be proportional to the trap stiffness (spring constant), c . (see Fig. 3.3). The relation is described by the following equation, known as Hooke's law,

$$\vec{F} = -c\Delta\vec{r}. \quad (3.7)$$

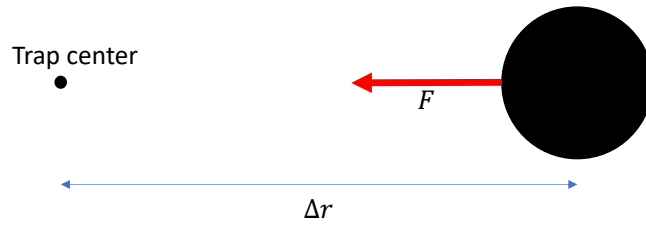


Figure 3.3: General trapping principle. The field interacting with the particle needs to generate a restoring force, \vec{F} , that increases with the distance, $\Delta\vec{r}$, to the trap center, with a magnitude scaled by trap stiffness, c . The relation is described in equation 3.7

In other fields, i.e electrical, optical, or acoustic fields, other forces give rise to a possible particle trap.

Trapping of charged particles with electrical fields has been realized by two pairs of electrodes that switch polarity simultaneously at a high enough frequency. Such a trap is called a Paul Trap [64] or a quadrupole ion trap (see Fig. 3.4) invented by Wolfgang Paul in 1990 and awarded the noble prize for its use to trap charged particles for long times [65].

This two-dimensional version of a quadrupole trap is described by the equation,

$$\Phi_0 = U + V \cos \omega t, \quad (3.8)$$

where Φ_0 is the total applied voltage between each pair of electrodes in the quadrupole, U is a DC voltage and, V is an AC voltage with driving frequency, ω [64]. The electric field strengths in the xy -plane, E_x and E_y , described in Fig. 3.4, is given by the two expressions,

$$E_x = -\frac{\Phi_0}{r_0^2}x, \quad E_y = \frac{\Phi_0}{r_0^2}y, \quad (3.9)$$

where r_0 is the distance to the trap center [64].

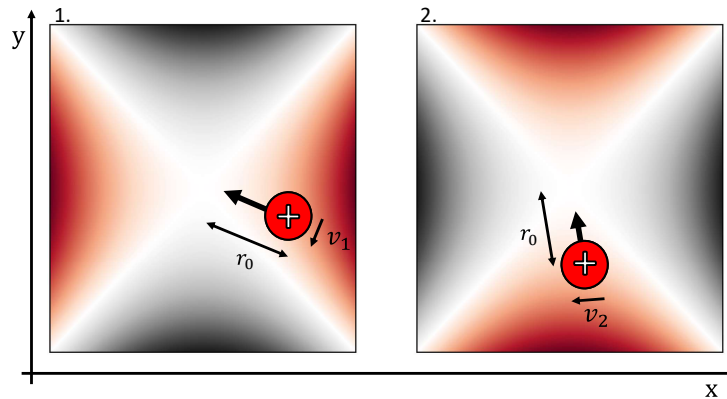


Figure 3.4: A simulation of the electric field in a Paul Trap. Changing the polarity of electrode pairs at a certain frequency introduces a varying electric field. 1) The electric field exerts an electric force on the positively charged particle directed to the trap center. The force changes the direction of the velocity v_1 . 2) The change in polarity of the electric field still exerts a force directed to the trap center. The force will increase in strength as the distance r_0 to the trap center increase. This keeps the particle trapped.

3.2.1 Optical traps

A qualitative understanding of optical levitation can be obtained by treating laser light as rays that hit a small transparent liquid droplet with a refractive index larger than the surrounding. The laser light can then be reflected, refracted or absorbed. As the light change direction, the linear momentum changes. The droplet must then undergo an equal and opposite momentum change due to the law of conservation of momentum. This results in optical forces. In an optical trap (see Fig. 3.5), a focused laser exhibits two types of forces on the levitated particles to hold them in place. The *scattering force* F_{scatter} , balances gravity and drives the particles along the laser's path, and the *gradient force* F_{grad} provides attraction towards the point of highest intensity (due to refracted light). For an upward-directed focused laser beam, these two forces combine to form the optical trap and provide lift and stability

To trap the particle, however, some air resistance or other frictional force is needed for the object to lose energy and eventually find a stable position. This makes it harder to trap at lower pressures. The magnitude of the net optical restoring force F on a particle in the ray-optics regime (particles not much smaller than the laser wavelength) in an optical trap is, for a Gaussian beam, directed to the

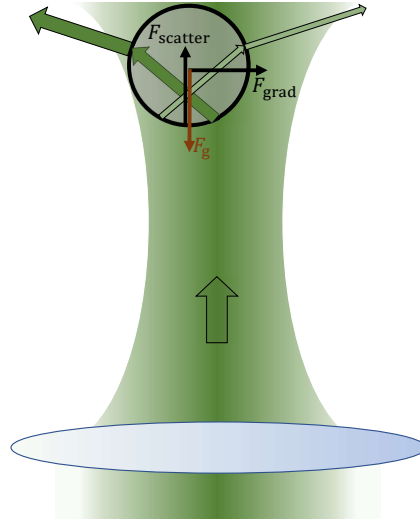


Figure 3.5: Optical forces on a transparent object in the optical field of green laser with Gaussian beam profile. The upward force (black arrow, up) is the scattering force from photons (light particles) pushing on the object when reflected. The gradient force (black arrow, right) is produced by light being refracted out from the center of the beam, pushing the object into the center due to the conservation of momentum. The field gradient is symbolized by the red arrows pointing toward the highest intensity. The direction of the gradient force is inwards if the refractive index for the trapped particle is higher than the medium it is immersed in.

beam center and can be calculated as

$$F = Q \left(\frac{n_m P}{c} \right), \quad (3.10)$$

where P , c , n_m , and Q are the incident laser power, the speed of light in vacuum, the refractive index of the surrounding medium, and a dimensionless quality factor encoding the angular contribution of F_{scatter} , and F_{grad} , respectively. For particles much smaller than the wavelength, Rayleigh theory is applicable instead.

3.2.1.1 Combining optical and electrical fields

Power is defined as energy over time and a change in energy is physical work that is described by $W = F \cdot \Delta s$, where, Δs , is a displacement and, F is the force doing the work. Hence, power and force are related in the expression

$$P = \frac{\Delta E}{\Delta t} = \frac{F \cdot \Delta s}{(\Delta t)^2}, \quad (3.11)$$

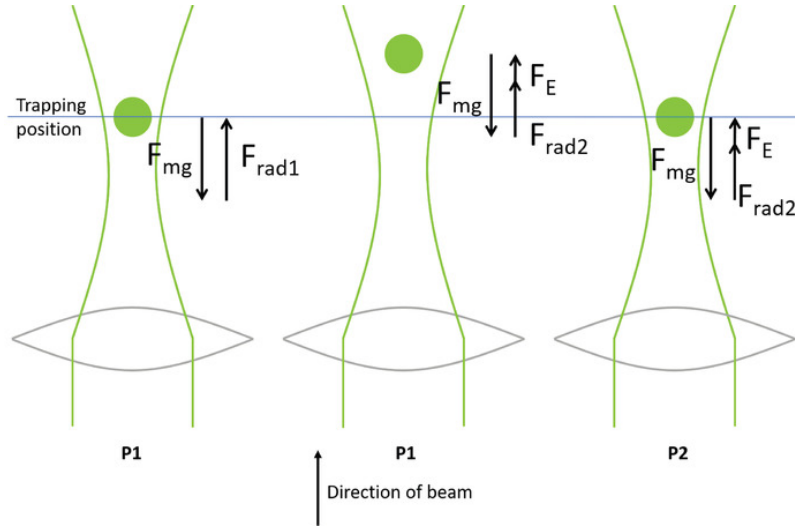


Figure 3.6: Using the laser power, P1, first the droplet is trapped as gravity is balanced by the optical force, F_{rad1} . As the electrical force, F_E , is applied (middle) the droplet is balanced at a higher level. There the wider beam provides a lower optical force, F_{rad2} , for the same laser power, P1. The laser power is then reduced (to P2) until the droplet is back at the original level of balance. Here the new optical force, F_{rad2} , and the electric force together balance gravity. The sum of the two forces is equal to the previous optical force, F_{rad1} . *P* is the power of the laser. ”This is adapted from Galán, D., Isaksson, O., Enger, J., Rostedt, M., Johansson, A., Hanstorp, D., de la Torre, L. Safe Experimentation in Optical Levitation of Charged Droplets Using Remote Labs. J. Vis. Exp. (143), e58699, doi:10.3791/58699 (2019).”

where ΔE is the change in energy and, Δt is the corresponding time change.

A homogeneous electric field in combination with an acoustic field can be used to measure the charge of an object immersed in these fields using a rewriting of Eq. 3.1 to

$$q = \frac{F_E d}{U}, \quad (3.12)$$

where the electrical force, F_E , is obtained from the force equilibrium, between the three forces, F_{rad} , F_E , and F_g , acting on a levitated object in the two force fields.

The resulting equation can, combining Eq. 3.12 with Eq. 3.11, be described in terms of two different laser powers, P1 and, P2 using

$$F_E = mg \cdot \left(\frac{F_{rad1} - F_{rad2}}{F_{rad1}} \right) = mg \cdot \left(\frac{P1 - P2}{P1} \right). \quad (3.13)$$

3.2.2 Acoustic traps

The acoustic field consists of velocity, density, and pressure differences in the medium the object is trapped in. The acoustic field will exert gradient forces in the direction from high pressure to low pressure (nodes). The forces need to be strong enough to balance gravity. There is a lot of friction in the acoustic field due to the large amounts of molecules to give energy to and the objects tend to be very stable when trapped.

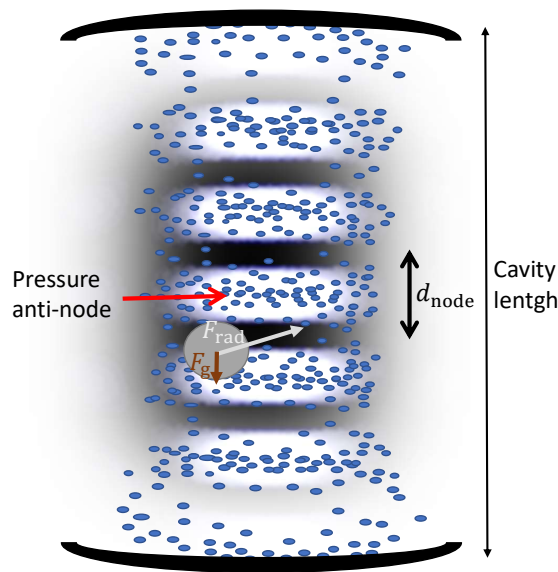


Figure 3.7: Acoustic pressure force F_{rad} (white arrow) on a small object immersed in the acoustic field balances the gravitational force F_g (brown arrow). Blue dots symbolize air particles. Anti-nodes are represented in the back by white regions, and in the front by high pressure (many particles). Nodes are represented in the back by black regions and few particles (low pressure)

Particles in all forms, no matter charge or transparency can be trapped using an acoustic trap. Limitations include the size and density of the object. Usually, the size cannot surpass half the acoustic wavelength, even if some exceptions exist [66–69]. Densities of up to 7.3 g/cm^3 have been rotation-locked during levitation [69] and even lead and mercury can be levitated [70]. Altogether, this means a lot of flexibility compared to other levitation techniques and this contributes to the recent success of acoustic levitation in scientific research [71]. Most research within acoustic levitation has used variants of the commercialized Langevin-type levitator [20, 72, 73]. In recent years, low-cost 3D-printed versions utilizing small transducers (sound emitters) mounted in arrays have brought acoustic levitation to

a new era. The simplest version of such a trap is the single-axis acoustic levitator, TinyLev[20]. Many spin-off designs have demonstrated impressive control of the acoustic field using phased array levitators[73, 74]. In single-axis acoustic levitators a standing wave can be generated by applying a phase shift of π between the two transducer arrays. The acoustic pressure producing the trap can be obtained by

$$p(x, y, z) = P_0 \sum_j J_0(ka_j \sin \theta_j) \frac{1}{d_j} e^{i\phi_j}, \quad (3.14)$$

where P_0 , J_0 , k , a_j , θ_j and, d_j respectively denote a voltage-dependent factor, the zeroth-order Bessel function of the first kind, the wavenumber, the radius of transducer j , the angle between the normal of transducer j and any point in space (x, y, z) , and d_j is the distance from transducer j to that point [69].

The most common way to calculate the acoustic radiation force on a levitated object is by first calculating Gor'kov potential U and then obtaining the force as the gradient. The calculations assume that a small incompressible sphere is immersed in the acoustic field of an ideal fluid. The acoustic wavelength, λ , has to be larger than the radius, R , of the sphere [75]. The Gor'kov potential, in air, is calculated as

$$U = 2\pi R^3 \left[\frac{f_1}{3\rho_0 c_0^2} \langle p^2 \rangle - \frac{f_2 \rho_0}{2} \langle u^2 \rangle \right], \quad (3.15)$$

where p and, u are the first-order incident acoustic pressure and particle velocity respectively. ρ_0 and, c_0 is the density of, and speed of sound in air and for dense objects like solids the two factors f_1 and, f_2 can be approximated to 1 [76]. The acoustic radiation force, F_{rad} , acting on the small sphere can now be calculated using the Gor'kov potential by

$$F_{\text{rad}} = -\nabla U. \quad (3.16)$$

For situations where these approximations don't apply more general but slower calculations can be used [76], but the reason the gradient of the Gor'kov potential is widely used is the simplicity and the corresponding gain in calculation speed.

3.2.2.1 Acoustically levitated droplets

Droplets levitated in single-axis acoustic levitators are deformed by the acoustic pressure and find equilibrium shapes. For droplets in the sub-microliter to milliliter size, these shapes are well approximated by oblate spheroids (ellipsoids, see Fig. 3.8). On of the cross-sections of these are an ellipse with a minor-axis, r_{min} , and a major-axis, r_{maj} .

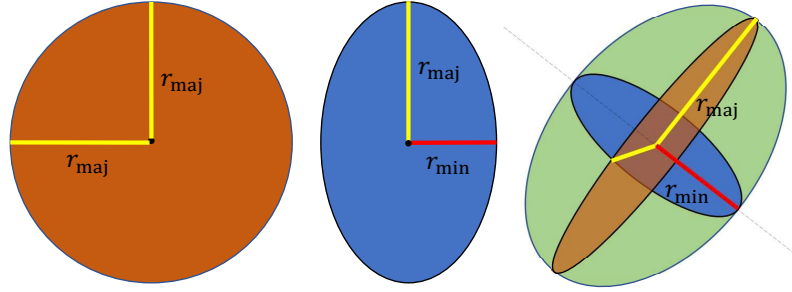


Figure 3.8: The oblate spheroid (ellipsoid) to the right is circular (brown, left) when viewed along the dashed axis of symmetry and elliptic (blue, middle) viewed orthogonal to that axis. r_{maj} is the semi-major axis of the blue ellipse. The semi-minor axis, r_{min} , in red, of the ellipse is aligned with the axis of symmetry for the oblate spheroid.

The roundness of the droplets can be described by their aspect ratio, A_r , calculated as

$$A_r = \frac{r_{\text{min}}}{r_{\text{maj}}}. \quad (3.17)$$

Depending on surface tension the same acoustic pressure will deform droplets of different materials into different aspect ratios. Very small droplets are well approximated by spheres if the amplitude of the acoustic field is sufficiently low. Ellipsoidal droplet volumes V_{ell} , can be calculated using r_{min} , and r_{maj} with

$$V_{\text{ell}} = \frac{4\pi}{3} r_{\text{maj}}^2 r_{\text{min}}. \quad (3.18)$$

Images of levitated droplets can then be used to calculate their volumes with

$$V_{\text{metric}} = V_{\text{pixels}} \times s^3, \quad (3.19)$$

where V_{metric} is volume in cubic-millimeters, V_{pixels} is the pixel-volume obtained via Eq. 3.18 from pixels corresponding to r_{min} and r_{maj} in an image of the droplets, and s is the scale factor between pixels and millimeters.

Method

4.1 Experimental setups

4.1.1 Electrical field (Paper I)

An experimental setup was designed for teachers as a tool to help their students develop mental models for the particle-field interaction of charged particles in electric fields. The setup was designed to visualize individual particles moving through and interacting with an electric field. The design was based on the chosen object of learning (the ability for students to predict the direction and relative magnitude (smaller/larger) of the electric force on particles in electric fields) and the required pattern of variation and invariance described in Sec. 4.2.

A custom-built charging unit was mounted on a piezoelectric micro-dispenser with a curved steel capillary (GeSim A010-002) capable of automatically and controllably ejecting small glycerol droplets with a size of $20\ \mu\text{m}$. With the charging unit switched off, the droplets are ejected with an undefined negative charge depending on the friction in the dispenser.

The charging unit can change the charge of the droplet by passing it through an electric field of 0-300 V. The field will rip off a number of electrons from the droplet. To produce drops with a neutral charge, a voltage of about 100 V was used. Voltages lower than 100 V will cause the paths of the droplets to deflect to the right, while higher voltages will cause movement to the left (see Fig. 4.1). Droplets with different charges can be produced with the charging device shown in the upper right part of Fig. 4.2. The ejected droplets lose velocity after traveling a few centimeters in the air and then fall vertically into an experimental chamber. In the chamber, two parallel ITO-coated (indium-tin-oxide) glass plates (the

electrodes of a capacitor) produce a statically homogeneous electric field when connected to a DC voltage. Voltages in the range of 0-50 V are used to control the falling trajectories of the charged droplets. LED light illuminates the experimental chamber through the transparent conductive ITO plates and scatters from the falling droplets, which are made visible to the naked eye.

For further visualization and video generation, a Logitech Brio 4K webcam was placed with the optical axis parallel to the ITO plates and collected the scattered light from the droplets (see left in Fig. 4.2). The velocity and size of the ejected droplets were controlled via the software accompanying the droplet dispenser control box (GeSim, multi-dos 2, A020-301).

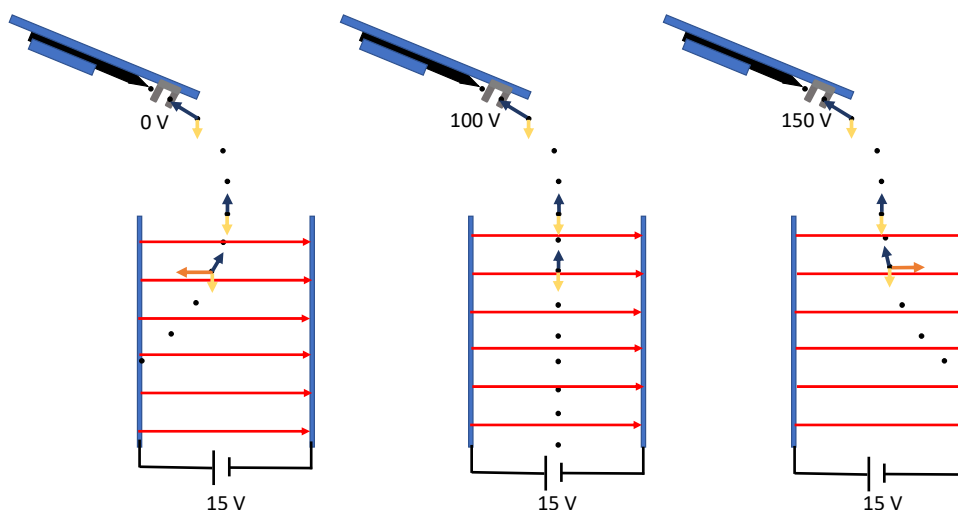


Figure 4.1: A droplet dispenser with a charger unit was placed a distance above the capacitor electrodes. Red arrows indicate the direction of the electric field between the electrodes of the capacitor. Another electric field between the dispenser tip and the charger electrode was applied to alter the charge of ejected glycerol droplets. The ejected droplets almost immediately after ejection reach terminal velocity and fall straight down with constant speed when entering the approximately homogeneous electric field of the capacitor. Arrows are force vectors indicating the strength and direction of electric- (orange), gravitational- (yellow), and drag (blue) forces. Left: 0 V applied, the droplets are negatively charged initially due to friction in the dispenser causing the electric force directed towards the positive electrode. Middle: 100 V is applied and this neutralizes the droplet charge, ripping off the extra electrons so the droplets fall unaffected by the electric field. Right: 150 V is applied, ripping off even more electrons making the droplet charges positive and attracted by the right negative electrode of the capacitor.

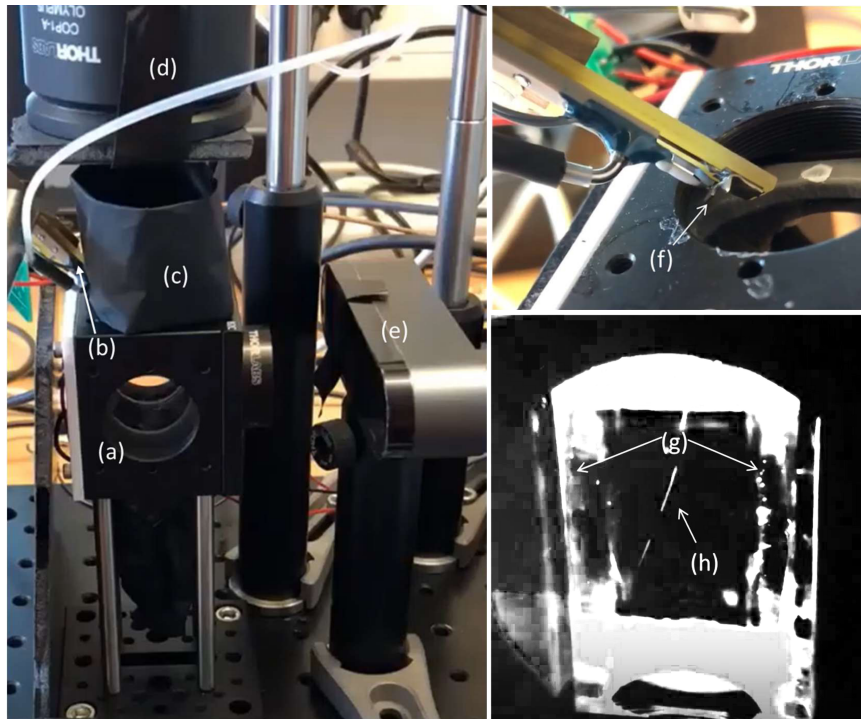


Figure 4.2: Left is the experimental setup: (a) experimental chamber, (b) droplet dispenser, (c) turbulence shielding tube, (d) LED-light source, (e) web camera connected to PC. Upper right: (f) close up on droplet charger mounted on the dispenser. Lower right: (g) ITO-plates connected to a voltage supply, (h) falling droplets in curved trajectories due to particle-field interaction (electric force).

4.1.2 Optical trap (Paper II and Paper III)

The experimental setup (see Fig. 4.3) consists of a droplet dispenser, an experimental chamber (glass cell) that can be vacuum pumped, a vertical laser with focus slightly under the center of the glass cell, electrodes with holes for letting the laser through, an alpha source (^{241}Am) mounted on an electric motor translation stage.

A voltage of up to 1000 V is applied between the plates (f in Fig. 4.3) to produce a vertical electric field. This setup in combination with a droplet ejection device has been used to trap liquid droplets optically and investigate their properties and their interaction with both optical and electrical fields as well as ionizing radiation [77].

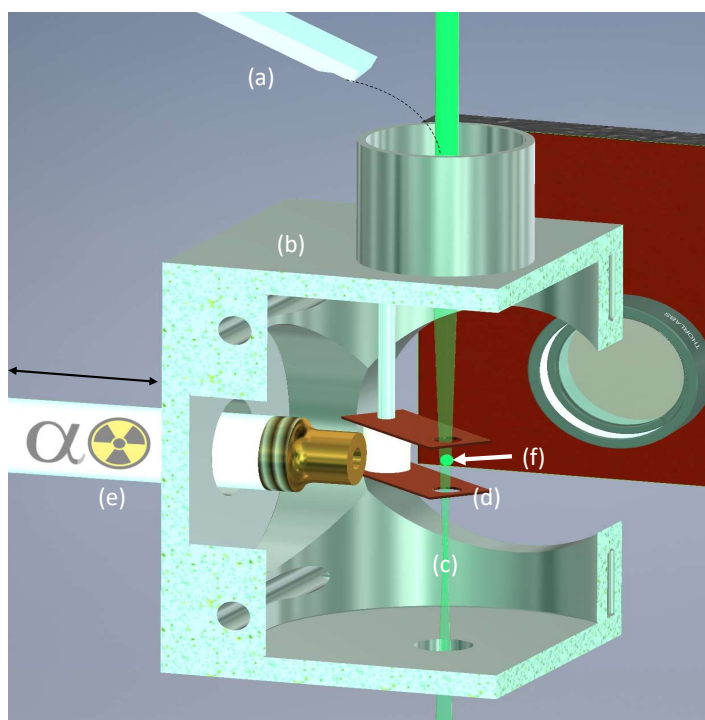


Figure 4.3: The experimental setup consists of (a) droplet dispenser and a charger, (b) experimental chamber, (c) a vertical and focused laser, (d) electrodes, (e) alpha source (^{241}Am) on motorized translation stage, (f) optically levitated droplet. The front and right walls are cut to visualize the center of the experimental chamber.

4.1.3 Acoustic trap (Paper IV)

The experimental setup used to measure volumes of levitated droplets is shown left figure of Fig. 4.4. Two opposite arrays of transducers (Manorshi, MSO-P1040H07T) are driven by the same square signal of about 40 kHz, amplified with a step motor and a DC-power supply. Trapped droplets scatter the diffused light from the LED source, producing a shadow that is projected onto the CCD chip via an Navitar Zoom 7000 macro objective mounted on a Logitech 4K Brio camera. The droplet images are directly visualized on a computer screen connected to the experiment. A CPU collects the pixel data and the thermometer readings. The transducer mounting caps are attached to motorized translation stages to controllably vary the cavity length.

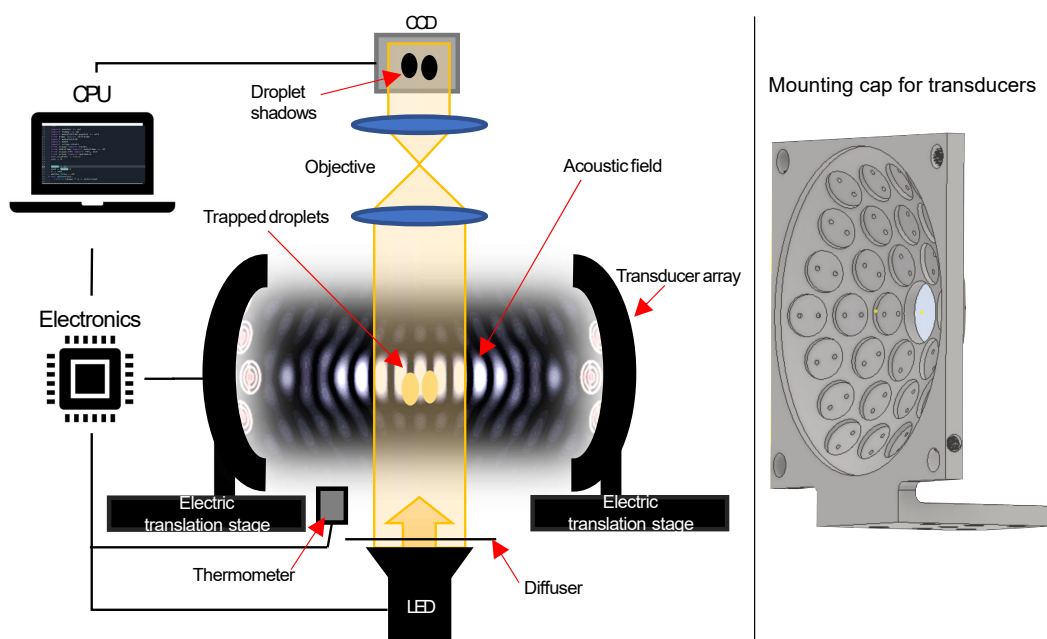


Figure 4.4: Left is the experimental setup. The traps acoustic field shown with white anti-nodes and black nodes. Two droplets (yellow) shadow diffused LED light. The shadows are projected via a camera objective on a CCD chip. The CPU collects the pixel data and the thermometer readings. Right is the design of the mounting cap for the transducers.

4.2 Method Paper I

In the Swedish upper secondary physics curriculum, two-dimensional motions of objects in electrical fields are part of the central content [12]. The experimental setup described above was developed to visualize the phenomenon and help students develop their corresponding mental models (see Ch. 2). With variation theory as the planned analytical and theoretical framework, the object of learning in this pilot study was the ability for students to predict the direction and relative magnitude (smaller/larger) of the electric force on particles in electric fields. To help students develop such mental models the experiment was designed with possible patterns of variation and invariance in mind, ready to be realized when needed during the lesson. The electric force acting on charged droplets immersed in an electric field depends on the magnitude and direction of the electric field, as well as the magnitude and polarity of the electric charge carried by the droplets. Therefore, droplet charge and polarity in addition to the strength and direction of the electric field were identified as some of the particle-field interactions' neces-

sary critical aspects. Their variability within the experiment design is imaged in the right of Fig. 4.5 and the pattern of variation and invariance is shown in Tab. 4.1. The electric field is varied by varying the voltage applied between the capacitor electrodes and the droplets' charge is varied by varying the voltage on the custom charger mounted on the dispenser as described in section 4.1.1.

Table 4.1: Pattern of variation and invariance made possible via experiment design. Contrast (c, white), generalization (g, gray), and fusion (f, olive). The bending of droplet paths can be observed, and it is the result of the droplet-field interaction (the electric force).

| | Electric field [V/m] | Charge on droplets [C] | Droplet path |
|---|-------------------------|---------------------------|--------------|
| c | Const. pos. | vary | co-vary |
| c | Const. neg. | vary | co-vary |
| c | vary | const. pos. | co-vary |
| c | vary | const. neg. | co-vary |
| g | vary | 0 | const. |
| g | 0 | vary | const. |
| f | vary | vary | vary/const. |

To further improve the students' mental models, relevant theoretical concepts should be included. The concepts of electric fields and charged particles and their representations (diagrams) were based on being central to the concepts selected as initial critical aspects for the development of the mental model. A pattern of variation and invariance using pictures with representations of gravitational fields and electric fields as well as particles within these fields was designed (see Fig. 4.6). Using the variation pattern and the principle of contrast, the possibility arises for students to distinguish differences between homogeneous and non-homogeneous fields. Furthermore, they can discern the field strength and direction as well as the magnitude of forces on objects in the field, within the representations of field lines and force vectors. The observed relationship is linked to Eq. 3.1. During a lesson, the teacher uses the ability to contrast the effects of changes in the experimental setup by varying one property value at a time. To connect theoretical concepts with physical observations, students are activated to explain the observation using the diagrams and concepts from the theory in a discussion with the teacher.

4.2.1 Educational data collection and analysis

Students from two upper secondary schools ($n=50$) in the Gothenburg area participated in a pilot study. The aim was to investigate the effect on students' learning when the teacher had access to an experimental setup or a video of such a setup

that could visualize physical phenomena related to the object being taught during the lesson or no demonstration at all. For this lesson, the object of learning was the concept of electric fields and their interaction with particles.



Figure 4.5: Example frame from a video recording. Left is a camera image of the experimental chamber. The trace of three falling droplets produces a visible projectile motion bending to the left in the electric field between the electrodes. To the right are the knobs controlling the voltages applied to the ITO plates in the experimental chamber (left) and the droplet charger electrodes (right). Top right is the droplet function generator giving suitable frequency and voltage to the droplet dispenser.

Students were divided into three groups: 1) Experiment live, 2) Video experiment, 3) No demonstration (only a thought experiment). Group 3 is the control group and does not receive any teaching using the experimental setup. The same teacher (the author) taught all three groups using the same script for the lesson to only vary the use of the experimental setup to visualize the phenomenon. An example slide from the script can be seen in Fig. 4.6. An example frame from the video used in group 2 can be seen in Fig. 4.5.

The data collection method consisted of a pre-test and a post-test. Students performed the pre-test immediately before the lesson and the post-test immediately after. The test questions of both tests were identical and consisted of four questions aimed at investigating students' mental models regarding the object of learning. The test questions are replications of some questions found in the Diagnostic

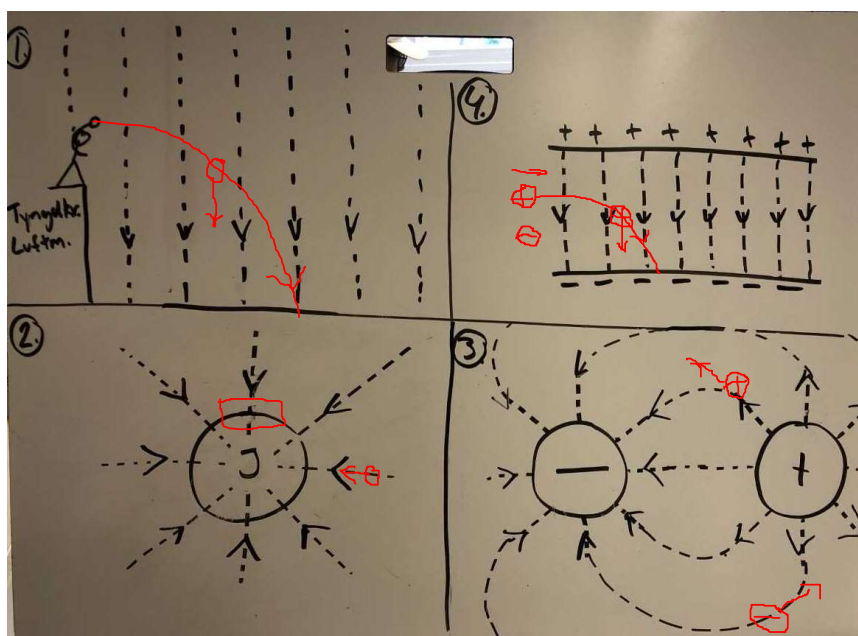


Figure 4.6: Example slide from the script used by the teacher during the three lesson variations.

Exam for Introductory, Undergraduate Electricity and Magnetism (DEEM) [78], translated to Swedish (see Fig. 4.7).

1. Vilken riktning, om någon, har kraften som verkar på partikeln på grund av fältet om partikeln initialt (vid start) är i vila och partikeln har positiv laddning?

De prickade pilarna representerar elektriska fältlinjer.

| | |
|--|--------|
| <input type="checkbox"/> ↑ |→ |
| <input type="checkbox"/> ↓ |→ |
| <input type="checkbox"/> → |→ |
| <input type="checkbox"/> ← |→ |
| <input type="checkbox"/> Det finns ingen resulterande kraft. |→ |

Figure 4.7: Example item from the pre- and post-tests (in Swedish).

Students' responses were analyzed and compared by first calculating a possibly improved version of the Hake gain [79], which differs in how zero or negative

changes are handled. To calculate the average normalized change, c_{ave} , [80] for each group, first the normalized change, c , for each student was calculated by

$$c = \begin{cases} \frac{\text{post}-\text{pre}}{100-\text{pre}} & \text{post} > \text{pre} \\ \text{drop} & \text{post} = \text{pre} = 100 \text{ or } 0 \\ 0 & \text{post} = \text{pre} \\ \frac{\text{post}-\text{pre}}{\text{pre}} & \text{post} < \text{pre}. \end{cases} \quad (4.1)$$

Then the standard error was calculated for each group by first calculating the standard deviation (but not assuming c-scores to be normally distributed) and then dividing by the square root of the number of students in the group N [80]. Average normalized change and the standard error can be used to measure and compare learning outcomes from interventions in classrooms, even if N is low since it does not assume the distribution of the population to be normal [80]. The results can be seen in Fig. 5.2.

4.3 Method Paper II

The experimental setup described in 4.1.2 was complemented with two video cameras. One camera for a view of the droplet dispenser so users could monitor droplet ejection and dispenser clogging. One camera for a view of the experimental chamber where the droplets are trapped. The two cameras, the position sensitive device (PSD), the laser, and the voltage amplitude and type were connected directly or via a NI-DAQ card to the lab computer that enabled control and monitoring via a LabView program.

A UniLabs moodle was designed as the user GUI (graphical user interface) to communicate with the lab computer via the internet. End users could connect their local computers to the internet and access the moodle via a web browser. A Swedish upper secondary physics class was invited to test use the setup from their classroom.

4.4 Method Paper III

To measure the electron's charge and visualize its quantization, a charged silicone oil droplet was first trapped in a focused laser beam. The radiation pressure balances gravity and the conservation of momentum due to the refracted light keeping it near the center of the vertical laser beam. The droplet dispenser ejected a charged droplet that was optically trapped and then neutralized using an alpha radiation source as the amplitude of droplet oscillations in a varying electrical field was monitored. A magnified image of the droplet was projected onto a distant wall. As the

droplet was neutral a voltage of a few hundred volts locally homogeneous electric field could be introduced without any impact on the droplet. The alpha source was then introduced again to ionize air molecules in the vicinity of the droplet. The ionized air surrounding the droplet added electrons to it during collisions, making the droplet and its projected image "jump". The jumping shadow could be analyzed with a ruler on the wall and we found a smallest possible jump, and all other jumps were multiples of this jump. These jumps are interpreted as quantization of the charge of the electron. By measuring these smallest charge jumps, we could confirm seeing individual electrons.

4.5 Method Paper IV

The acoustic trap is operated at a 40 kHz driving voltage. Two droplets are levitated in adjacent central nodes produced by the superposition of sound waves emitted from the transducers. The droplets shadow the light from the LED as it passes through the trap and is imaged on a CCD chip via a camera lens.

A simulation that can predict node-to-node distances in air depending on the specific details of transducers, trap geometry, frequency, cavity length, and temperature (in the outer regions of the trap), was developed (see Fig. 4.8).

Two droplets were trapped in the neighboring most central nodes and the temperature of the air in the outer region of the trap was measured. Iterations between predictions of cavity lengths that have symmetric node geometries, and live pixel data collection of two levitated droplets using that cavity length were done to establish a match between the simulation and the real experiment.

The images and the temperature measured by the thermometer were timestamped, recorded, and analyzed via a custom python script based on the skimage library. Pixel data from the sharp contour images were collected with the below image-processing algorithm:

1. Convert to gray-scale.
2. Apply a mask, using a dilation method.
3. Binarize the image using a threshold to make objects white and the background black.
4. Label connected regions of white pixels.
5. Extract pixel values (x,y) of centroid, minor-axis length, major-axis length, and the orientation.

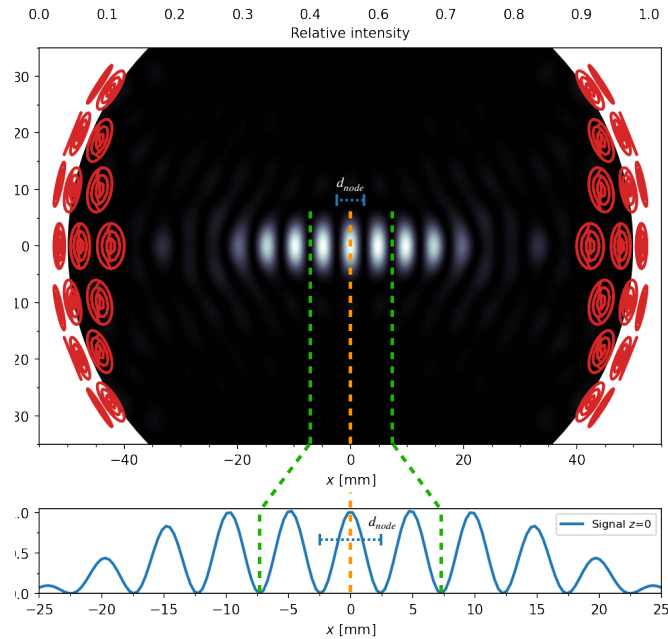


Figure 4.8: Simulation of the acoustic trap. The black area shows a simulation of the acoustic field with relative intensity (greyscale) in the region accessible to the CCD. The structures in red color represent the positions and orientations of the transducers. The lower subfigure shows the relative intensity of the acoustic field along the x-axis for the central nodes of the trap.

Fig. 4.9 shows the captured camera image (upper) and the extracted image data (lower); the distance between droplet centroids (weighted pixel center of a labeled region), semi-minor and semi-major axis length of each labeled region. The centroid, the semi-minor axis, and the semi-major axis are used to paint a red ellipse on the image and it can be concluded that the droplet can be well approximated as an ellipsoid since it is circular from the perpendicular side view and elliptic viewed from the camera.

Cavity lengths that have symmetrical central nodes were obtained by constructing simulations in a loop that stops at the cavity length that predicts similar amplitudes of the acoustic field in the four central anti-nodes (see Fig. 4.8). This ensured equal pressure gradients at different levitation heights of droplets levitated in the nodes and thus they won't move sideways during alterations of driving voltages or droplet volumes.

The above procedure is done once and establishes a match between the simulation of the acoustic field and the acoustic field in the trap. The simulation was then used to accurately predict node-node distance in millimeters and a scale factor s [pixels/mm] was automatically established using the pixel information contained in images of the two droplets (see Fig. 4.9). A spheroidal approximation of droplet

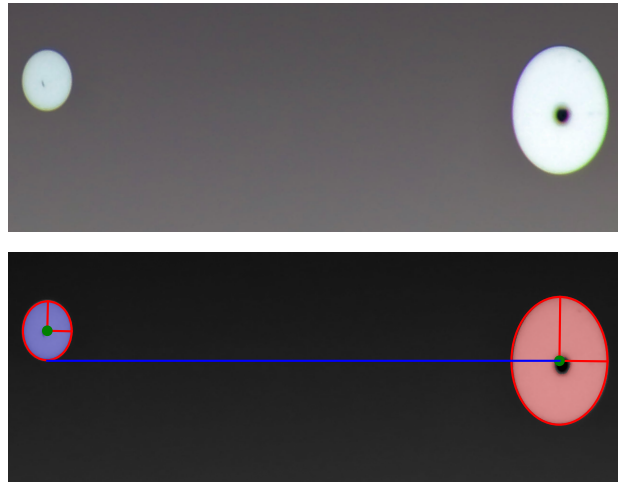


Figure 4.9: Upper: Image of two levitated droplets. Lower: Extracted pixel data from the upper image. The custom software finds the regions of white pixels in the upper image and then measures the region's major and minor axes (red lines), as well as the centroid positions (green dot) and the horizontal distance between the centroids (blue line). The red ellipses are painted afterward using the extracted data, only to show the quality of the elliptic approximation.

shape was used to calculate a pixel volume by Eq. 3.18. The droplet volume was finally calculated with Eq. 3.19 using the scale factor s .

Results and Discussions

5.1 Experiments increases understanding of particles in electric fields (Paper I)

Results are presented from the three interventions where a teacher taught the same lecture to three similar student groups with, without, and with a video of an experimental setup visualizing particles' movement in an electrical field.

Fig. 5.1 shows a comparison of the three interventions. In the diagram, the x-coordinate, x_n , for each point is obtained by $x_n = n \cdot 100/N$. Where N is the number of students in each group. The students' scores in percent on the pre-test and the post-test was sorted and plotted against the list of x-coordinates (students %). The pre-test scores show that the three groups had similar pre-knowledge. The post-test scores reveal that more students increase their conceptual understanding, as measured by the test if the lecture includes an experimental setup either live or videotaped, than without an experiment. However, even if all groups had the same amount of time, the same teacher, that also used the same script for the lesson except for how the experiment was used. In the lesson with no experiment, a thought experiment was used to illustrate the same conceptual critical aspects that the pattern of variation and invariance (see Fig. 4.1) aims to. The two plots in Fig. 5.1 show statistical floor and ceiling effects and this suggests the number of items on the tests need to be increased for better measurements.

Fig. 5.2 shows the three interventions' scores as normalized change against pre-test scores in percent. This way of displaying the data indicates that a video of the experiment and using the experiment live as a teaching tool during a lecture increases students' conceptual understanding more than not using an experiment

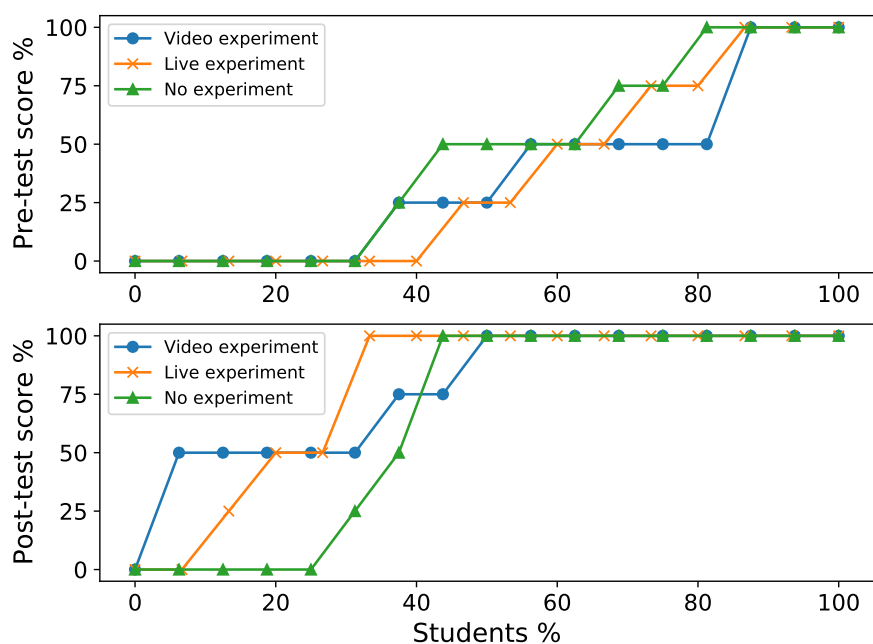


Figure 5.1: Upper: Students pre-test scores from the three groups; video experiment (blue), live experiment (orange), and without experiment (green). Lower: Students post-test scores. On the horizontal axis students from a specific group are equally spaced from 0-100 (labeled students %).

during the same lecture.

The two interventions with higher average normalized change (experiment live and video), had also lower pre-test scores on average. The pre-and post-test consisted of only four questions. There is a relatively high probability that this biased the normalized change scores in favor of the interventions that had low scores in the pre-test. In addition, the higher average score on the pre-test means that there is less room for improvement (floor and ceiling effects). The low number of test questions was a clear shortcoming of the pilot study and therefore four additional test questions were created as variants of the previous questions to address this issue before the next round of data collection. During this first pilot study, qualitative data were not collected systematically or analyzed, but it was observed that the students in all three groups were concentrated most participated in the class discussions.

5.1. Experiments increases understanding of particles in electric fields (Paper I)

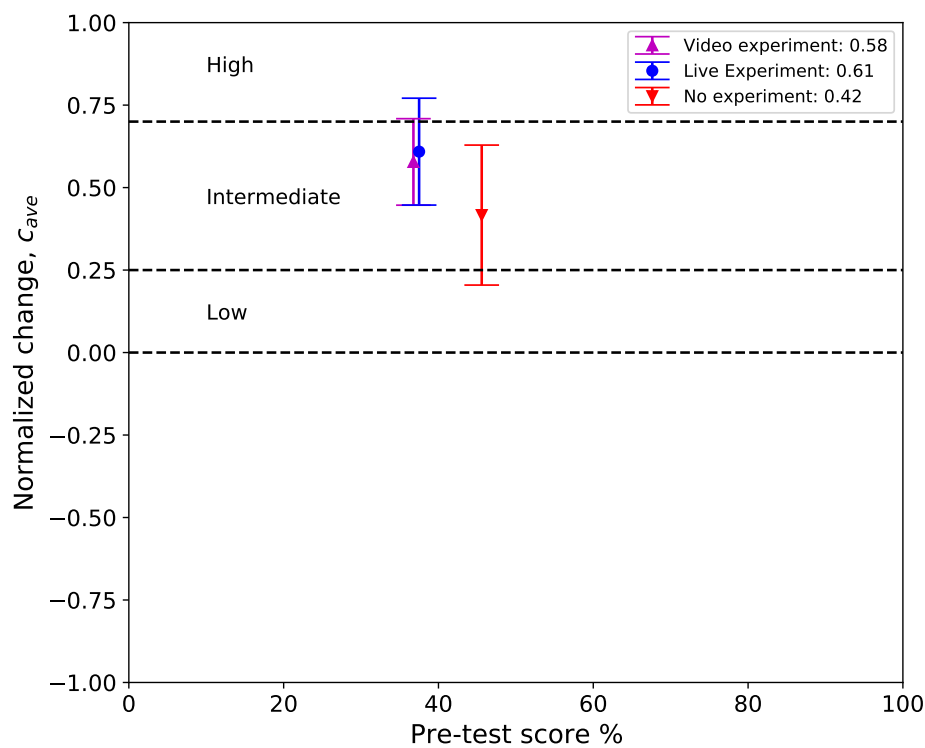


Figure 5.2: Normalized change vs pre-test score %. The error bars are the standard errors. Intervention with no experimental setup (red, arrow down), showed a low intermediate impact. Interventions with the aid of the experimental setup, live (blue, dot) or on video (magenta, arrow up) showed higher intermediate impact, as measured by the average normalized change, C_{ave} .

Summary

An experimental setup to visualize particle-field interaction with charged particles falling in an electric field has been successfully developed to be used as a teaching tool. More research is needed to confirm the results of a carried out pilot study, which show that experiments and video experiments produced better learning outcomes than teaching without demonstrations. To gain a better understanding, future studies need to incorporate qualitative data collection and a number of test items need to be added.

5.2 Optical trapping and investigation of a particle remotely from a school (Paper II)

A webcam and an internet connection as well as motorized equipment was controlled from a PC to convert an experimental setup to a remote setup (see Fig. 5.3). For the above-described experiment, a remote laboratory activity was developed to let students investigate the field-droplet interaction in a combination of optical and electric fields. Students connected to the experiment via the web portal University Network of Interactive Laboratories (UNILabs) and controlled the experimental setup located in Gothenburg, Sweden.

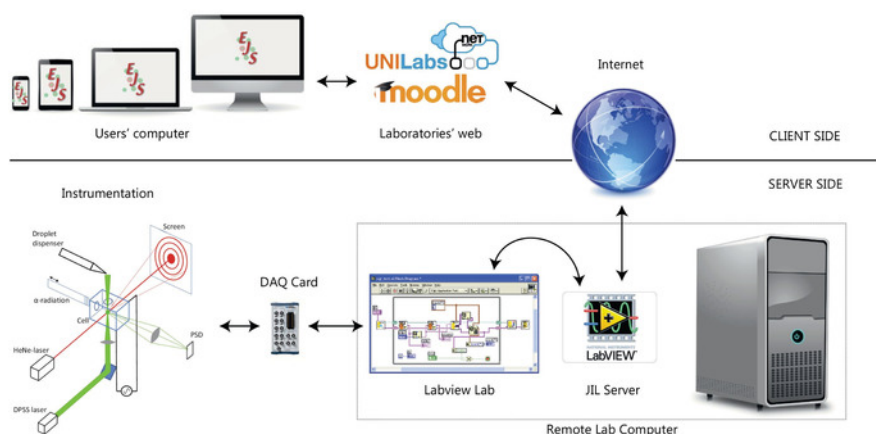


Figure 5.3: Remotely controlled experimental setup. "This is adapted from Galán, D., Isaksson, O., Enger, J., Rostedt, M., Johansson, A., Hanstorp, D., de la Torre, L. Safe Experimentation in Optical Levitation of Charged Droplets Using Remote Labs. *J. Vis. Exp.* (143), e58699, doi:10.3791/58699 (2019)."

The experimental procedure, which is described fully in Paper I, enables students to trap a droplet, and measure its' size, charge polarity, and absolute charge. The students monitor their operations via the digitally transferred images from the web camera and the signal from the Position Sensitive Device (PSD). This view is shown in Fig. 5.4 together with the respective inputs and outputs students can control and receive from the experiment.

Extensive instruction about how to operate the experimental setup hands-on as well as remotely to perform measurements of the levitated droplets' size, charge polarity, and charge is provided in Paper I. A trapped droplet can stay trapped for over half an hour. It can take up to one minute to capture the droplet but when it's trapped it is stable enough for the students to perform all the described

5.3. Visualizing the electron's quantization with a ruler (Paper III)

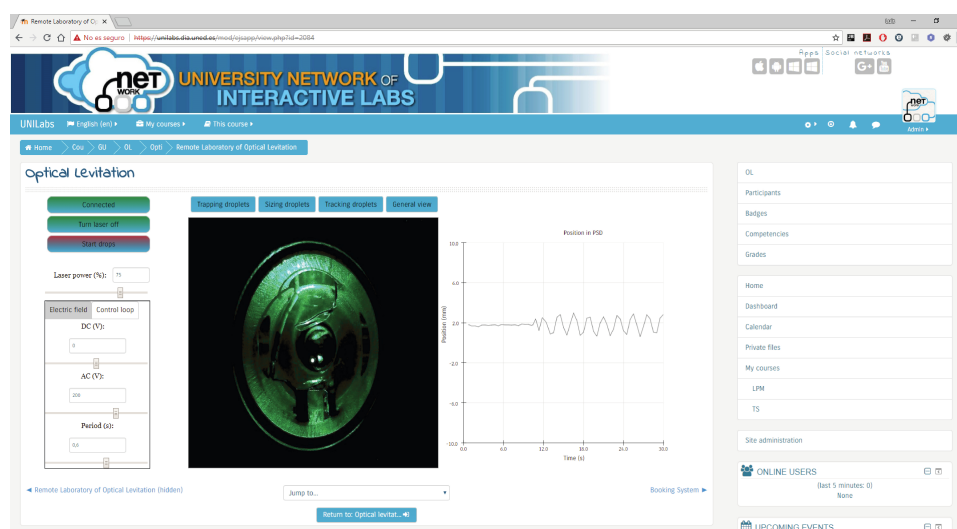


Figure 5.4: Student view of the experiment. To the left: controls for the laser and the electric field. Middle left: Control of camera view and droplet dispenser. Middle right: PSD monitor. Right: UniLab homepage navigation. "This is adapted from Galán, D., Isaksson, O., Enger, J., Rostedt, M., Johansson, A., Hanstorp, D., de la Torre, L. Safe Experimentation in Optical Levitation of Charged Droplets Using Remote Labs. *J. Vis. Exp.* (143), e58699, doi:10.3791/58699 (2019)."

measurements. This has been extensively tested, first locally, and then remotely by students from a Swedish upper-secondary physics class.

Summary

An experimental setup was developed and connected to the Internet of Things (IoT). The setup used high-power lasers and high-voltage electric fields but could be safely controlled remotely. A student lab was developed for students to measure the size, charge polarity, and charge of a levitated droplet using the experiment and it was tested both hands-on and by students remotely.

5.3 Visualizing the electron's quantization with a ruler (Paper III)

In this paper, we managed to visualize the quantization of electric charge by showing single electrons' impact on the net charge of an optically levitated droplet surrounded by an electric field. The effects were magnified, to be seen with the bare

eye, on a wall, or on a screen as a visual experience for future students to incorporate into their mental models.

The ability to visualize single quantized electron jumps has been developed. The experimental setup is based on trapping charged liquid droplets in an optical trap. By approaching the trapped droplet with an alpha emitter, air molecules are ionized, which in turn knocks off single charges on the trapped droplet. Since the droplet is in a homogeneous electric field, it will jump when its charge changes. These jumps are directly proportional to the number of electrons removed from the surface of the droplet. The smallest of the observed jumps corresponds to the charge of a single electron. These jumps are visualized on a ruler hanging on a wall (see Fig. 5.5). The optical trap stiffness $k = 5.00 \pm 0.49$ nN/m and a rewriting of Eq. 3.12, using Hooke's law (Eq. 3.7) and, the definition of electric field strength in homogeneous electric fields, $E = U/d$, where E is the electric field strength, U is the applied voltage to the electrodes, and d is the distance between the parallel electrode plates, was used to calculate the corresponding charge q for the smallest jump as

$$q = \frac{k\Delta y}{E}, \quad (5.1)$$

where Δy is the distance from the particle to the trap center. The known charge of the electron is 1.602×10^{-19} and our measurement agrees within the limits with this number and it confirmed the visualization of quantized single electron effects.

Summary

An experimental setup to visualize the quantization of electric charge was developed. With the experiment single electron addition to a levitated droplet can be seen with the naked eye. The experience of seeing quantum phenomena can be incorporated into students' mental models to improve their conceptual understanding. A video of the experiment visualizing the phenomenon is available in the online version of the paper.

5.4. Zoom-independent volume measurements calibrated by acoustic field (Paper IV)

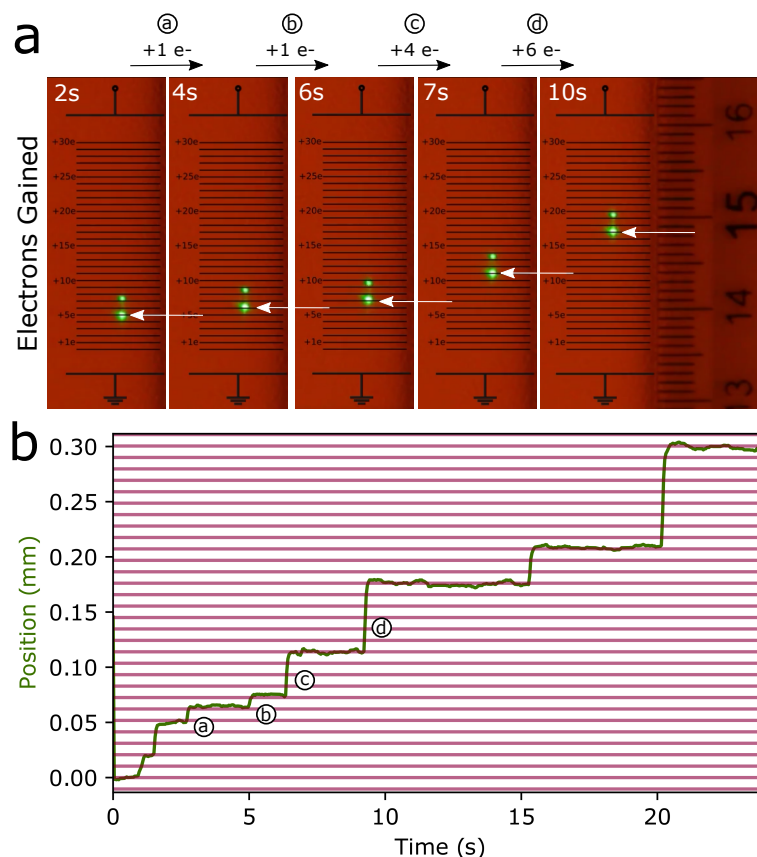


Figure 5.5: Visualization and quantification of the quantized charge of the electron. Upper, **a**: Captured images of droplet position due to, charge additions of (a) +1e, (b) +1e, (c) +4e, and (d) +6e. Black horizontal lines mark the displacement caused by a single electron addition and are set to the lower bright image of the droplet. The last image to the right shows a millimeter ruler that had been attached to the wall. Lower, **b**: The displacement of the droplet (green) calculated from the video of the projected droplet image displacement on the wall. Distance between red lines visualizes the corresponding jump of the known charge of an electron.

5.4 Zoom-independent volume measurements calibrated by acoustic field (Paper IV)

This paper describes a self-calibrating method for measuring the volume of levitated droplets in a single-axis acoustic trap. A match between the real trap and a simulation of the trap enabled this. The method showed similar performance in the precision of volume measurements as a standard method and it was demonstrated to function during evaporation (see the upper figure in Fig. 5.6). Lower figures

indicate that the perceptual differences between the two methods are mainly attributed to oscillations in the inter-droplet distance. Furthermore, the novelty of zoom-independent measurements was realized. This is shown in Fig. 5.7 where eight different zooms were used during measurements of a single droplet's unaltered volume. The red line in the upper figure is droplet volume measured by the new and zoom-independent method. The blue line shows how a standard method performs on volume measurements of the same droplet during the different zooms.

The demonstrated measurements were made from images either in real-time or from a video recording, so the volume can be monitored and timestamped. The method can be used along with collected data from other parts of an experimental setup within fields such as trace analysis using spectroscopy, chemical micro-analysis, and evaporation studies.

Compared to a conventional method (with $d = 1 \text{ mm} \pm 0.02 \text{ mm}$ spheres), the results show that a similar precision can be achieved when measuring the volume ($\pm 1.5\%$) in the range of 1.5 nl to 2 μl . The self-calibrating nature gives researchers a previously unknown ability to zoom in and out or reconfigure the experiment without the need to re-calibrate.

Summary

A new method has been developed and demonstrated that it is possible to calibrate an acoustic trap quickly and accurately even during measurements. The strength is that camera pixel size is against a distance in the acoustic field and becomes zoom-independent. The method is based on simulating the selected trap and then performing a sequential measurement of two trapped droplets. The method differs from others, such as optical diffraction patterns and standard image analysis, which rely on fixed geometries in the experimental setup as this means that each change requires a new calibration. The method described in this section lacks this drawback.

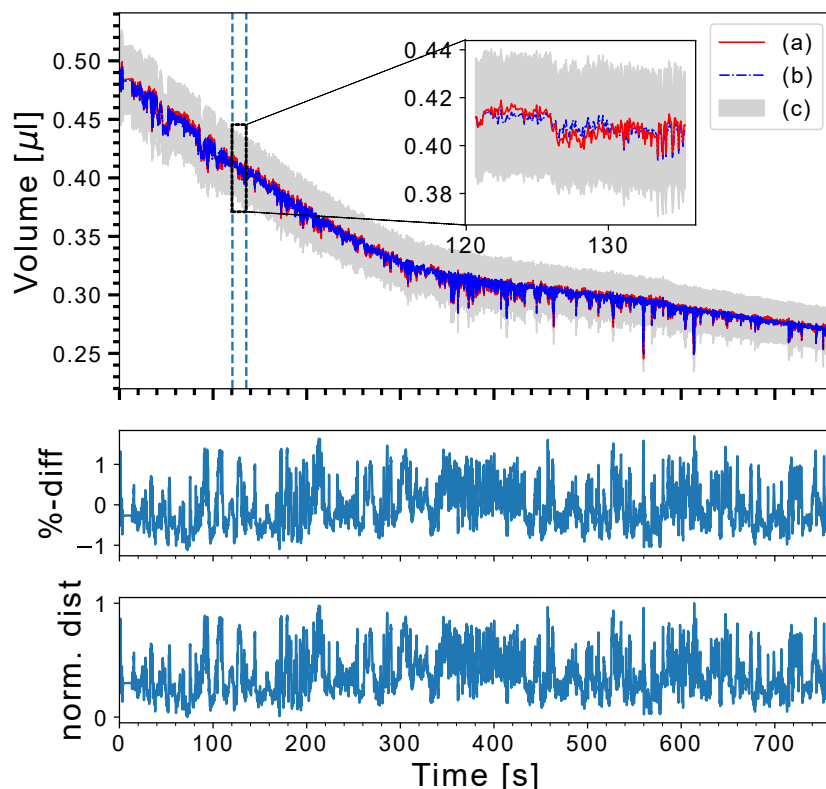


Figure 5.6: A trapped water-oil mixture droplet is evaporating for 763 seconds. Upper: Line (a) is droplet volume calculated using the presented method. Line (b) is the droplet volume calculated by an average from the calibration spheres. The shaded grey area (c) is the corresponding confidence interval boundary from the calibration spheres ($d = 1.00 \pm 0.02$ mm) converted to volume. The red line and the blue line is overlapping almost perfectly. Inset: A smaller interval corresponding to data (200 frames) between the two vertical blue dashed lines, showing small oscillations of volume measurement using the new method around the volume measurements of the standard method. Middle: The percentage difference between the two methods. The variations are of similar order during the entire time as the droplet is losing about half of its volume. Lower: Normalized distance between the two droplets. The oscillations of the inter-droplet distance are the major cause of the larger variations of volume measurements as compared to the standard method, seen above.

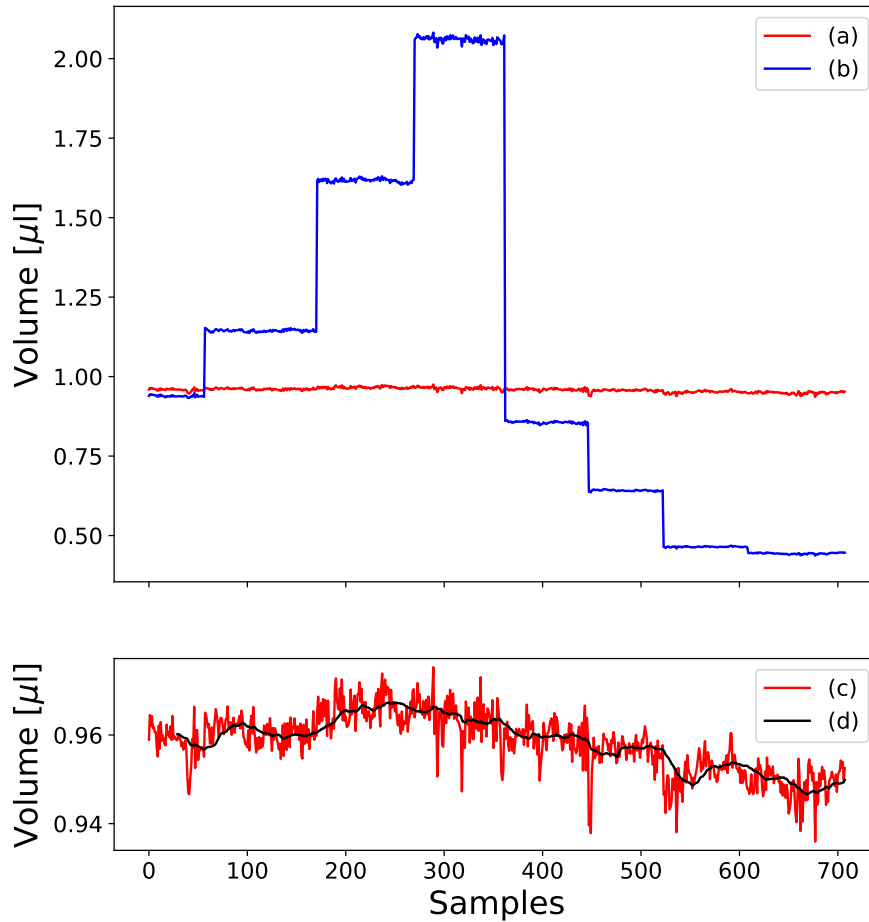


Figure 5.7: The zoom-independent self-calibration is demonstrated. The effects of zooming in and out while measuring droplet volume are negligible. Upper: Oil drop volume measurement using eight different camera zooms. Line (a) is the droplet volume calculated by the presented method. Line (b) is droplet volume as calculated using a pixel-to-millimeter ratio from the average of several $1 \text{ mm} \pm 0.02 \text{ mm}$ calibration spheres for the first of the eight zooms. Lower: Line (c) is zoom-in on droplet volume calculated using the presented method. Line (d) is a moving average of the last 30 frames.

Conclusion and Outlook

This chapter, is dedicated to answer the research questions posed at the end of the introduction of this thesis:

Are students' conceptual knowledge increased as the teacher uses an experimental setup to visualize particle movement in electrical fields directly or via a movie clip, compared to a classical lesson without any experiment available?

In Section 5.1 (Paper I), results from a pilot study measuring students' conceptual knowledge, in three groups (live experiment, video experiment, no experiment), before and after an intervention lesson, is presented. A positive effect of each lesson was recorded, but the groups taught with a demonstration experiment, either live or on video, learned more. The effects of demonstration with live experiment and video experiment were of similar magnitude. Floor and ceiling effects on the tests were noted and therefore the results are preliminary and the tests need to be extended to increase reliability.

In conclusion, indicative results present that experiments visualizing particle movements in electrical fields, either live or videotaped, can enhance students' conceptual learning during a lecture as compared to lectures without such visualizations, but more research is needed.

How can experiments to visualize important physical phenomena, but with expensive or inappropriate equipment, be made available to use in a classroom?

In Section 5.2 (Paper II), an optical trap experiment, with a high-power laser and a high voltage (1kV) power supply was safely operated by students from a Swedish

upper secondary school. It was realized by enabling remote control, and monitoring of the experiment, as well as providing the teacher with a detailed protocol. The students were through the remote visual experience able to manipulate and make measurements of the size, mass, and charge of an optically levitated droplet.

Remote labs can, to conclude, provide opportunities to let students operate experiments with hazardous or expensive equipment that is used to manipulate and visualize important physical phenomena such as optical levitation of charged droplets.

Can the quantization of the elementary charge be visualized directly to the students?

Section 5.3 (Paper III), presented an experiment able to visualize the quantization of the electron's charge as "jumps" in the projected image of an optically levitated droplet. The magnified projection could be seen with the naked eye. The experiment also verified that single electron impacts were observed by balancing the forces from a surrounding electric field and the optical force on the trapped droplet.

Although observations of quantum phenomena in the macroscopic world are rare, the presented experiment can, in conclusion, add the quantization of the elementary charge to that list to be used by teachers and students.

Can self-calibration of volume measurements of acoustically trapped liquid droplets be realized using low-cost equipment?

Standard image analysis methods levitate precision produced spherical calibration beads in the trap, to calibrate the pixel-to-millimeter ratio (scale factor) of the camera at a fixed distance and with a fixed zoom, to measure the size and volume of levitated objects. In Section 5.4 (Paper IV), a simulation of the acoustic field was matched with the real trap and used to automatically obtain a calibrated scale factor used to determine trapped liquid droplet volumes via image analysis. Furthermore, an iterative process to establish a match between the simulation and the real trap was presented. Volume measurements with similar precision as standard image analysis and robustness during alterations in driving voltage, droplet size, camera zoom, and camera distance were achieved. The novel method used equipment available for many schools; a 3D-printed acoustic trap with low-cost transducers, a function generator, a standard web camera with a zoom objective on a 3D-printed mount, and a LED.

To conclude, self-calibrated volume measurements in acoustic levitation can indeed be realized with low-cost equipment.

Outlook

With these four questions answered, I will finish this thesis by outlining the remaining time of my graduate studies. I will focus my efforts on PER research and design learning activities based on students' observation of and engagement with the physical phenomena from the three presented experimental setups, either live, remote, or via video. Based on the pilot study, a larger number of test questions will be used and a larger number of participants will be involved to investigate, in a design-based approach with the addition of interviews and classroom observations, whether variation theory can make video observation and/or live observation provide similar bases for the construction of students' mental models during learning activities. I also want to study remote labs as a tool, with a comparative study between Swedish and Mexican education. The acoustic trap is a possible experiment to be connected online and used for learning activities in a remote classroom in such a study.

Bibliography

1. Fraser, J. M. *et al.* Teaching and physics education research: bridging the gap. *Reports on Progress in Physics* **77**, 032401 (2014).
2. Redish, E. F. Implications of cognitive studies for teaching physics. *American Journal of Physics* **62**, 796–803 (1994).
3. Deslauriers, L., Schelew, E. & Wieman, C. Improved learning in a large-enrollment physics class. *science* **332**, 862–864 (2011).
4. Wieman, C. *Change: The Magazine of Higher Learning Why Not Try a Scientific Approach to Science Education?* 2010.
5. Docktor, J. L. & Mestre, J. P. Synthesis of discipline-based education research in physics. *Physical Review Special Topics-Physics Education Research* **10**, 020119 (2014).
6. Etkina, E. & Van Heuvelen, A. Investigative science learning environment—A science process approach to learning physics. *Research-based reform of university physics* **1**, 1–48 (2007).
7. Gericke, N., Högström, P. & Wallin, J. A systematic review of research on laboratory work in secondary school. *Studies in Science Education* **0**, 1–41 (2022).
8. Bewley, G. P., Lathrop, D. P. & Sreenivasan, K. R. Visualization of quantized vortices. *Nature* **441**, 588–588 (2006).
9. Cheuk, L. W. *et al.* Observation of collisions between two ultracold ground-state CaF molecules. *Physical review letters* **125**, 043401 (2020).
10. Deli'c, U. *et al.* Cooling of a levitated nanoparticle to the motional quantum ground state. *Science* **367**, 892–895 (2020).
11. Etkina, E., Brookes, D. & Planinsic, G. *The investigative science learning environment (ISLE) approach to learning physics* in *Journal of Physics: Conference Series* **1882** (2021), 012001.

Bibliography

12. Skolverket. *Fysik*
<https://www.skolverket.se/undervisning/gymnasieskolan/laroplan-program-och-amnen-i-gymnasieskolan/gymnasieprogrammen/amne?url=1530314731>. 2022-10-24.
13. Thomson, J. J. XL. Cathode rays. *The London, Edinburgh, and Dublin Philosophical Magazine and Journal of Science* **44**, 293–316 (1897).
14. Webb, J. I. P. The fine-beam cathode-ray tube and the observant and enquiring student part 8. *The Physics Teacher* **23**, 277–282 (1985).
15. Ashkin, A. & Dziedzic, J. Optical levitation by radiation pressure. *Applied Physics Letters* **19**, 283–285 (1971).
16. Trinh, E. H. Compact acoustic levitation device for studies in fluid dynamics and material science in the laboratory and microgravity. *Review of Scientific Instruments* **56**, 2059 (1985).
17. Fang, Z., Huang, X., Taslim, M. E. & Wan, K.-t. Flexural bending resonance of acoustically levitated glycerol droplet. *Physics of Fluids* **33**, 071701 (2021).
18. Leiterer, J., Delißen, F., Emmerling, F., Thünemann, A. F. & Panne, U. Structure analysis using acoustically levitated droplets. *Analytical and Bioanalytical Chemistry* *2008 391:4* **391**, 1221–1228 (4 Mar. 2008).
19. Yang, T.-H., Yang, H.-C., Chang, C.-H., Prabhu, G. R. D. & Urban, P. L. Microanalysis Using Acoustically Actuated Droplets Pinned Onto a Thread. *IEEE Access* **7**, 154743–154749 (2019).
20. Marzo, A., Barnes, A. & Drinkwater, B. W. TinyLev: A multi-emitter single-axis acoustic levitator. *Review of Scientific Instruments* **88**, 085105 (8 Aug. 2017).
21. Schappe, R. S. & Barbosa, C. A Simple, Inexpensive Acoustic Levitation Apparatus. *The Physics Teacher* **55**, 6–7 (1 Jan. 2017).
22. Sever, S., Oguz-Unver, A. & Yurumezoglu, K. The effective presentation of inquiry-based classroom experiments using teaching strategies that employ video and demonstration methods. *Australasian Journal of Educational Technology* **29**, 450–463 (3 2013).
23. Kestin, G., Miller, K., McCarty, L. S., Callaghan, K. & Deslauriers, L. Comparing the effectiveness of online versus live lecture demonstrations. *Physical Review Physics Education Research* **16**, 013101 (2020).
24. Del Alamo, J. *et al.* *The MIT microelectronics weblab: A web-enabled remote laboratory for microelectronic device characterization in World Congress on Networked Learning in a Global Environment, Berlin (Germany)* (2002).

25. Ling Lo, M. *Variation theory and the improvement of teaching and learning* (Göteborg: Acta Universitatis Gothoburgensis, 2012).
26. Bowden, J. A. & Walsh, E. *Phenomenography* (RMIT University Press, 2000).
27. Marton, F. & Booth, S. *Learning and awareness* (Routledge, 2013).
28. Marton, F. *Necessary conditions of learning* (Routledge, 2014).
29. Pang, M. F. & Ki, W. W. Revisiting the idea of “critical aspects”: *Scandinavian Journal of Educational Research* **60**, 323–336 (2016).
30. Kullberg, A., Vikström, A. & Runesson, U. Mechanisms enabling knowledge production in learning study. *International Journal for Lesson and Learning Studies* **9**, 78–91 (2019).
31. Pang, M.-F. & Marton, F. Learning theory as teaching resource: Enhancing students’ understanding of economic concepts. *Instructional science* **33**, 159–191 (2005).
32. Zull, J. E. *The art of changing the brain: Enriching the practice of teaching by exploring the biology of learning* (Stylus Publishing, LLC, 2020).
33. Li, J. *et al.* Set-shifting ability is specifically linked to high-school science and math achievement in Chinese adolescents. *PsyCh Journal* **9**, 327–338 (2020).
34. Houdé, O. *et al.* Shifting from the perceptual brain to the logical brain: The neural impact of cognitive inhibition training. *Journal of cognitive neuroscience* **12**, 721–728 (2000).
35. Foisy, L.-M. B., Potvin, P., Riopel, M. & Masson, S. Is inhibition involved in overcoming a common physics misconception in mechanics? *Trends in Neuroscience and Education* **4**, 26–36 (2015).
36. Nieoullon, A. Dopamine and the regulation of cognition and attention. *Progress in neurobiology* **67**, 53–83 (2002).
37. Logue, S. F. & Gould, T. J. The neural and genetic basis of executive function: attention, cognitive flexibility, and response inhibition. *Pharmacology Biochemistry and Behavior* **123**, 45–54 (2014).
38. Bandura, A. Social Cognitive Theory of Mass Communication. *Media Psychology* **3**, 265–299 (3 2001).
39. Luria, E., Shalom, M. & Levy, D. A. Cognitive Neuroscience Perspectives on Motivation and Learning: Revisiting Self-Determination Theory. *Mind, Brain, and Education* **15**, 5–17 (1 Feb. 2021).
40. Pezzulo, G. & Castelfranchi, C. *Intentional action: from anticipation to goal-directed behavior* 2009.

Bibliography

41. Beilock, S. L. & DeCaro, M. S. From poor performance to success under stress: working memory, strategy selection, and mathematical problem solving under pressure. *Journal of Experimental Psychology: Learning, Memory, and Cognition* **33**, 983 (2007).
42. Vosniadou, S. *et al.* *Executive Functions and Conceptual Change in Science and Mathematics Learning*. in *CogSci* (2015).
43. Rhodes, S. M. *et al.* Executive functions predict conceptual learning of science. *British Journal of Developmental Psychology* **34**, 261–275 (2016).
44. Bascandziev, I., Powell, L. J., Harris, P. L. & Carey, S. A role for executive functions in explanatory understanding of the physical world. *Cognitive Development* **39**, 71–85 (2016).
45. Abdullah, M. N. S., Karpudewan, M. & Tanimale, B. M. Executive function of the brain and its influences on understanding of physics concept. *Trends in Neuroscience and Education* **24**, 100159 (2021).
46. Cheng, S. C., She, H. C. & Huang, L. Y. The Impact of Problem-Solving Instruction on Middle School Students' Physical Science Learning: Interplays of Knowledge, Reasoning, and Problem Solving. *Eurasia Journal of Mathematics, Science and Technology Education* **14**, 731–743 (3 Nov. 2017).
47. Walker, M. P. The Role of Slow Wave Sleep in Memory Processing. *Journal of Clinical Sleep Medicine : JCSM : Official Publication of the American Academy of Sleep Medicine* **5**, S20 (2 Suppl Apr. 2009).
48. Hendrikse, J. *et al.* Regular aerobic exercise is positively associated with hippocampal structure and function in young and middle-aged adults. *Hippocampus* **32**, 137–152 (3 Mar. 2022).
49. Sapey-Triomphe, L. A. *et al.* Ventral stream hierarchy underlying perceptual organization in adolescents with autism. *NeuroImage: Clinical* **25**, 102197 (Jan. 2020).
50. Richter, D. & de Lange, F. P. Statistical learning attenuates visual activity only for attended stimuli. *Elife* **8**, e47869 (2019).
51. Redish, E. F. *Oersted Lecture 2013: How should we think about how our students think?* 2014.
52. Goodman, J. Place vs. Response learning: History, controversy, and neurobiology. *Frontiers in Behavioral Neuroscience* **14**, 598570 (2021).
53. Regt, H. W. D. Visualization as a Tool for Understanding. *Perspectives on Science* **22**, 377–396 (3 2014).
54. Black, M. *Models and metaphors: Studies in language and philosophy.* (1962).

55. Johnson-Laird, P. N. Mental models in cognitive science. *Cognitive science* **4**, 71–115 (1980).
56. Crouch, C. H. & Mazur, E. Peer instruction: Ten years of experience and results. *American journal of physics* **69**, 970–977 (2001).
57. Hanfstingl, B., Arzenšek, A., Apschner, J. & Göllly, K. I. Assimilation and Accommodation: A Systematic Review of the Last Two Decades. *European Psychologist* **27** (Nov. 2021).
58. Hammer, D. Force concept inventory The Physics Teacher. *Students' preconceptions in introductory mechanics American Journal of Physics* **64**, 66 (1996).
59. Wood, D., Bruner, J. S. & Ross, G. The role of tutoring in problem solving. *Child Psychology & Psychiatry & Allied Disciplines* (1976).
60. Margolis, A. A. Zone of proximal development, scaffolding and teaching practice. *Cultural-Historical Psychology* **16**, 15–26 (2020).
61. Vygotsky, L. The development of everyday and scientific concepts in school age. *Psychol. Sci. Educ* **1**, 5–16 (1996).
62. Gess-Newsome, J. in *Examining pedagogical content knowledge* 3–17 (Springer, 1999).
63. Arons, A. B. Student patterns of thinking and reasoning. *The Physics Teacher* **22**, 21–26 (1984).
64. Paul, W. Electromagnetic traps for charged and neutral particles. *Reviews of modern physics* **62**, 531 (1990).
65. Paul, W. Electromagnetic traps for charged and neutral particles (Nobel lecture). *Angewandte Chemie International Edition in English* **29**, 739–748 (1990).
66. Andrade, M. A., Bernassau, A. L. & Adamowski, J. C. Acoustic levitation of a large solid sphere. *Applied Physics Letters* **109**, 044101 (2016).
67. Andrade, M. A., Okina, F. T., Bernassau, A. L. & Adamowski, J. C. Acoustic levitation of an object larger than the acoustic wavelength. *The Journal of the Acoustical Society of America* **141**, 4148–4154 (2017).
68. Zang, D. *et al.* Acoustic levitation of soap bubbles in air: Beyond the half-wavelength limit of sound. *Applied Physics Letters* **110**, 121602 (2017).
69. Röthlisberger, M., Schmidli, G., Schuck, M. & Kolar, J. W. Multi-Frequency Acoustic Levitation and Trapping of Particles in All Degrees of Freedom. *IEEE Transactions on Ultrasonics, Ferroelectrics, and Frequency Control* **69**, 1572–1575 (2022).
70. Contreras, V. & Marzo, A. Adjusting single-axis acoustic levitators in real time using rainbow schlieren deflectometry. *Review of Scientific Instruments* **92**, 015107 (1 Jan. 2021).

Bibliography

71. Santesson, S. & Nilsson, S. Airborne chemistry: acoustic levitation in chemical analysis. *Analytical and bioanalytical chemistry* **378**, 1704–1709 (2004).
72. Baer, S. *et al.* Analysis of the particle stability in a new designed ultrasonic levitation device. *Review of Scientific Instruments* **82**, 105111 (10 Oct. 2011).
73. Marzo, A. *et al.* Holographic acoustic elements for manipulation of levitated objects. *Nature Communications* **6** (Oct. 2015).
74. Marzo, A., Corkett, T. & Drinkwater, B. W. Ultraino: An open phased-array system for narrowband airborne ultrasound transmission. *IEEE transactions on ultrasonics, ferroelectrics, and frequency control* **65**, 102–111 (2017).
75. P., G. L. On the forces acting on a small particle in an acoustical field in an ideal fluid. *Sov. Phys. Dokl.* **6**, 773–775 (1962).
76. Andrade, M. A., Pérez, N. & Adamowski, J. C. Review of progress in acoustic levitation. *Brazilian Journal of Physics* **48**, 190–213 (2018).
77. Isaksson, O., Karlsteen, M., Rostedt, M. & Hanstorp, D. *Manipulation of optically levitated particles* in *Optical Trapping and Optical Micromanipulation X* (eds Dholakia, K. & Spalding, G. C.) **8810** (SPIE, 2013), 88100O.
78. Marx, J. D. *Creation of a diagnostic exam for introductory, undergraduate electricity and magnetism* (Rensselaer Polytechnic Institute, 1998).
79. Hake, R. R. Interactive-engagement versus traditional methods: A six-thousand-student survey of mechanics test data for introductory physics courses. *American journal of Physics* **66**, 64–74 (1998).
80. Marx, J. D. & Cummings, K. Normalized change. *American Journal of Physics* **75**, 87–91 (2007).

Appended papers



**Charged liquid droplets in
electromagnetic fields - An
experiment for developing
conceptual understanding during
student activity**

Max 500 ord (<http://events.saip.org.za/conferenceDisplay.py?confid=93>)

Authors: Andreas Johansson, Dag Hanstorp, Ingela Bursjö and Jonas Enger,

Titel: Charged liquid droplets in electromagnetic fields - An experiment for developing conceptual understanding during student activity

Concepts for the students to learn in this experimental setup:

Electric Fields, Electric Force, Electric Charge, Motion in electric fields, Newton's laws

Introduction

What is the relative impact on learning when the abstraction in lessons changes?

Things that are too small to be seen by the human eye need to be visualized to be well understood. Visualisations can be realized with digital tools but at the cost of introducing a higher level of abstraction. The visualizations could also be made by observing and experimenting with an analog macroscopic object that behaves in a similar way as the object of study, and this is the main idea behind the experiment presented in this work.

We limit our study to scientific questions, whereas social factors affecting learning in the lab is left for future studies.

Research questions

What can students learn about the concepts and properties of electric fields, electric charge, electric force, Newton's laws while building their experience on direct observations of charged droplets moving through electric fields?

What kind of teaching, such as direct observations during experiments, pre-recorded videos of experiments or classical theoretical studies with literature and lectures, presents the subject in a way that enables the students to learn efficiently, which we interpret as students having obtained long-term knowledge of the subject matter.

Physical experimental setup

During the study, an experimental setup was used to teach the above mentioned concepts. The experimental set-up consist of: charged macroscopic liquid droplets that fall through an electric field that can be controlled by the observer. This gives the students the opportunity to experience ideas and concepts that otherwise only appear as particle-motion exercises in the Physics textbook. When illuminated by a strong light-diode the 20 microns in diameter droplets are made visible for the human eye. By a simple web-camera we can directly record and observe the motion of of the droplet as it moves a curved path in an electric field created.

Students are able to change a number of parameters and simultaneously observe how the changes affects the paths of the droplets. We investigate in this study how work with this experimental system affects the learning of the students.

Design of Study

All students performed a pre-test.

Three groups of students got an equal amount of teaching-time:

Group one: Short introduction to the concepts in the lab while the teacher uses the experimental setup as a teaching tool. Students can interact with the setup.

Group two: Short introduction while the teacher is showing a short video of the experiment. Held in ordinary classroom.

Group three: A theoretical lecture about the concepts in an ordinary classroom.

All three groups then received the same task: "Design an experiment where a charge droplet will move in a circle." This task was conducted in groups of two or three students.

All these lessons were recorded with video cameras.

The post-test was given within two weeks after the lessons.

We will discuss our first results and give suggestions for further studies to improve both the understanding of the teaching situation and the knowledge gained by the students.



Safe experimentation in optical levitation of charged droplets using remote labs

Video Article

Safe Experimentation in Optical Levitation of Charged Droplets Using Remote Labs

Daniel Galán¹, Oscar Isaksson², Jonas Enger², Mats Rostedt², Andreas Johansson², Dag Hanstorp², Luis de la Torre¹

¹Departamento de Informática y Automática, UNED

²Department of Physics, University of Gothenburg

Correspondence to: Daniel Galán at dgalan@dia.uned.es

URL: <https://www.jove.com/video/58699>

DOI: [doi:10.3791/58699](https://doi.org/10.3791/58699)

Keywords: Engineering, Issue 143, Optical Levitation, Remote Laboratory, Laser, Photon Pressure, Diffraction, Electrical Fields, Liquid Droplets

Date Published: 1/10/2019

Citation: Galán, D., Isaksson, O., Enger, J., Rostedt, M., Johansson, A., Hanstorp, D., de la Torre, L. Safe Experimentation in Optical Levitation of Charged Droplets Using Remote Labs. *J. Vis. Exp.* (143), e58699, doi:10.3791/58699 (2019).

Abstract

The work presents an experiment that allows the study of many fundamental physical processes, such as photon pressure, diffraction of light or the motion of charged particles in electrical fields. In this experiment, a focused laser beam pointing upwards levitate liquid droplets. The droplets are levitated by the photon pressure of the focused laser beam which balances the gravitational force. The diffraction pattern created when illuminated with laser light can help measure the size of a trapped droplet. The charge of the trapped droplet can be determined by studying its motion when a vertically directed electrical field is applied. There are several reasons motivating this experiment to be remotely controlled. The investments required for the setup exceeds the amount normally available in undergraduate teaching laboratories. The experiment requires a laser of Class 4, which is harmful to both skin and eyes and the experiment uses voltages that are harmful.

Video Link

The video component of this article can be found at <https://www.jove.com/video/58699/>

Introduction

The fact that light carries momentum was first suggested by Kepler when he explained why the tail of a comet always points away from the sun. The use of a laser to move and trap macroscopic objects was first reported by A. Ashkin and J. M. Dziedzic in 1971 when they demonstrated that it is possible to levitate micrometer sized dielectric objects¹. The trapped object was exposed to an upward directed laser beam. Part of the laser beam was reflected on the object which imposed a radiation pressure on it that was sufficient to counterbalance gravity. Most of the light, however, was refracted through the dielectric object. The change of the direction of the light causes a recoil of the object. The net effect of the recoil for a particle placed in a Gaussian beam profile is that the droplet will move towards the region of highest light intensity². Hence, a stable trapping position is created in the center of the laser beam at a position slightly above the focal point where radiation pressure balances gravity.

Since the optical levitation method allows small objects to be trapped and controlled without being in contact with any objects, different physical phenomena can be studied using a levitated droplet. However, the experiment presents two limitations to be reproduced and applied at schools or universities since not all institutions can afford the required equipment and since there are certain risks in the hands-on operation of the laser.

Remote laboratories (RLs) offer online remote access to the real laboratory equipment for experimental activities. RLs first appeared at the end of the 90s, with the advent of the Internet, and their importance and use have been growing over the years, as the technology has progressed and some of their major concerns have been solved³. However, the core of RLs has remained the same over time: the use of an electronic device with Internet connection to access a lab, and control and monitor an experiment.

Due to their remote nature, RLs can be used to offer experimental activities to users without exposing them to the risks that may be associated with the realization of such experiments. These tools allow students to spend more time working with laboratory equipment, and hence develop better laboratory skills. Other advantages of RLs are that they 1) facilitate for handicapped people to perform experimental work, 2) expand the catalog of experiments offered to students by sharing RLs between universities and 3) increase the flexibility in scheduling laboratory work, since it can be performed from home when a physical laboratory is closed. Finally, RLs also offer training in operating computer-controlled systems, which nowadays are an important part of research, development and industry. Therefore, RLs cannot only offer a solution to both the financial and safety issues that traditional labs present, but also provide more interesting experimental opportunities.

With the experimental setup used in this work, it is possible to measure the size and charge of a trapped droplet, investigate the motion of charged particles in electric fields and analyze how a radioactive source can be used to change the charge on a droplet⁴.

In the experimental setup presented, a powerful laser is directed upwards and focused into the center of a glass cell⁴. The laser is a 2 W 532 nm diode-pumped solid-state laser (CW), where usually about 1 Watt (W) is used. The focal length of the trapping lens is 3.0 cm. Droplets are generated with a piezo droplet dispenser and descend through the laser beam until they are trapped just above the focus of the laser. Trapping

occurs when the force from the upward directed radiation pressure is equal to the downward directed gravitational force. There is no upper time limit observed for trapping. The longest time a droplet has been trapped is 9 hours, thereafter, the trap was turned off. The interaction between the droplet and the laser field produces a diffraction pattern which is used to determine the size of the droplets.

The droplets emitted from the dispenser consist of 10% glycerol and 90% water. The water part quickly evaporates, leaving a 20 to 30 μm sized glycerol droplet in the trap. The maximum size of a droplet that can be trapped is about 40 μm . There is no evaporation observed after about 10 s. At this point, all water is expected to have evaporated. The long trapping time without any observable evaporation indicates that there is minimal absorption and that the droplet essentially is at room temperature. The surface tension of the droplets makes them spherical. The charge of the droplets generated by the droplet dispenser depends on the environmental conditions in the laboratory, where they most commonly become negatively charged. The top and the bottom of the trapping cell consists of two electrodes placed 25 mm apart. They can be used to apply a vertical electric direct current (DC) or alternating current (AC) field over the droplet. The electric field is not strong enough to create any arcs even if 1000 volts (V) is applied over the electrodes. If a DC field is used, the droplet moves up or down in the laser beam to a new stable equilibrium position. If an AC field is applied instead, the droplet oscillates around its equilibrium position. The magnitude of the oscillations depends on the size and charge of the droplet, on the intensity of the electric field, and on the stiffness of the laser trap. An image of the droplet is projected onto a position-sensitive detector (PSD), which allows users to track the vertical position of the droplet.

This work presents a successful initiative of modernizing teaching and research using Information and Communication Technologies through an innovative RL on optical levitation of charged droplets which illustrates modern concepts in physics. **Figure 1** shows the architecture of the RL. **Table 1** shows the possible injuries that lasers can cause according to their class; In this setup, a Class IV laser has been used, which is the most dangerous one. It can operate with up to 2.0 W of visible laser radiation, so the safety provided by the remote operation is clearly suitable for this experiment. The optical levitation of charged droplets RL was presented in the work of D. Galan *et al.* in 2018⁵. In this work, it is demonstrated how it can be used online by teachers who want to introduce their students to modern concepts of physics without having to be concerned about the costs, the logistics or the safety issues. Students access the RL through a web portal called University Network of Interactive Laboratories (UNILabs - <https://unilabs.dia.uned.es>) in which they can find all the documentation regarding the theory related to the experiment and the use of the experimental setup by means of a web application. By using the concept of a remote laboratory, experimental work in modern physics that requires costly and dangerous equipment can be made available to new groups of students. Furthermore, it enhances the formal learning by providing traditional students with more laboratory time and with experiments that normally are inaccessible outside research laboratories.

Protocol

NOTE: The laser used in this experiment is a class IV laser delivering up to 1 W of visible laser radiation. All personnel present in the laser laboratory must have conducted adequate laser safety training.

1. Hands-On Experimental Protocol

1. Safety

1. Make sure everyone in the lab is aware that a laser will be turned on.
2. Turn on the laser warning lamp in the lab.
3. Check that no watch or metal rings are worn and put on the laser goggles.
4. Check that the four light absorbing boards, closest to the experiment, are in place.
5. Check the space between the laser and the absorbing board for obstacles. Also check that the space between the trapping cell and the beam block is free from objects.

2. Prepare the software and the experiment.

1. Turn on the lab computer. Wait until it is ready to operate.
2. Open the **Remote Startup** folder from the desktop and click the icon **Main1806.vi**. Run the program by pressing the arrow in the top left corner.
NOTE: This opens the control program (e.g., Labview) shown in **Figure 2** and **Figure 3** and automatically turns on both the power supply for the laser and the electric field. All buttons referenced from now on in this section refer to those that appear in these figures.
3. Under "**EJS variables**", mark the checkbox named "**Laser Remote Enable2**" power and set "**laser current2**" to 25 so that the laser power slide to the right ends up at 25%. Observe the laser beam using alignment laser goggles to make sure that the beam ends up in the beam dump. If not, adjust the position of the beam dump.
4. Check **Drops2** and move the tip of the droplet dispenser until the droplets are falling into the laser beam. Do this by adjusting the translation stage marked with letter A in **Figure 4**. For that purpose, gently turn the driving screws at the base of the translation stage until the desired position is reached.
 1. If no drops are coming, apply some pressure in the syringe until a droplet is shown in the tip of the dispenser. Wipe it off carefully (fragile tip) using a paper with acetone. The droplets should now start coming. When this occurs, start over from point 1.2.4.
5. Raise the laser power to about 66% using the **Laser Current 2** input field and trap a droplet. Uncheck **Drops2** as soon as a droplet is trapped.

NOTE: **Figure 5** shows a droplet captured in the experimental environment. The lower green dot corresponds to the real droplet, while the upper one is its reflection on the glass of the cell in which the droplet is located. From this moment on, it will be The trapped droplet is now imaged onto the PSD.

3. Determine the size of a droplet.

1. Adjust the laser power until the PSD position is as close as possible to zero.
NOTE: As droplets can be trapped below or above previous trapping positions, depending on the laser power or the size/weight. This step is performed to move the droplet image to the center of the PSD.

2. Observe the diffraction pattern created on the screen (see **Figure 1**). Take a picture with the web camera that is positioned to observe the screen from underneath.
NOTE: The pattern is caused by laser light diffracted by the trapped droplet.
3. Use the picture to determine distances from the line marked 1 to two arbitrary minima in the image. The distance is positive if it is further from the droplet than the line marked 1, else negative. Then, add 40 cm to both distances. Call the shortest a_1 , and the longest a_2 . Use Equation 1 to calculate the size of the droplet:

$$d = \frac{\Delta n \cdot \lambda}{\frac{a_2}{\sqrt{x^2 + a_2^2}} - \frac{a_1}{\sqrt{x^2 + a_1^2}}} \quad (1)$$

where, x is the vertical distance from the droplet to the screen ($x = 23.5$ cm), λ is the wavelength of the laser light ($\lambda = 532$ nm) and Δn is the number of fringes (integer) between the two minima used in the calculation.

NOTE: When the droplet is imaged in the middle of the PSD, the distance (x), from the droplet to the screen is 23.5 ± 0.1 cm. A more detailed explanation of the process can be found in the work of J. Swithenbank *et al.*⁶.

4. Determine the polarity of the charge of the droplet.
 1. Choose the tab **run** to the right of **EJS variables** and set the **E-Field DC control2** to +2 V (see **Figure 3**). Be careful, since the voltage on the electrode is now 200 V.
NOTE: The polarity of the droplet charge is determined by observing how the droplet respond to an applied vertical electric field. A sketch of how the electric field is applied can be seen in **Figure 6**
5. Determine the charge of the droplet
NOTE: To calculate the charge of the droplet, it is necessary first to measure the size of the droplet. The weight of the droplet can then be determined since the density of the liquid is known. **Figure 7** describes the procedure schematically.
 1. Set the **E-field DC control2** to zero.
 2. Estimate and note an average value for the position of the droplet by the **PSD Normalize Position** trace in the **Chart Waveform**.
 3. Note the value of the laser power. This value will be F_{Rad1} in Equation 2.
 4. Set the **E-field DC control2** between +1 and +5 Volts or -1 and -5 Volts so that the drop moves upwards. The droplet is now at a new position. Slowly reduce the laser power until the droplet is back in its original position as noted in Step 1.5.2. Write down the new laser power (F_{Rad2}).

If the droplet is lost, check **Drops2** and start over from Step 1.2.4.

5. Use the following procedure to calculate the charge. First, calculate the force from the electric field:

$$F_E = \left(\frac{F_{Rad1} - F_{Rad2}}{F_{Rad1}} \right) F_{mg} \quad (2)$$

6. Determine the absolute charge using the expression

$$Q = \frac{F_E d}{U} \quad (3)$$

Here d is the distance between the electrodes and U is the applied voltage.

2. Remote Experimentation Protocol

1. Access the remote laboratory.
 1. Open UNILabs webpage on a web browser: <https://unilabs.dia.uned.es/>
 2. Select the desired language if needed. The option is found at the first item of the menu under the header.
 3. Log in with the following data:
Username: test
Password: test
NOTE: The login frame is under the news and introduction info of the webpage.
 4. In the course area, next to the login area, left click on the logo of the University of Gothenburg (GU).
 5. Click on **Optical Levitation** to access the material of this experiment.
 6. Access the remote laboratory by clicking on **Remote Laboratory of Optical Levitation**. After that, ensure that the main frame of the webpage show the user interface of the remote laboratory, as shown in **Figure 8**.
2. Connect to the Optical Levitation laboratory.
NOTE: All the instructions here refer to **Figure 8**.
 1. Click on the **Connect** button. If the connection is successful, the button text will change to **Connected**.
NOTE: When a user connects to the remote laboratory, it emits an acoustic signal that warns other people in the surrounding area that someone will power on and manipulate the laser remotely.
 2. Click on **Tracking droplets** and check that the PSD data is being received.
NOTE: As there are no droplets captured at this point, the value obtained is not relevant.
 3. Click on **General view** to identify all elements of the setup: the laser, the droplet dispenser, the trapping cell and the PSD.
3. Trap a droplet.

NOTE: All the instructions here refer to **Figure 8**.

1. Once the remote laboratory is connected, click on the **Trapping droplets** button to visualize the pipette and the droplet dispenser nozzle.
 2. Click on the **Turn on laser** button to establish the connection to the laser.
NOTE: The laser is started manually and independently of the rest of the instruments because it can damage the environment if it is not correctly aligned.
 3. Set the laser power around the first quarter of the control strip, which is situated under the **Turn on laser** button. Wait until the green light is visible.
 4. Check the laser alignment.
NOTE: If the laser is correctly aligned, a thin green light beam will be seen. Otherwise, a scattered green spot will be perceived. In case of incorrect alignment, shut down the system, and contact the lab maintenance services. To contact the maintenance services, click on the icon that represents a speech bubble, located in the upper left corner of UNILabs webpage. Then click on the **Admin user** message, write down the message at the bottom describing the problem and press **Send**. This usually does not happen, since all the optics are fixed.
 5. Increase the laser power to 3/4 of the bar.
NOTE: A power of 60% (550 mW) is enough to capture and keep a droplet levitated.
 6. Press the **Start drops** button to turn on the droplet dispenser.
 7. Watch the webcam image and wait until a flash is produced. At that moment, a droplet has been captured. Check the webcam image again and verify that a droplet is levitating in the center of the trapping cell. Press the **Stop drops** button to turn off the droplet dispenser.
NOTE: Optionally, it is possible to obtain a larger droplet by catching several of them and waiting for them to merge with the one already captured. It is necessary to bear in mind that if several are caught, the droplet mass increases so that the laser power may not be enough to keep it levitated.
4. Determine the size of a droplet.
NOTE: All instructions here refer to **Figure 9**.
1. Press the **Sizing droplets** button to observe the diffraction pattern formed by the trapped droplet.
 2. Follow the same procedure as in the hands-on experimentation protocol (Step 1.3) to determine the size of the droplet by means of the diffraction pattern.
5. Determining the droplet charge polarity.
NOTE: All instructions here refer to **Figure 10**.
1. Click on the **Tracking droplets** button to view the PSD graph and the webcam view of the pipette.
 2. Click on the **Electric Field** tab at the bottom left of the user interface.
 3. Set the DC voltage to 100 V. To do this, click on the numeric field to the right of the **DC (V)** label and enter the value 100.
 4. Check the PSD graph showing the position of the droplet and observe whether the droplet moves upwards or downwards when the electrical field is applied.
NOTE: The polarity of the plates is arranged so that if a positive voltage is applied, a negatively charged droplet will move downwards and a positively charged droplet will move upwards.
 5. Now change the value of the electric field and check that the droplet moves in the opposite direction; for this purpose, enter -100 in the **DC (V)** numeric field.
6. Determine the charge of the droplet.
NOTE: All instructions here refer to **Figure 10**.
1. Having a droplet trapped, click on the **Tracking droplets** view.
 2. Select the **Electric Field** menu.
 3. Set the DC electric field to zero with the **DC (V)** numeric field.
 4. Estimate and note an average value of the droplet position given by the chart and note the laser power.
 5. Set the DC electric field to a value between +500 V and -500 V to make the droplet change its position.
 6. Reduce or increase the laser power with the slider until the droplet is back in its original position and write down the new value of the laser power.
 7. Follow the procedure described in Step 1.5.5 to calculate the droplet charge.

Representative Results

When the laser beam is well aligned, and the bottom plate is clean, the drops are almost immediately trapped. When a droplet is trapped it can stay in the trap for several hours, giving plenty of time for investigations. The radius r of the droplets is in the range of $25 \leq r \leq 35 \mu\text{m}$ and the charge has been measured between $1.1 \times 10^{-17} \pm 1.1 \times 10^{-18} \text{ C}$ and $5.5 \times 10^{-16} \pm 5.5 \times 10^{-17} \text{ C}$. The size of the droplets stays, according to our measurements, constant over time, but the charge will slowly diffuse away, giving smaller and smaller reactions from the position of the droplet when applying an electric field. This gives the user a chance to measure different charges on the same droplet if he or she is patient enough.

The remote laboratory has been developed using Easy Java/JavaScript Simulations⁷ and is accessible via the UNILabs website⁸. As for the local control software of the laboratory, it has been developed using the control software program. The connection of the remote and local software has been developed following the, widely tested, work of D. Chaos *et al.*⁹. The idea of creating a remote laboratory for optical droplet levitation is based on two pillars: 1) to allow researchers from other parts of the world who do not have this setup to work with it and 2) to make this type of experiment available to Physics students.

The environment has been extensively tested both locally and remotely to support the researchers work. It has been shown that droplet capture can take between 2 seconds and 1 minute. This variation is due to pipette cleaning and laser alignment. For this reason, a small amount of maintenance is carried out every day to enable the laboratory to function correctly. Once the droplet has been captured, it can withstand levitating for long periods of time, reaching more than half an hour, a period sufficient to perform all the tasks that the system provides. The fact that several drops can collapse and be trapped, enables users to quickly check the correction of the protocols relating to the calculation of mass and electrical charge, as the difference in the results between two drops collapsed, and a single drop is more significant than if they only compare two unique droplets caught at different moments. In addition, given the stability and reconfigurability of the environment, it serves as a basis for adding new instrumentation and thus enabling new functionality. An example of this fact is an analysis, being carried out nowadays at the University of Gothenburg, to study the influence of radioactive samples on the phenomenon of optical levitation.

The only effective way to allow many students to access this type of experience is through a remote laboratory, mainly for security reasons. Also, research such as that of Lundgren *et al.* shows that students' experience of working with a remote laboratory is as useful as that of a traditional laboratory¹⁰. The environment allows younger students to discover the concept of optical levitation by observing how the laser beam can effectively levitate matter. The teacher can also introduce electric charge to the students by studying the polarity of the droplets. For more advanced students, the calculation of the droplet mass and charge can be included in the work protocol.

This laboratory has been used in a physics class in Halmstad, Sweden, with students from the International Baccalaureate (IB) Diploma Program (www.ibo.org). The teacher followed the remote protocol described in Step 2. After the experience, the students were interviewed by asking them questions about the environment, the measurements made, the underlying physical concepts they had learned, and the benefits and disadvantages they perceived from using the remote laboratory. Overall, the students understood the process followed and calculated the size of the drops, obtaining results close to the real size of the trapped drop. They understood the risks involved in using high-powered lasers, and some suggested adding improvements to the visualization of the experiment, such as buying better cameras or including augmented reality elements.

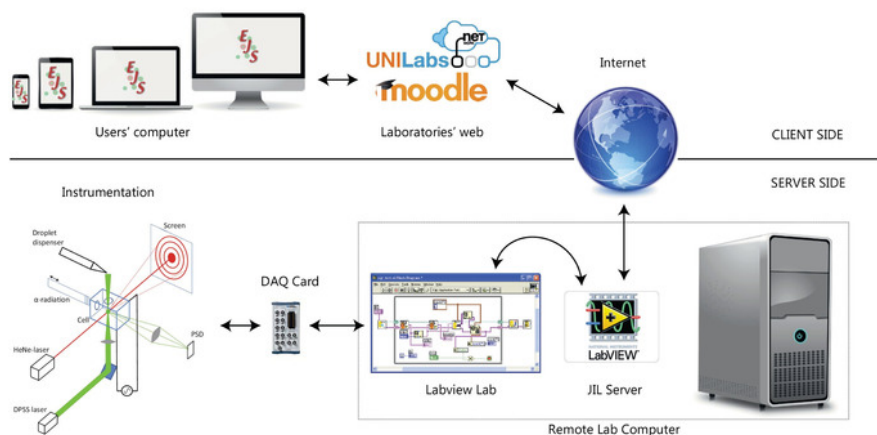


Figure 1: Architecture of the remote laboratory experimentation. Internet users connect to the UNILabs webpage using their computer or mobile devices. The web environment serves the remote lab JavaScript application that allows to remotely operate the experiment. This application connects to a computer located in the laboratory through the JIL server middleware, which enables the communication between JavaScript applications and LabVIEW programs. Finally, the lab computer communicates with the experimental setup using the necessary DAQ cards and a LabVIEW program. [Please click here to view a larger version of this figure.](#)

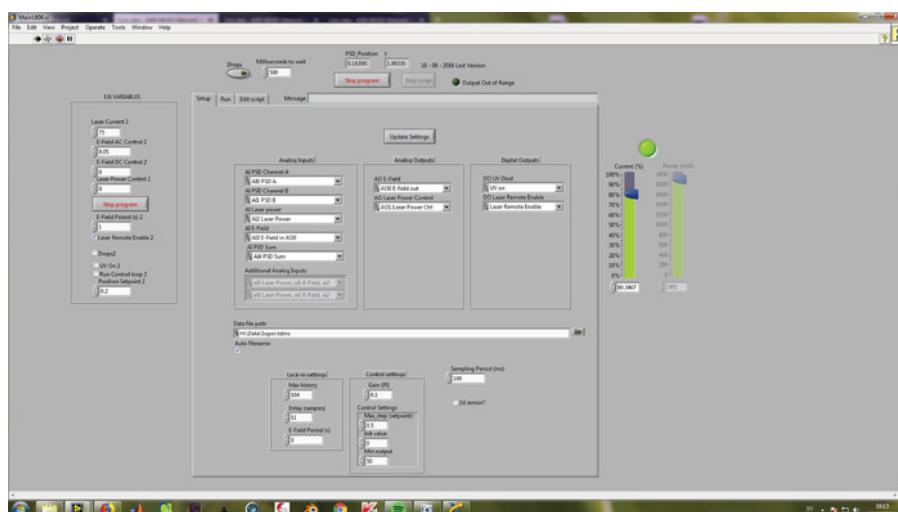


Figure 2: LabVIEW program: Configuration panel. The configuration tab in the LabVIEW program is used in hands-on mode experimentation for starting the experiment by turning on the laser on and starting the droplets. [Please click here to view a larger version of this figure.](#)

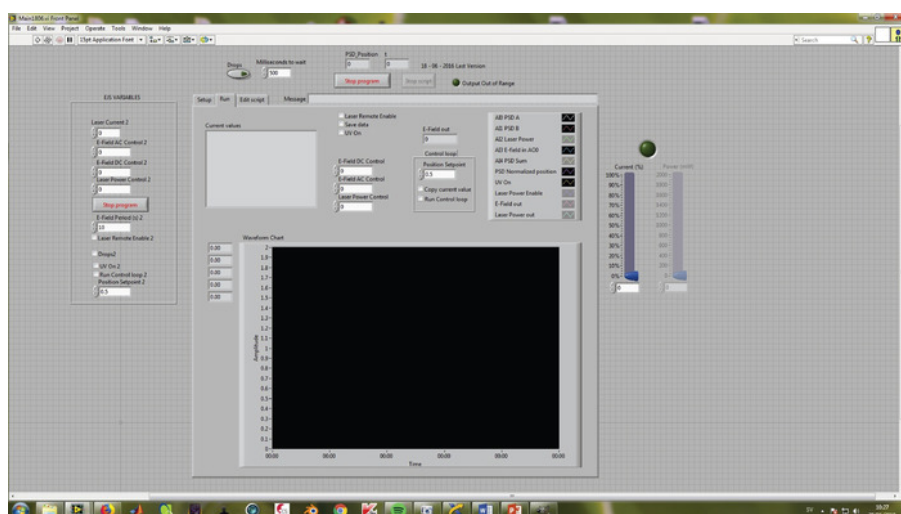


Figure 3: LabView program: Run panel. The configuration tab in the LabView program is used in hands-on mode experimentation for determining the charge of the trapped droplets. [Please click here to view a larger version of this figure.](#)

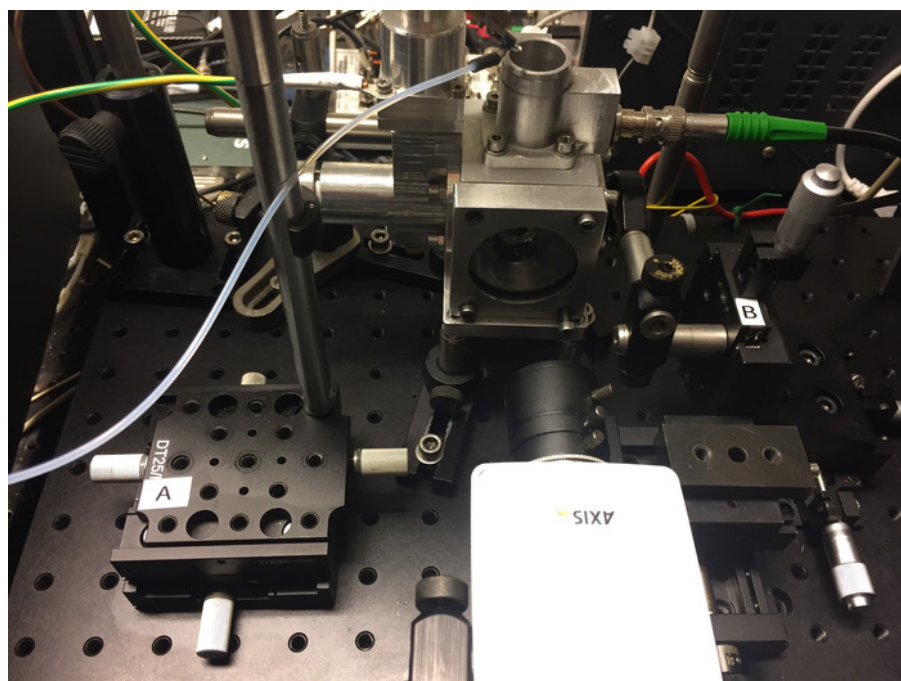


Figure 4: Detail of the experimental setup. The droplet dispenser is shown at the top of the image, the cell in the middle and, at the bottom, the web camera. Letter A: the translation stage used to adjust the position of the dispenser inside the cell. Letter B: The lens used by the PSD to perceive the trapped droplet. [Please click here to view a larger version of this figure.](#)

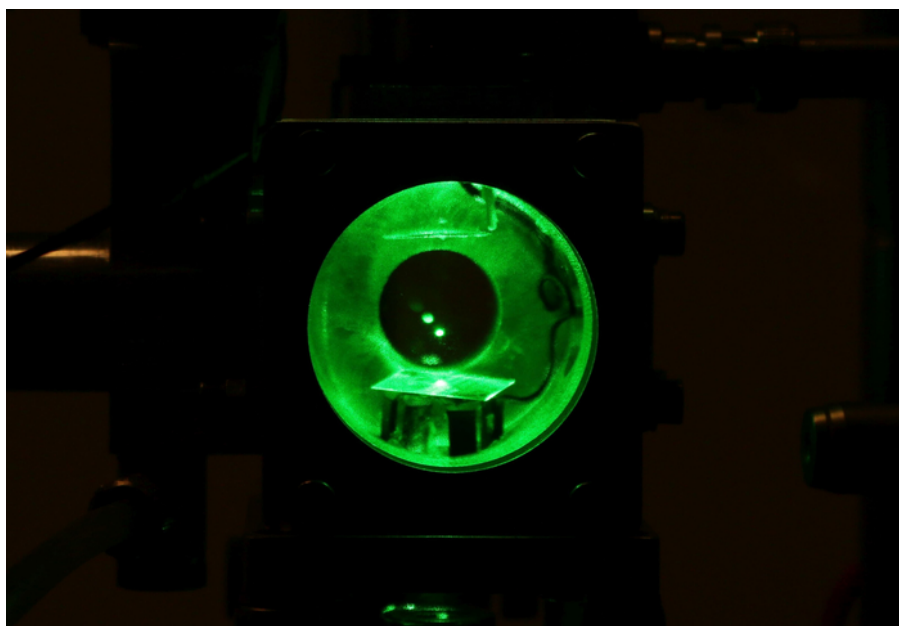


Figure 5: A trapped droplet levitating. In the image it is possible to see one of the droplets levitating inside the cell of the setup. The green color is due to the laser and the fact of seeing two dots instead of one is that the droplet is reflected on the glass of the cell. In this case, the upper point is the reflection and the lower point is the droplet. [Please click here to view a larger version of this figure.](#)

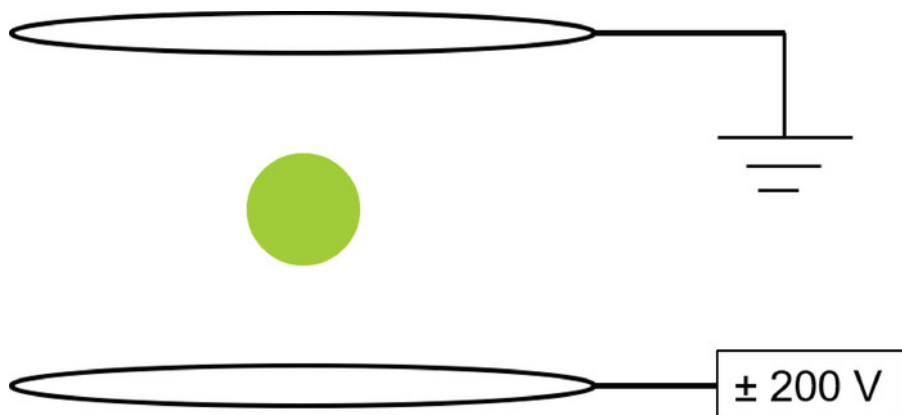


Figure 6: Electrode configuration for applying electrical fields. Experimental setup for applying the electric field onto the droplet. When a positive voltage is applied, negative charged droplets will move downwards and droplets with positive charge will move upwards. [Please click here to view a larger version of this figure.](#)

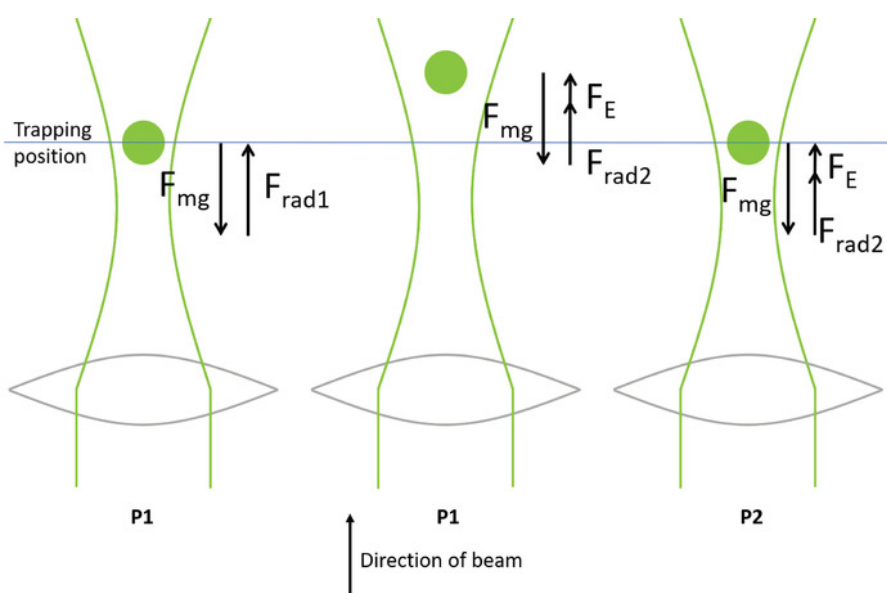


Figure 7: Determination of droplets charge. A schematic sketch of the procedure to determine the absolute charge of an optically levitated droplet. [Please click here to view a larger version of this figure.](#)



Figure 8: Remote lab interface: trapping a droplet. In remote experimentation, this web application interface is used to trap a droplet. A trapped droplet can be seen in the image provided by the lab webcam due to the scattered light. [Please click here to view a larger version of this figure.](#)

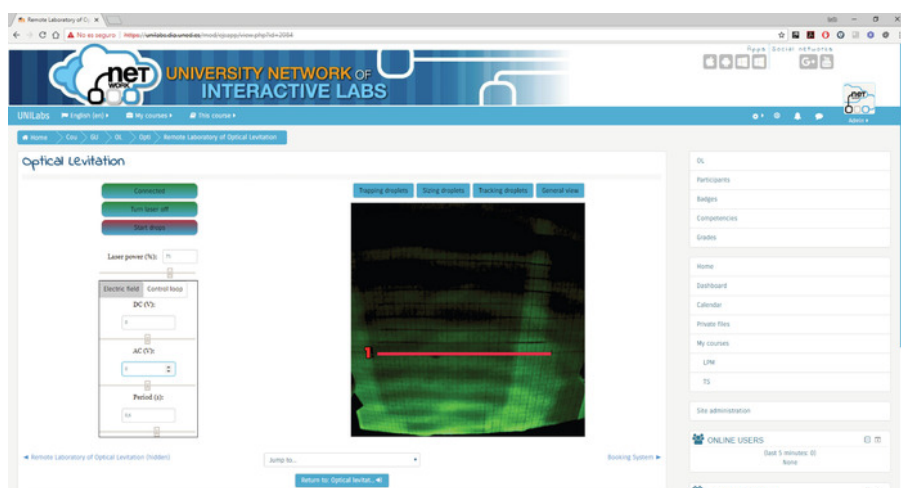


Figure 9: Remote lab interface: sizing a droplet. In remote experimentation, this web application interface is used to determine the size of a trapped droplet. The diffraction pattern displayed by the lab webcam and the scale allow users to determine the size of the trapped droplet. [Please click here to view a larger version of this figure.](#)

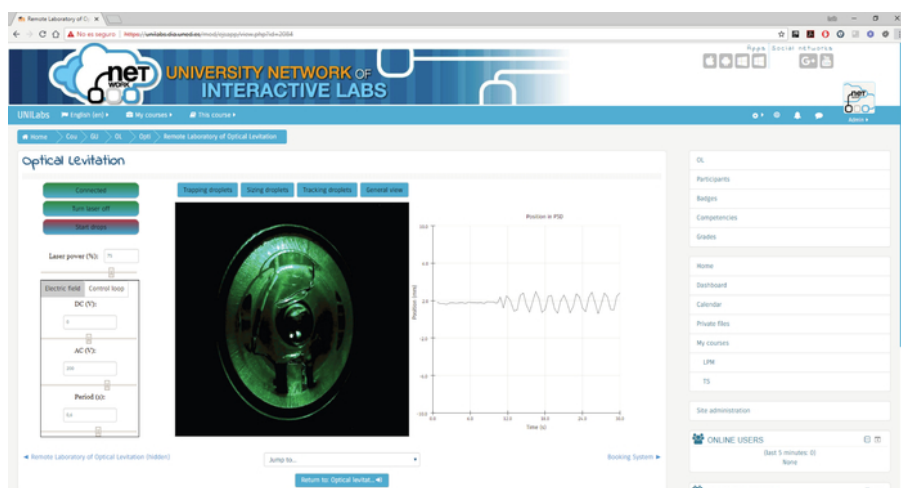


Figure 10: Remote lab interface: applying an electric field. In remote experimentation, this web application interface is used to apply an electric field to the trapped droplet. In this example, a 200 V AC electric field is applied. The lab PSD signal is displayed on the graph at the right and it shows the oscillating movement of the droplet following an electric field change which was applied at around $t = 10$ s. [Please click here to view a larger version of this figure.](#)

| Laser class | Possible injury |
|-------------|---|
| Class 1 | Incapable of causing any injury during a normal operation |
| Class 1M | Do not cause any type of injury if no optical collectors are used. |
| Class 2 | Visible lasers that do not cause injuries in 0.25 s |
| Class 2M | If no optical collectors are used, they are incapable of causing injury in 0.25 s. |
| Class 3R | Slightly unsafe for intrabeam viewing; up to 5 times the class 2 limit for visible lasers or 5 times the class 1 limit for invisible lasers |
| Class 3B | Eye hazard to direct vision, usually not an eye hazard to diffuse vision |
| Class 4 | Eye and skin hazard for both direct and scattered exposure |

Table 1: Laser classification summary. The different lasers on the market can be classified according to their hazardousness and the risks involved in their use. The table shows the different types of lasers available (in the left column) and their potential danger (in the right column).

Discussion

This work presents a setup for carrying out a modern physics experiment in which droplets are optically levitated. The experiment can be performed either in a traditional hands-on way or remotely. With the remote system establishment, students and researchers all over the

world can get access to the experimental set-up. This also guarantees the users' safety, since they do not need to be in presence of the high-power laser and electric fields required for the experiment. In addition, the users can interact with the instrumentation in a very simple way, by sending high-level commands via the computer due to the automation of the set-up. When compared to the hands-on procedure, the remote experimentation offers a very similar experience. One of the key-points of the experiment presented is obtaining the size of the droplets, since it has a big influence on the calculations of the absolute charge. Three different methods have been used to determine the size, and they all agree very well: (1) The method described above (using the diffraction pattern) (2) to oscillate the droplet with a vertical electric field and use the phase difference between the electric field and the position and (3) to visualize the shadow of the droplet on a screen, and with a camera determine the size. The setup is also being prepared for researching trapped droplets in vacuum. First the droplet is trapped in air, then the cell is enclosed, and the air is removed. In this way, it will be possible to investigate the properties of a trapped droplet in vacuum.

With the presented remote lab, the charge and the size of micrometer-sized dielectric particles can be determined. A further development of the setup has provided a way to study micrometer-sized droplet collisions using high speed cameras¹¹. With the experimental set-up as a base, it has been investigated as a sensitive way to track the position of particles using a Sagnac Interferometer¹². Our method is used to obtain the charge and size of droplets one by one. The measurements take quite some time to perform, so it is mainly a tool to work with single droplets. If the goal is a good statistic capturing of large numbers of droplets, other methods are better, such as the method presented by Polat¹³.

When the measurements are made, the droplet is released and descends onto the bottom of the cell, unfortunately making the bottom glass dirty. This is a long-term constraint since the laser light can scatter, making harder to trap the next droplet. However, it is easily solved with a periodical cleaning of the cell.

Disclosures

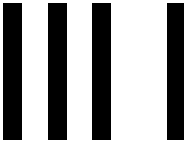
The authors have nothing to disclose.

Acknowledgements

This work has been supported by the Swedish Research Council, Carl Trygger's Foundation for Scientific Research and the Spanish Ministry of Economy and Competitiveness under the project CICYT DPI2014-55932-C2-2-R. Thanks to Sannarpsgymnasiet for letting us try the RL with students.

References

1. Ashkin, A., Dziedzic, J. Optical levitation by radiation pressure. *Applied Physics Letters*. **19**, 283 - 285 (1971).
2. Roosen, G., Imbert, C. Optical levitation by means of two horizontal laser beams: A theoretical and experimental study. *Physics Letters*. **59** (1), 6 - 8 (1976).
3. Heradio, R., de la Torre, L., Galan, D., Cabrerizo, F.J., Herrera-Viedma, E., Dormido, S. Virtual and remote labs in education: A bibliometric analysis. *Computers & Education*. **98**, 14-38 (2016).
4. Isaksson, O., Karlsteen, M., Rostedt, M., Hanstorp, D. An optical levitation system for a physics teaching laboratory, *American Journal of Physics*. **88**(10), 88-100 (2018).
5. Galan, D., Isaksson, O., Rostedt, M., Enger, J., Hanstorp, D., de la Torre, L. A remote laboratory for optical levitation of charged droplets. *European Journal of Physics*. **39** (4), 045301 (2018).
6. Swithenbank, J., Beer, J., Taylor, D., Abbot, D., and McCreath, G. A laser diagnostic technique for the measurement of droplet and particle size distribution. *14th Aerospace Sciences Meeting, Aerospace Sciences Meetings*. (1976).
7. Christian, W. and Esquembre, F. Modeling physics with easy java simulations, *The Physics Teacher*. **45**, 475-480 (2007).
8. de la Torre, L., Sanchez, J., Heradio, R., Carreras, C., Yuste, M., Sanchez, J., and Dormido S. Unedlabs - an example of ejs labs integration into moodle. *World Conference on Physics Education*. (2012).
9. Chaos, D., Chacon, J., Lopez-Orozco, J. A., and Dormido S. Virtual and remote robotic laboratory using ejs, matlab and labview. *Sensors*. **13**, 2595-2612, ISSN 1424-8220 (2013).
10. Lundgren, P., Jeppson, K., and Ingerman, A. Lab on the web-looking at different ways of experiencing electronic experiments. *International journal of engineering education*., **22**, 308-314 (2006).
11. Ivanov, M., Chang, K., Galinskiy, I., Mehlig, B., Hanstorp, D. Optical manipulation for studies of collisional dynamics of micron-sized droplets under gravity, *Optics Express*. **25**, 1391-1404 (2017).
12. Galinskiy, I., et al. Measurement of particle motion in optical tweezers embedded in a Sagnac interferometer. *Optics express*. **23**, 27071-27084 (2015).
13. Polat, M., Polat, H., Chander, S. Electrostatic charge on spray droplets of aqueous surfactant solutions. *Journal of Aerosol Science*. **31**, 551-562 (2000).



Visualizing the electron's quantization with a ruler



OPEN

Visualizing the electron's quantization with a ruler

Javier Tello Marmolejo^{1✉}, Mitzi Urquiza-González^{1,2}, Oscar Isaksson¹, Andreas Johansson¹, Ricardo Méndez-Fragoso² & Dag Hanstorp¹

More than 100 years ago, Robert Millikan demonstrated the quantization of the electron using charged, falling droplets, but the statistical analysis on many falling droplets did not allow a direct visualization of the quantization of charge. Instead of letting the droplets fall, we have used optical levitation to create a single droplet version of Millikan's experiment where the effects of a single electron removal can be observed by the naked eye and measured with a ruler. As we added charges to the levitated droplet, we observed that its equilibrium position jumped vertically in quantized steps. The discrete nature of the droplet's jumps is a direct consequence of the single-electron changes in the charge on the droplet, and therefore clearly demonstrates the quantization of charge. The steps were optically magnified onto a wall and filmed. We anticipate that the video of these *single electron additions* can become a straightforward demonstration of the quantization of charge for a general audience.

The idea of quantization is one of the most important concepts in physics and an essential component of our conceptualization of the microscopic world. Nevertheless, because of the very fact that it concerns the microscopic world, macroscopic observations of quantization are rare.

Since their invention in 1970 by Nobel Prize winner Arthur Ashkin, optical trapping techniques have allowed us to isolate and manipulate micro- and nano-particles¹. This can now be performed so precisely that relatively large objects can be employed to explore quantum phenomena. Examples include the search of milli-charged particles², collisions of ultracold ground-state molecules³, and the investigation of macroscopic quantum states⁴. These experiments, along with others like the visualization of quantized vortices⁵ or of quantum cat states⁶, continue to bring the concept of quantization to the macroscopic world.

In this paper, we add a new macroscopic visualization of quantization through a modern single-droplet version of Millikan's experiment⁷. In past experiments, quantized amounts of electric charge in the form of electrons have been added to trapped particles using optical^{8–10} and electrostatic¹¹ levitation. However, these observations were not direct and necessitated the use of feedback loops or post-experiment mathematical analysis to discern the quantization. The technique we present here is direct and shows the magnified effect of adding individual electrons to trapped particles live on a screen and visible with the naked eye.

The quantization was observed in the stability position of a $29.5 \pm 1.4 \mu\text{m}$ silicone oil droplet optically levitated between two horizontal electrodes. A potential difference between the electrodes produced a vertically-directed and locally homogeneous electric field around the droplet. The net amount of charge on the droplet created a force that displaced it in the vertical direction. Since the optical trap held the droplet in a harmonic potential, the displacement was proportional to the force, which, in turn, depended on the droplet's net amount of charge. The position dependence of the droplet's net charge was sufficiently enhanced to clearly observe the result of depositing individual electrons on the levitated droplet.

The technique we used to visualize the effect of adding individual electrons to the droplet requires three elements: (i) an optical levitation trap with a very low trap stiffness (i.e. the spring constant of the harmonic potential) to make the movement per unit force large, (ii) a strong electric field, and (iii) a method of adding individual electrons to the levitated droplet.

We created the trap by directing a 532 nm continuous wave laser beam (LaserQuantum gem532) vertically upwards and focusing it with a 100 mm plano-convex lens. The long focal distance produced a weak optical trap. The laser beam had a diameter of 0.9 mm, resulting in a numerical aperture (NA) of 4.5×10^{-3} and in a trap stiffness of $5.00 \pm 0.49 \text{ nN/m}$ (see Supplementary Information).

¹Department of Physics, University of Gothenburg, 412 96 Gothenburg, Sweden. ²Facultad de Ciencias, Universidad Nacional Autónoma de México, Av. Universidad 3000, Circuito Exterior S/N Delegación Coyoacán, C.P. 04510 Ciudad Universitaria, Ciudad de México, México. ✉email: javier.marmolejo@physics.gu.se

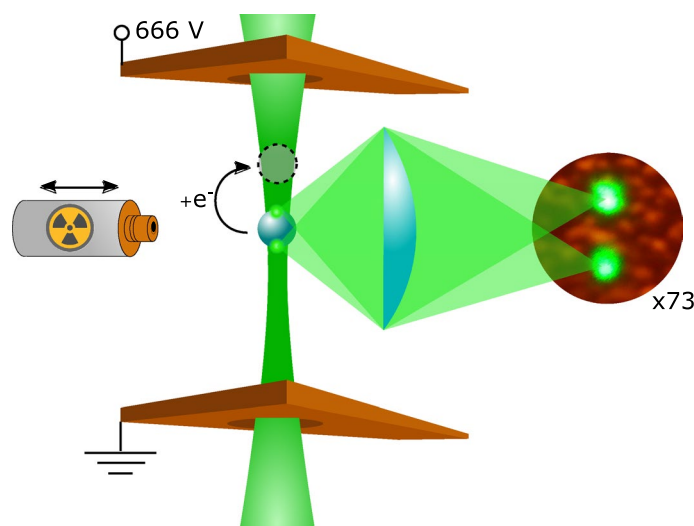


Figure 1. Schematic of the experimental setup. A silicone oil droplet is levitated between two flat, horizontal electrodes with a separation of 1.0 mm and a voltage difference of 666 ± 0.5 V. A ^{241}Am alpha radiation source is placed close to the droplet in order to create free electrons. Some of these electrons become attached to the droplet and change its net charge. The levitated droplet scatters mostly from the bottom and top where the laser enters and exits the droplet. This creates a double point image when focused by a lens.

We produced the electric field by applying a voltage difference of 666 ± 0.5 V across a pair of horizontal electrodes with a vertical separation of 1.0 mm. The laser passes through each electrode via a circular hole with a radius of 1.0 mm. The small distance between the electrodes and the large voltage difference were chosen to produce a strong electric field.

We used a numerical simulation to determine the magnitude and homogeneity of the electric field. We defined a working volume between the electrodes inside of which we know the experiment took place. In this volume, the electric field was found to have a vertical direction and a magnitude of 360 ± 45 kV/m. In a smaller volume sufficient for the droplet to make a couple of jumps, the homogeneity of the field is even greater, which results in equispaced jumps (see Supplementary Information).

We added individual electrons to a previously neutralized droplet (see Supplementary Information) using a ^{241}Am alpha radiation source. The emitted alpha particles produced free electrons in the trap either directly by striking the droplet or indirectly by striking the electrodes or ionizing the air in the trap. The free electrons were subsequently deposited on the surface of the droplet. In this manner, we were able to change the charge on the droplet in randomly distributed steps of either single or small multiples of the elementary charge.

We projected an image of the droplet onto a wall in the laboratory using an aspheric planoconvex lens ($f = 50$ mm, Thorlabs AL2550G) with a magnification of 73 ± 1.4 . With this magnification, we were able to observe micro-metric movements of the droplet with the naked eye. The light scattered from the droplet comes mostly from the bottom where the laser beam hits the droplet and the top where the beam leaves the droplet. Hence, the image of the droplet is observed as two separate images on the screen, as seen in Fig. 1.

When we set the alpha radiation source at the appropriate distance from the droplet, it gains charges randomly. This causes it to jump discontinuously from one equilibrium point to another. We filmed a video of a series of electron additions (see online). Some selected frames are shown in Fig. 2a. Between each of the frames, the droplet gained an additional amount of charge causing it to jump from one equilibrium position to another. Equally spaced horizontal reference lines are added to Fig. 2a. The separation between the equally spaced horizontal lines corresponds to the distance the droplet moves when absorbing a single elementary charge. The quantization of the charge immediately stands out. The position of the droplet always falls on one of the horizontal lines and, by simply counting the number of lines between the steps, one can determine the number of electrons the droplet has gained.

Figure 2b presents the position as function of time for the droplet shown in the video. The magenta equally spaced lines represent the displacement, Δy , caused by a single electron addition and all the steps are multiples of this distance. In this graph, one can clearly see the full series of 8 steps that fall on a horizontal line, where the droplet gains 2, 3, 1, 1, 4, 6, 3, and 9 electrons. Once again, one can observe the quantization of the electronic charge arising from the discrete nature of the individual steps.

We determined the displacement Δy by fitting the positions of the droplet to a step function, which is shown in Fig. 3a. The fit produced a value of Δy of 10.36 ± 0.26 μm , which is almost three times smaller than the droplet's diameter. The two fit variables were a global *single electron displacement* Δy , and an individual *number of electrons added* for each point in time. The uncertainty in Δy stems mostly from the droplet's oscillation around the stability positions.

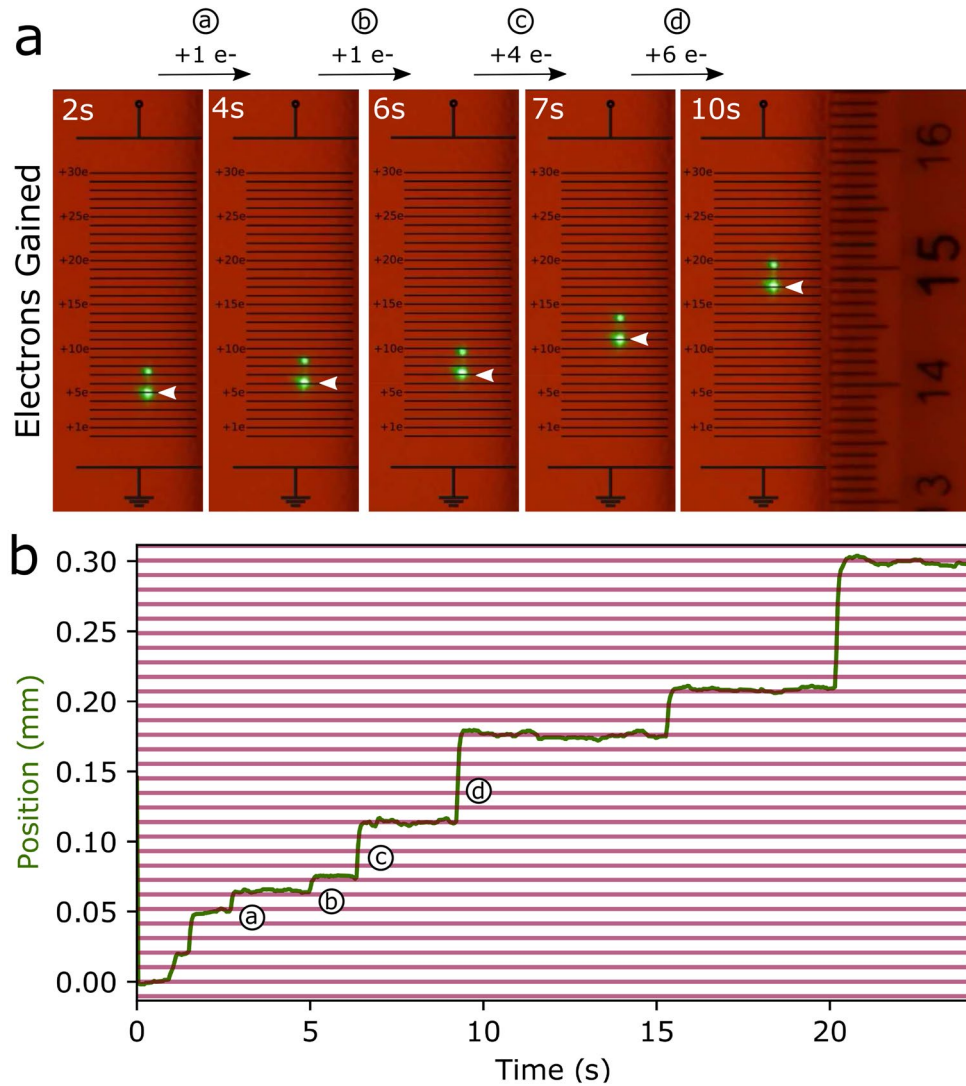


Figure 2. Visibly quantized steps of a levitated droplet as it gains electrons. **(a)** Screenshots of the droplet’s projection on the wall before and after steps a (+ 1e), b (+ 1e), c (+ 4e) and d (+ 6e). Black horizontal lines mark the displacement caused by a single electron addition and are set to the lower bright image of the droplet. The last image to the right shows a mm ruler that had been attached to the wall. **(b)** Real displacement of the droplet (green) calculated from the video of the displacement on the wall.

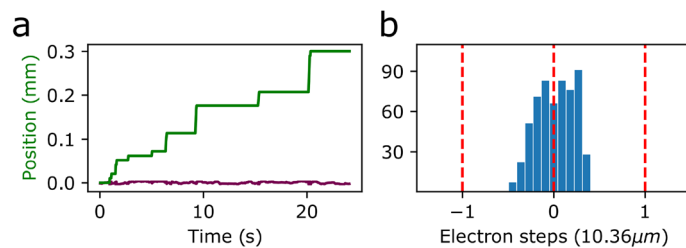


Figure 3. Discrete steps in the vertical position of droplet in the trap. **(a)** The green line shows a fit of the data shown in Fig. 2b using a step function. The height of the steps is an integer multiple of the *single electron step* fitting parameter (see discussion in text). The magenta line shows a plot of the residue between the data and the fit. **(b)** Histogram of the residue measured in units of electron steps. The normal distribution around zero results from the discrete nature of the steps.

The residue between the fit and the data is plotted in magenta at the bottom of Fig. 3a and a histogram of this residue is plotted in Fig. 3b. The histogram follows a normal distribution around zero and its FWHM is less than half an electron step, providing further evidence that we are observing quantized steps.

To confirm that these steps were indeed caused by electron additions, we used them to calculate the charge of the electron. Balancing the electrostatic ($F_e = qE$) and optical restoring ($F_r = k\Delta y$) forces results in

$$q = \frac{k\Delta y}{E}, \quad (1)$$

where q is the charge of the electron, Δy the displacement caused by a single electron addition, k the trap stiffness and E the magnitude of the electric field. The method to determine the trap stiffness is described in the methods section. Using Eq. (1), we calculated the charge of the electron to be of $1.44 \pm 0.25 \times 10^{-19} \text{C}$, which agrees within the statistical uncertainty with the known value of $1.602 \times 10^{-19} \text{C}$ ¹². The uncertainty was calculated through error propagation in Eq. (1) where the biggest contributors were the uncertainties of the electric field and the trap stiffness.

The series of electron jumps serve as straight forward evidence of the quantization of the electric charge. We have magnified the effect to a level where the step caused by adding a single electron can be seen with the naked eye and measured with a simple ruler. The discrete steps are the result of the charge on the droplet changing by a single electron. In contrast, other methods of observing the effects of quantization such as the photoelectric effect or atomic emission lines are indirect in the sense that they involve the use of many photons or electrons. Our experiment allows one to directly visualize charge quantization, a quantum phenomenon, in the macroscopic world.

Data availability

All relevant data generated or analysed for this study are available within the article and the associated Supplementary Information. Any other data are available from J.T.M. (javier.marmolejo@physics.gu.se) upon reasonable request.

Received: 15 February 2021; Accepted: 28 April 2021

Published online: 25 May 2021

References

1. Ashkin, A. & Dziedzic, J. M. Optical levitation by radiation pressure. *Appl. Phys. Lett.* **19**, 283–285 (1971).
2. Moore, D. C., Rider, A. D. & Gratta, G. Search for millicharged particles using optically levitated microspheres. *Phys. Rev. Lett.* **113**, 251801 (2014).
3. Cheuk, L. W. *et al.* Observation of collisions between two ultracold ground-state CaF molecules. *Phys. Rev. Lett.* **125**, 043401 (2020).
4. Delić, U. *et al.* Cooling of a levitated nanoparticle to the motional quantum ground state. *Science* **367**, 892–895 (2020).
5. Bewley, G., Lathrop, D. & Sreenivasa, K. Visualization of quantized vortices. *Nature* **441**, 588 (2006).
6. Liu, S. *et al.* Classical analogy of a cat state using vortex light. *Commun. Phys.* **2**, 75 (2019).
7. Millikan, R. A. On the elementary electrical charge and the Avogadro constant. *Phys. Rev.* **2**, 109–143 (1913).
8. Frimmer, M. *et al.* Controlling the net charge on a nanoparticle optically levitated in vacuum. *Phys. Rev. A* **95**, 061801(R) (2017).
9. Ashkin, A. Applications of laser radiation pressure. *Science* **210**(4474), 1081–1088 (1980).
10. Beunis, F. *et al.* Beyond Millikan: the dynamics of charging events on individual colloidal particles. *Phys. Rev. Lett.* **108**, 016101 (2012).
11. Stephen, A. Determination of particle mass and charge by one electron differentials. *J. Aerosol. Sci.* **10**(1), 49–53 (1979).
12. The NIST Reference on Constants, Units and Uncertainty. Fundamental Physical Constants. elementary charge. https://physics.nist.gov/cgi-bin/cuu/Value?e|search_for=elecmag_in!

Acknowledgements

Financial support from the Swedish Research Council (2019-02376) is acknowledged. J.T.M and M.U.G. acknowledge the support from the Linneaus-Palme foundation. R.M.F. acknowledges the support from the projects DGAPA-UNAM PAPIIT IN-114518 and PAPIME PE-112919. Johan Wingborg is acknowledged for his assistance in the filming of the video.

Author contributions

D.H. conceived the experiment and coordinated the project. O.I. performed the initial experimental design. J.T.M. built the final experimental system. J.T.M., M.U.-G., O.I. and A.J. conducted the experiments. J.T.M. performed the data analysis. R.M.-F. provided the numerical simulations. J.T.M. wrote the draft of the manuscript. All authors contributed to the final version of the manuscript.

Funding

Open access funding provided by University of Gothenburg.

Competing interests

The authors declare no competing interests.

Additional information

Supplementary Information The online version contains supplementary material available at <https://doi.org/10.1038/s41598-021-89714-2>

Correspondence and requests for materials should be addressed to J.T.M.

Reprints and permissions information is available at www.nature.com/reprints.

Publisher's note Springer Nature remains neutral with regard to jurisdictional claims in published maps and institutional affiliations.



Open Access This article is licensed under a Creative Commons Attribution 4.0 International License, which permits use, sharing, adaptation, distribution and reproduction in any medium or format, as long as you give appropriate credit to the original author(s) and the source, provide a link to the Creative Commons licence, and indicate if changes were made. The images or other third party material in this article are included in the article's Creative Commons licence, unless indicated otherwise in a credit line to the material. If material is not included in the article's Creative Commons licence and your intended use is not permitted by statutory regulation or exceeds the permitted use, you will need to obtain permission directly from the copyright holder. To view a copy of this licence, visit <http://creativecommons.org/licenses/by/4.0/>.

© The Author(s) 2021

Terms and Conditions

Springer Nature journal content, brought to you courtesy of Springer Nature Customer Service Center GmbH (“Springer Nature”).

Springer Nature supports a reasonable amount of sharing of research papers by authors, subscribers and authorised users (“Users”), for small-scale personal, non-commercial use provided that all copyright, trade and service marks and other proprietary notices are maintained. By accessing, sharing, receiving or otherwise using the Springer Nature journal content you agree to these terms of use (“Terms”). For these purposes, Springer Nature considers academic use (by researchers and students) to be non-commercial.

These Terms are supplementary and will apply in addition to any applicable website terms and conditions, a relevant site licence or a personal subscription. These Terms will prevail over any conflict or ambiguity with regards to the relevant terms, a site licence or a personal subscription (to the extent of the conflict or ambiguity only). For Creative Commons-licensed articles, the terms of the Creative Commons license used will apply.

We collect and use personal data to provide access to the Springer Nature journal content. We may also use these personal data internally within ResearchGate and Springer Nature and as agreed share it, in an anonymised way, for purposes of tracking, analysis and reporting. We will not otherwise disclose your personal data outside the ResearchGate or the Springer Nature group of companies unless we have your permission as detailed in the Privacy Policy.

While Users may use the Springer Nature journal content for small scale, personal non-commercial use, it is important to note that Users may not:

1. use such content for the purpose of providing other users with access on a regular or large scale basis or as a means to circumvent access control;
2. use such content where to do so would be considered a criminal or statutory offence in any jurisdiction, or gives rise to civil liability, or is otherwise unlawful;
3. falsely or misleadingly imply or suggest endorsement, approval, sponsorship, or association unless explicitly agreed to by Springer Nature in writing;
4. use bots or other automated methods to access the content or redirect messages
5. override any security feature or exclusionary protocol; or
6. share the content in order to create substitute for Springer Nature products or services or a systematic database of Springer Nature journal content.

In line with the restriction against commercial use, Springer Nature does not permit the creation of a product or service that creates revenue, royalties, rent or income from our content or its inclusion as part of a paid for service or for other commercial gain. Springer Nature journal content cannot be used for inter-library loans and librarians may not upload Springer Nature journal content on a large scale into their, or any other, institutional repository.

These terms of use are reviewed regularly and may be amended at any time. Springer Nature is not obligated to publish any information or content on this website and may remove it or features or functionality at our sole discretion, at any time with or without notice. Springer Nature may revoke this licence to you at any time and remove access to any copies of the Springer Nature journal content which have been saved.

To the fullest extent permitted by law, Springer Nature makes no warranties, representations or guarantees to Users, either express or implied with respect to the Springer nature journal content and all parties disclaim and waive any implied warranties or warranties imposed by law, including merchantability or fitness for any particular purpose.

Please note that these rights do not automatically extend to content, data or other material published by Springer Nature that may be licensed from third parties.

If you would like to use or distribute our Springer Nature journal content to a wider audience or on a regular basis or in any other manner not expressly permitted by these Terms, please contact Springer Nature at

onlineservice@springernature.com

IV

Self-calibrated droplet volume measurements in acoustic levitation

Self-calibrated droplet volume measurements in acoustic levitation

Andreas Johansson,¹ Ricardo Méndez-Fragoso,² and Jonas Enger¹

¹*Department of Physics, University of Gothenburg, SE-412 96 Gothenburg, Sweden*

²*Facultad de Ciencias, Universidad Nacional Autónoma de México, Av. Universidad 3000, Circuito Exterior S/N Alcaldía Coyoacán, C.P. 04510 Ciudad Universitaria, Ciudad de México, México*

(*Electronic mail: andreas.johansson@physics.gu.se)

(Dated: November 2, 2022)

Volume measurements using acoustic levitation is conventionally done via image analysis using a levitated precision produced sphere for pixel calibration. The problems are the frequent time-consuming re-calibration that comes with this approach and that more precise calibration spheres are expensive. A fast and self-calibrating method to measure the volumes of acoustically levitated droplets is presented as a versatile, low-cost alternative. The distance between two levitated droplets in a horizontally oriented acoustic trap, is processed via image analysis of real-time or recorded frame data. A simulation of the acoustic field is used to assist in setting the cavity-length for the acoustic trap based on the temperature in the trap and to predict the distance between the central nodes in millimeters. The volumes of the spheroidal shaped levitated droplets can thus be calculated using a custom analysis-software, built using open source programming language. The droplets dimensions and the droplet-to-droplet distance in pixels are extracted and used to calculate the volume. In comparison with a conventional method (using $d = 1 \text{ mm} \pm 0.02 \text{ mm}$ spheres), results shows that a similar volume measurement precision ($\pm 1.5\%$) as conventional methods, in the range 1.5 nl to $2 \text{ }\mu\text{l}$ can be achieved. The cost of the two droplets needed for pixel calibration in this new technique is virtually zero and the self-calibrating nature gives researchers the previously unheard of opportunity to zoom in and out or reconfigure the experiment without the need for re-calibration.

I. INTRODUCTION

Contactless measurements of droplet volume in an acoustic trap is often performed using optical methods. For this purpose diffraction patterns has been used¹ but the most common method is image analysis. The standard way of doing image analysis is to levitate a precision produced spherical bead in the focal plane of the camera and use it to calibrate the pixel to mm ratio²⁻⁴.

Levitating samples with other techniques can also be used for high precision volume measurements. Bradshaw and Schmidt report on a system that can produce accurate volume measurements using image analysis and electrostatic levitation, with the disadvantage of frequent re-calibration⁵.

The common issue of mentioned droplet volume measurement techniques in acoustic levitation is the requirement of the equipment to be static. If there is a change, the system needs to be re-calibrated, and time is lost. Even a simple change in camera zoom impose the need for re-calibration in order for standard image analysis to perform well as a volume measurement technique.

As an alternative technique using acoustic levitation we propose a simple, fast and self-calibrating method to measure droplet volumes using a simulation of the acoustic pressure and two droplets levitated in an acoustic trap. By measuring the droplet-to-droplet distances in pixels and temperature in the levitator orange to calculate the optimal parameters for the trap, and using the driving frequency of the transducers the pixel to millimeter ratio is calibrated. The suggested method can be useful in increasing the versatility of volume measurements involving acoustically levitated droplets in fields such as chemical micro analysis, spectroscopy studies and evaporation studies^{6,7}.

II. BACKGROUND

In 1933 Bücks and Müller were first to describe that small samples including droplets could be levitated by ultrasonic standing waves⁸. Levitation of a liquid sample can also be achieved using mainly optical levitation or electrostatic levitation. Levitated samples can be studied without being contaminated by container walls and this is very useful in especially micro-analysis⁹ and trace-analysis³. Acoustic levitation has the main advantage over other experimental techniques that it can levitate non-conducting, non-transparent and non-magnetic materials and this to a fraction of the cost, especially using recently developed levitators¹⁰⁻¹². An acoustic levitator also have the advantage that no dangerous or disturbing electromagnetic fields interfere with measurements. One version of such levitators is the open-source available TinyLev¹² that focuses the acoustic field by two transducer arrays mounted on opposite sections of a sphere. The acoustic trapping force to voltage ratio is higher in this kind of trap than using flat phased-array levitators¹³ or the commercialized Langevin-type levitators^{11,12,14}. Trapped objects are therefore stable even at low voltage experiments which in addition to low costs as well as the low requirement on sample properties, the accessibility of the sample and a wide volume range is desirable for a levitation technique as a tool for researchers¹⁵.

A. Concave radiators

The calculations for the acoustic pressure of concave radiators, such as the TinyLev¹² where parts of a spherical geometry emits sound, were introduced by H. T. O'Neil¹⁶. These calculations follows the work done by Lord Rayleigh¹⁷, on

how to integrate the contribution of each element of an arbitrary surface that vibrates and sets a fluid in motion to calculate the total velocity-potential (which here corresponds to the acoustic pressure). They were shown¹⁶ to have simple solutions along the axis of symmetry for coherent emitters. The acoustic far-field pressure could be described as:

$$P(\theta) \propto \text{sinc}(k \times a \times \sin(\theta)) \quad (1)$$

as long as the cavity length is much greater than the wavelength. Here $k = \frac{2\pi}{\lambda}$ is the wavenumber, θ is the azimuthal angle and a is the radius of the piston. This method is well described by Liu, Ming, Tan, et al¹⁸ and has also been used in other studies involving simulations of the acoustic field^{12,16,18-20}.

B. Image analysis of droplets,

The need to accurately measure droplet dimensions and calculate their volumes arises in contexts where concentration requires to be determined such as evaporation studies, spectroscopy studies and micro-analysis^{6,7}.

In acoustic standing wave single axis levitators such as TinyLev¹², the acoustic field interacts with droplets to both levitate and deform them. Here the surface-tension keeps the droplets round and the acoustic forces flatten them as they work mostly along the axis of symmetry and this results in the deformation of the droplet into a spheroidal shape^{21,22}. The utilization of the axis-symmetry of spheroidal droplets have been used to calculate volumes of levitated droplets before^{2,5}, however variations of this technique exists^{4,23}. Leiterer et al made comparison between three volume calculation methods for droplets in a single-axis acoustic trap. Their results indicate that spherical approximation (a) tends to give an estimation of droplet volumes 10-15% lower than the other two; spheroidal approximation (b) and using the rotational volume from the droplet shadow (c)⁴. However Contreras et al, found that for droplets in their experiments ranging from 250 to 780 μm in diameter (8.2 nl - 0.25 μl), the droplet deformation was non-significant and a spherical approximation could suffice²⁴. For large droplets of about 2 mm in diameter, Yarin et al found the aspect ratios to vary between 1.3 - 2 mm, depending on driving voltage²⁵ and thus a spherical approximation no longer suffice.

III. METHODS

Self-calibrated volume measurements can be achieved using computer vision by always having a known distance visible in the focus plane. In the experimental setup shown in Fig. 1, two droplets are levitating in neighboring nodes (see supplementary material for equipment used). Their center-to-center distance is ideally the same as the node to node distance of the acoustic field produced by the trap. The acoustic trap is mounted with its axis of symmetry horizontally oriented. Using a simulation of the acoustic field, the millimeter distance

between two nodes/droplet-centers can be predicted with respect to frequency, temperature and the geometry of the trap. This distance is always in the focus plane and have the desired characteristic for a self-calibrated volume measurement method.

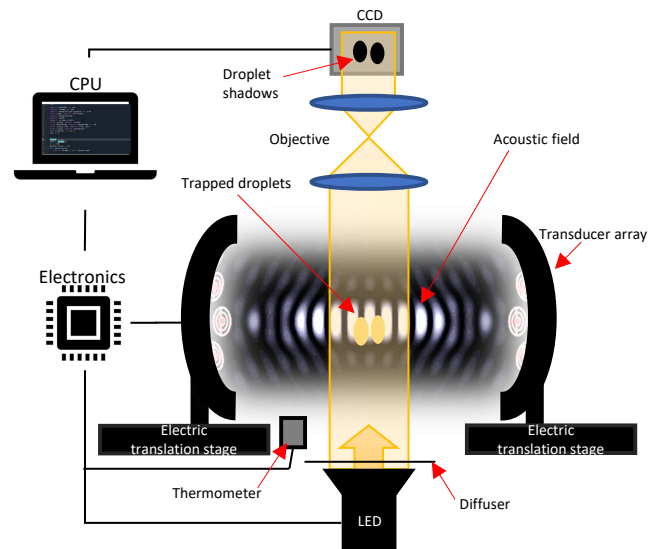


Figure 1. Experimental setup in which the CPU controls the frequency and voltage applied to the transducer arrays of the acoustic levitator. Diffused light from a LED-source passes the acoustic field and is focused on a CCD chip and monitored by the CPU.

A. Setup

1. Orientation of the acoustic trap

The acoustic trap in this experiment is mounted horizontally to minimize the impact of gravity on the droplet-to-droplet distance along the axis of symmetry and thus producing a reliable distance in the image plane that can be used for self-calibration. In previous studies on vertically oriented acoustic traps, the displacement of objects from the node center due to the gravitational pull has been investigated²⁵. Horizontally oriented acoustic traps are rare in the research literature, except for some examples^{7,8,20}. However, for the same driving voltage the acoustic force that counteracts gravity in a horizontally oriented trap is lower than in a vertical trap. Gravity will ideally not have any significant impact on the droplet-to-droplet distance using this trap-orientation while in the vertical trap gravity will introduce deviations in the distance between droplets, that vary with droplet size. When using concave radiators there will often be an asymmetry in the potential wells of the nodes and this was empirically found to introduce deviations in the distance between two levitated droplets, even in the horizontally oriented trap. A simulation of the intensity of the acoustic field in the trap was used to find cavity-lengths that produced equal intensities in the three central anti-nodes, and therefore two corresponding symmetrical

potential wells in the nodes in-between.

B. Predictions of the acoustic field intensity

In order to achieve self-calibration a simulation of the acoustic trap was developed to find the cavity length that produces the necessary symmetrical potential wells in the central nodes depending on temperature in the acoustic trap. The corresponding distance in millimeters between the two center nodes was also calculated via the simulation. In the simulation, the transducers was modeled as 4.5 mm pistons and placed in a hexagonal pattern to match the physical trap. Careful measurements of the physical trap's dimensional properties was done using a caliper to implement in the simulation. The simulation was developed in an iterative loop (see Fig. 2) by first predicting cavity length for symmetrical potential wells with the same intensity for the central nodes as shown in Fig. 3 (see the video in supplementary material). The simulation accounts for the variations in the speed of sound dependent on the temperature²⁶. Second, data collection of the position of two droplets in the acoustic trap as their size or the voltage controlling the acoustic fields intensity was altered. If the droplets centroid-trajectories both were approximately vertical during these alterations the prediction from the simulation was judged as valid and the settings was used for volume measurements. There is a trade-off between number of anti-nodes with equal and large magnitude, and the trapping force in the nodes due to the spreading of energy over larger parts of the experiment. After the fit between the acoustic trap and the simulation was established a Table showing the relationship between the speed of sound v for specific temperatures T and the optimized distance D between the transducer arrays, that produces the droplet to droplet distance d_{node} , in the center of the acoustic trap was produced using the simulation to use as a shortcut during volume measurements (see Table I).

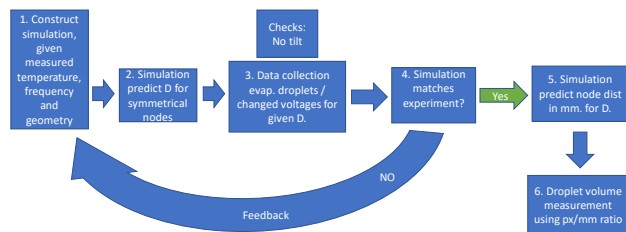


Figure 2. The match between simulation and reality was developed in an iterative loop, using droplet trajectories in the acoustic field as they evaporated or the field intensity was varied.

Table I. Distance between central nodes, d_{node} , as a function of temperature, T , and the optimized distance, D , between the transducer arrays for two symmetric potential wells with the same intensity.

| T [°C] | v [m/s] | D [mm] | d_{node} [mm] |
|-----------|--------------|-------------|--------------------|
| 18.0 | 342.200 | -1.182 | 4.804 |
| 18.5 | 342.490 | -1.067 | 4.807 |
| 19.0 | 342.780 | -0.956 | 4.809 |
| 19.5 | 343.075 | -0.840 | 4.812 |
| 20.0 | 343.370 | -0.725 | 4.815 |
| 20.5 | 343.665 | -0.610 | 4.818 |
| 21.0 | 343.960 | -0.495 | 4.820 |
| 21.5 | 344.250 | -0.384 | 4.823 |
| 22.0 | 344.540 | -0.269 | 4.826 |
| 22.5 | 344.830 | -0.158 | 4.829 |
| 23.0 | 345.120 | -0.042 | 4.831 |
| 23.5 | 345.415 | 0.073 | 4.834 |
| 24.0 | 345.710 | 0.188 | 4.837 |

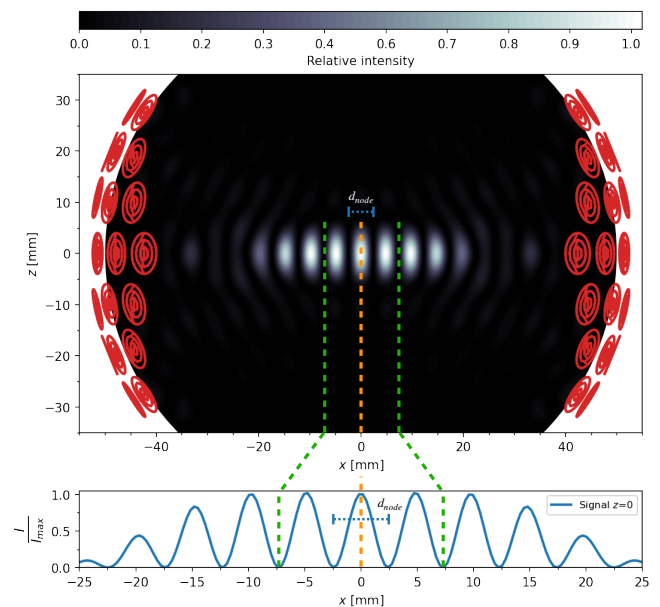


Figure 3. Simulation of acoustic trap. The black area shows the simulation of the acoustic field with relative intensity (grey scale) in the region accessible to the CCD. The structures in red color represent the positions and orientations of the transducers. The lower subfigure shows the relative intensity of the acoustic field along the x-axis for the central nodes of the trap.

C. Measuring droplet volume using images

Droplets in the acoustic trap are levitated due to the acoustic forces that balances gravity and at the same time they deform the droplet by compressing it along the axis of symmetry and the surface tension acts to keep the droplets spherical. The interaction of all forces produces the equilibrium spheroidal shape and the droplets levitate with their center of gravity in a position slightly lower than the horizontal axis (the axis of symmetry) of the acoustic trap.

For each video frame the pixel distance between droplets centroids is measured and from the simulation of the trap we can extract the node to node distance in millimeters and then use the ratio between them as a scale factor. To calculate any volume derived from pixel measurements the cube of the scale-factor, s can be used as in:

$$V_{metric} = V_{pixels} \times s^3. \quad (2)$$

where V_{metric} is volume in cubic-millimeters and V_{pixels} is the pixel-volume.

Below is the method used to extract data from the images of the droplets.

1. Pixel-data extraction

To collect pixel-data of value from the sharp contour images, these image-processing algorithms are used which closely resembles (with some deviations) the steps used by Kremer et al²³:

1. Convert to gray-scale.
2. Apply a mask, using a dilation method.
3. Binarize image using otsu-threshold to make objects white and background black.
4. Label connected regions of white pixels.
5. Extract pixel values (x,y) of centroid, minor axis length, major axis length and orientation.

The above algorithm is illustrated in Fig. 4.

It is thus possible to calculate the metric values for the semi-major axis and semi-minor axis of each droplet. Since gravity pull droplets slightly down from the symmetry axis of the trap, the force field is not fully symmetric. However, in Figure 4 we show that even for large droplets the spheroidal approximation is quite good. Using their elliptical cross-section as seen from the camera, their volumes can be calculated as shown below.

2. Calculating the oblate spheroid shaped droplet volume

Droplets are deformed by the acoustic field and as in a method investigated by Leiterer et al and described in section II B, their shapes are well approximated as oblate spheroids⁴. An oblate spheroid is symmetric along one of its axes as is visualized in Figure 5. When viewed along the axis of symmetry the cross-section is a circle with a specific radii. When viewed orthogonal to the axis of symmetry the cross-section is an ellipse. In the case of the oblate spheroid the semi-major axis is of the same length as the circle's radius. Thus the information about the shape and the corresponding volume can be derived from extracting the lengths of the semi-major axis, b , and the semi-minor axis, c , as a droplet is viewed orthogonal to the axis of symmetry and the droplet shadow is of elliptic shape.

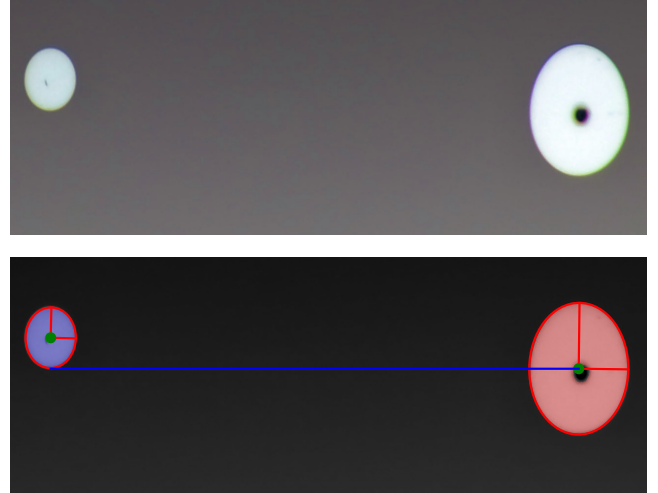


Figure 4. Upper: Image of two levitated droplets. Lower: Extracted pixel-data from upper image. The custom software, finds the regions of white pixels in the upper image and then measures the regions major and minor axis (red lines), as well as the centroid positions (green dot) and the horizontal distance between the centroids (blue line). The red ellipses are painted afterwards using the extracted data, only to show the quality of the elliptic approximation.

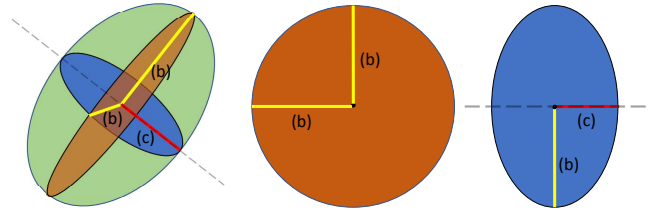


Figure 5. The oblate spheroid to the left is circular (brown, middle) when viewed along the dashed axis of symmetry and elliptic (blue, right) viewed orthogonal to that axis. The radius (b), in yellow, of the brown circle corresponds to the semi-major axis of the blue ellipse. The semi-minor axis (c), in red, of the ellipse is aligned with the axis of symmetry for the oblate spheroid.

The volume, $V_{ellipsoid}$, of an ellipsoid is calculated using the formula

$$V_{ellipsoid} = \frac{4\pi}{3} b^2 c, \quad (3)$$

which is the same case of the oblate spheroid and the droplets levitated in this experiment. The problem of measuring the three dimensional volume have thus been reduced to the singular dimension problem of measuring lengths in pixels on an image of two droplets.

Using Eq. (3), a value for the pixel volume V_{pixels} is calculated for each droplet in each frame. Using Eq. (2) the metric volume is then calculated for each frame. The measured and reported volume is then calculated as the mean and standard deviation of these volumes for many frames.

The method uses a simple simulation of the acoustic field and relies on the assumption that the presence of two droplets in the acoustic field doesn't affect the field significantly.

D. Summary of volume measurement method in steps:

1. Measure temperature in the acoustic trap (not in center, as thermometer absorbs energy and gets heated).
2. Use table produced by simulation to find out the correct cavity-length D and corresponding distance between center nodes d (see Table I).
3. Set correct experimental cavity length in accordance with previous point.
4. Levitate two droplets in the center nodes and collect pixel data using video-camera.
5. Analyze pixel data for each frame and extract centroid-to-centroid distances and the droplets dimensions, using custom python software based on the packages skimage and OpenCV.
6. Calculate volume of droplets for each frame.
7. During data collection, if necessary zoom in and out as needed. As shown in section IV, the measurements are not dependent on these changes.

E. Verifying volume measurements

The results from volume-measurements using the technique presented in this article and the results from a standard method of calibrating pixels using precision produced spheres was compared in order to verify the technique. We use levitated glass precision spheres of with $d = 1 \pm 0.02$ mm in one of the center nodes. Image-data was collected and analyzed to extract the diameter in pixels of these spheres. The mean of the pixel diameter from the frames for each sphere was used to calculate the average mean pixel diameter for all spheres. The average was used to calibrate the pixel-millimeter ratio, which were used to calculate droplet volumes and was compared to the results achieved from the new method. Since all data needed to calculate the volume of the droplets can be found in the image plane, it was conceivable that zooming in and out, while maintaining focus, would not affect the volume measurements using the new method. This cannot be achieved by other methods common in the literature, making it a versatile and low cost method.

F. Verifying self-calibration

Two non-evaporating oil droplets was levitated in the central nodes. The temperature of the trap was measured and the simulation generated table was consulted for the appropriate cavity-length which was set via the electric translation stage. The pixel-millimeter ratio was calibrated in the same two ways as before; using the calibration spheres and the new method respectively. During data collection the zoom of the camera was changed for a total of 8 different zooms, as is shown in section IV C.

IV. RESULTS AND DISCUSSION

In this section first the results from validating the simulation against data are presented and discussed. Second, to verify the method, results from a wide range volume measurements using the proposed method will be evaluated and compared to the method of using a precision produced sphere for calibration. Third, results from volume measurements while altering camera-zoom during data collection will be presented to demonstrate the robustness and self-calibrating nature of the new method.

A. Predictions from the simulation

The developed simulation was used to predict at what cavity-length the intensity distribution of the acoustic field produce symmetric potential wells at the center nodes, based on temperature (variable) and the geometry of each transducer array. The output is the cavity-length and the corresponding node-node horizontal distance between the two center-nodes. The predicted cavity-length for the temperature in the acoustic trap was used during data collection and the mapping between simulation and the actual acoustic field was verified via tracking two levitated oil droplet's centroid-trajectories while the driving voltage of the transducers producing the acoustic field is altered. The results can be seen in Fig. 6. The approximately vertical movement and the similarity in the two droplet's centroid-trajectories verify that the simulation has predicted a useful cavity-length for volume measurements. The error-bars correspond to one standard deviation and each point is the mean of 100 frames. The vertical overlap between the error-bars as well as the two droplets has moved in sync indicates that the prediction from the simulation was valid and that it now can be used in the method for volume measurements. This is further confirmed by the lower diagram in Fig. 6 showing stationarity in the pixel deviations from the mean pixel distance between the droplet's centroids over time.

Since the transducers that were used in the acoustic trap had a working frequency at 40 kHz the best performance seems to come near the spherical geometry that corresponds to a multiple of half wavelengths for that frequency. During the development of the presented method, the importance of the symmetric potential wells for the levitated droplets emerged as limitation for the method to work well. The speed of sound changes with temperature and so the exact distance between the two transducer arrays that produces symmetric potential wells also varies by temperature. Temperature measurements was found to be more reliable at the outer part of the trap as a more central position of the thermometer would make it absorb energy from the acoustic field and show misreadings.

B. Self-calibrated volume measurements

Two droplets, one oil and the other a mixture of mostly water and some oil was levitated and their volumes were measured. In Fig. 7, the mixed droplets volume measurement

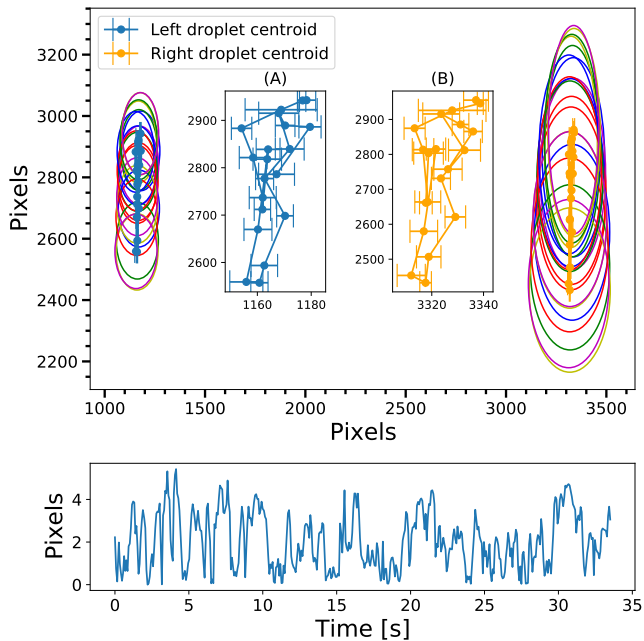


Figure 6. Two trapped oil droplets move vertically due to manually induced variations in the driving voltage of the transducers. Upper: The droplets has moved together synchronously and the coordinates (x,y) in pixels of the centroids is plotted as well as the droplets contours. Insets (A) and (B) is the zoom-in on the two droplets centroid movement. The error-bars correspond to one standard deviation and each point is the mean of 22 frames. Lower: The deviations in pixel-distance from the mean pixel distance of the two droplet centroids are plotted over time. The deviations are of similar magnitude regardless of the difference in vertical droplet positions.

data is shown. The change in slope comes from oil constituting a higher percentage of the droplet as the water evaporates. The conventional method's volume measurement is shown as a blue line. The red line is the volume measurements from the presented method. Both shows approximately the same volume with the new method having slightly larger deviations ($\pm 1.5\%$) but approximately the same mean. From the two lower diagrams in the figure it is clear that the larger variations in volume calculation using the new method comes from variations in the inter-droplet distance (shown as norm. dist in Fig. 7). Compensating for this and using the average of the inter-droplet distance to calculate the volume instead of the momentary, erases the differences between the methods. The larger volume oscillations that both volume measurements methods shows is due to the droplet's movement back and forth to the camera causing variations in the measured dimensions with slightly higher pixel readings when the droplet is closer to the camera and vice versa. The described effects is visible in the inset of Fig. 7.

The demonstrated measurements was made from images either in real-time or from a video-recording, and so the volume can be monitored and timestamped along with collected data from other parts of an experimental setup in fields such as trace analysis using spectroscopy, chemical micro-analysis

and evaporation studies.

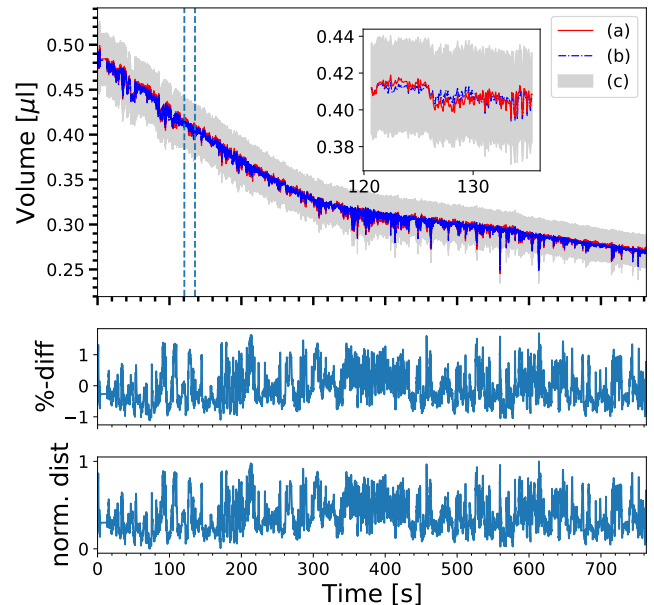


Figure 7. A trapped water-oil mixture droplet is evaporating during 12 minutes and 43 seconds. Upper: Line (a) is droplet volume calculated using the presented method. Line (b) is droplet volume calculated using an average from the calibration spheres. The shaded grey area (c) is the corresponding confidence interval boundary from the calibration spheres ($d = 1.00 \pm 0.02$ mm) converted to volume. The red line and blue line is overlapping almost perfectly. Inset: A smaller interval corresponding to data (200 frames) between the two vertical blue dashed lines, showing small oscillations of volume measurement using the new method around the volume measurements of the standard method. Middle: The percentage difference between the two methods. The variations is of similar order during the entire time as the droplet is loosing about half of its volume. Lower: Normalized distance between the two droplets. The oscillations of the inter-droplet distance is the major cause of the larger variations of volume measurements as compared to the standard method, seen in above.

C. Zoom-independent self-calibration

In Fig. 8 the self-calibrating nature of the proposed method is demonstrated. The data is gathered from one of two levitated oil drops for eight different camera zooms as shown in the right image without any manual re-calibration. The droplet volume is as previously measured in two ways, using calibration spheres and the new method. At first they show the same result but only the new method maintains same volume measurement while zooming in and out with the camera. The highest volume readings does not occur at the largest zoom and the volume changes are not proportional to the changes in zoom. The trend of lower volume readings from frame 250 to frame 700 is thus likely caused by slow oscillations back and forth to the camera. Since the volume of the droplet initially is approximately $1 \mu\text{l}$ the blue line after zooming can

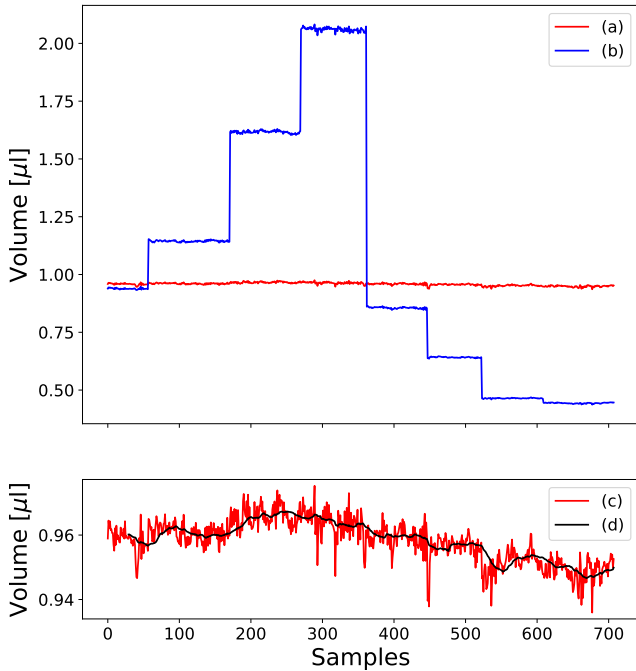


Figure 8. The zoom-independent self-calibration is demonstrated. Effects of zooming in and out while measuring droplet volume are negligible. Upper: Oil drop volume measurement using 8 different camera-zooms. Line (a) is droplet volume calculated using the presented method. Line (b) is droplet volume as calculated using pixel to millimeter ratio from the average of several $1 \text{ mm} \pm 0.02 \text{ mm}$ calibration spheres for the first of the eight zooms. Lower: Line (c) is zoom-in on droplet volume calculated using the presented method. Line (d) is a moving average of last 30 frames.

represent the percentage current zoom to the initial zoom. It also represents the error of using the standard method without re-calibration after zooming.

The process of levitating many precision produced spheres to get an average good enough for volume measurements is time consuming and these spheres are expensive. However in comparison the presented method is self-calibrating and the results are consistent, zoom-independent volume measurements with similar precision.

D. Limitations and the future

Since most of the equipment used in this research comes at low cost it is expected that the results could be improved with more precise equipment such as state of the art image-recognition instruments, higher quality transducers, more sensitive temperature sensor.

Our results are proof of concept and the precision of volume measurements achieved so far is comparable to results that only can be surpassed by the more expensive calibration spheres using the conventional method, and thus is expected to already be useful to research teams where funding is low or where the self-calibrating feature is of value for the workflow.

The advantages of having real-time temperature monitoring and simulation predicting cavity length and node-to-node distances provide great versatility of the measurement process. With this, a completely automated and self-calibrating system can be produced. This and a more controlled environment in addition to more precise instruments is expected to produce more accurate measurements than has yet been achieved.

V. CONCLUSIONS

A new and self-calibrating method for volume measurements of droplets (75 nl to $1.3 \mu\text{l} \pm 1.5\%$) has been proposed and demonstrated. For a fraction of the cost of conventional image analysis methods to measure droplet volumes, similar accuracy have been achieved. The intrinsic properties of the acoustic trap have been harnessed via a fit between a simulation and the acoustic trap, and used to measure the volumes of two levitated droplets. This new versatile method can help research teams save time-consuming calibration time that occurs every time the equipment for research are mounted, re-mounted or either intentionally or unintentionally have been altered during the research trial-n-error process. The self-calibrating aspect makes it possible to zoom in and out during data collection. Thus the presented method has the potential to be an easy to use technique that solves the versatility issue of repeated re-calibration and could be used for research in spectroscopy and chemistry studies as well as in studies that monitor the geometric properties of a droplets such as evaporation studies.

SUPPLEMENTARY MATERIAL

See supplementary material for a list of equipment used in the experimental setup and a video visualizing the results from the simulation regarding node to node d_{node} distance with respects to cavity length D and temperature T .

ACKNOWLEDGEMENTS

R.M.-F. acknowledges the financial support from The Wenner-Gren Foundations and the grants DGAPA-PASPA, PAPIIT IN-112721 and PAPIME PE-103021.

AUTHORS DECLARATIONS

Conflict of Interest

The authors have no conflicts to disclose.

DATA AVAILABILITY

The data and code that support the findings of this study are available from the corresponding author upon reasonable

request.

REFERENCES

- ¹H. Yu, F. Xu, and C. Tropea, *Journal of Quantitative Spectroscopy and Radiative Transfer* **126**, 105 (2013).
- ²B. Al Zaitone, *International Journal of Heat and Mass Transfer* **126**, 164 (2018).
- ³O. Rohling, C. Weitkamp, and B. Neidhart, *Fresenius' Journal of Analytical Chemistry* 2000 368:2 **368**, 125 (2000).
- ⁴J. Leiterer, F. Delißen, F. Emmerling, A. F. Thünemann, and U. Panne, *Analytical and Bioanalytical Chemistry* 2008 391:4 **391**, 1221 (2008).
- ⁵R. C. Bradshaw, D. P. Schmidt, J. R. Rogers, K. F. Kelton, and R. W. Hyers, *Review of Scientific Instruments* **76**, 125108 (2005).
- ⁶J. Leiterer, F. Emmerling, A. F. Thünemann, and U. Panne, *Zeitschrift für anorganische und allgemeine Chemie* **632**, 2132 (2006).
- ⁷T.-H. Yang, H.-C. Yang, C.-H. Chang, G. R. D. Prabhu, and P. L. Urban, *IEEE Access* **7**, 154743 (2019).
- ⁸K. Bücks and H. Müller, *Zeitschrift für Physik* **84**, 75 (1933).
- ⁹S. Santesson and S. Nilsson, *Analytical and Bioanalytical Chemistry* **378**, 1704 (2004).
- ¹⁰E. H. Brandt, *Nature* **413**, 474 (2001).
- ¹¹S. Baer, M. A. Andrade, C. Esen, J. C. Adamowski, G. Schweiger, and A. Ostendorf, *Review of Scientific Instruments* **82**, 105111 (2011).
- ¹²A. Marzo, A. Barnes, and B. W. Drinkwater, *Review of Scientific Instruments* **88**, 085105 (2017).
- ¹³A. Marzo, S. A. Seah, B. W. Drinkwater, D. R. Sahoo, B. Long, and S. Subramanian, *Nature Communications* **6**, 10.1038/ncomms9661 (2015).
- ¹⁴E. H. Trinh, *Review of Scientific Instruments* **56**, 2059 (1985).
- ¹⁵E. Welter and B. Neidhart, *Fresenius' Journal of Analytical Chemistry* 1997 357:3 **357**, 345 (1997).
- ¹⁶H. T. O'neil, Citation: *The Journal of the Acoustical Society of America* **21**, 516 (1949).
- ¹⁷B. J. W. S. Rayleigh, *The theory of sound* (Macmillan and co., 1877-78, England, 1878).
- ¹⁸P. Liu, D. Ming, S. Tan, and B. Lin, *Applied Acoustics* **155**, 216 (2019).
- ¹⁹A. Marzo, A. Ghobrial, L. Cox, M. Caleap, A. Croxford, and B. W. Drinkwater, *Applied Physics Letters* **110**, 014102 (2017).
- ²⁰V. Contreras and A. Marzo, *Review of Scientific Instruments* **92**, 015107 (2021).
- ²¹Y. Tian, R. G. Holt, and R. E. Apfel, Citation: *The Journal of the Acoustical Society of America* **93**, 3096 (1993).
- ²²Y. Tian, R. G. Holt, and R. E. Apfel, *Review of Scientific Instruments* **66**, 3349 (1995).
- ²³J. Kremer, A. Kilzer, and M. Petermann, *Rev. Sci. Instrum* **89**, 15109 (2018).
- ²⁴V. Contreras, R. Valencia, J. Peralta, H. Sobral, M. A. Meneses-Nava, and H. Martinez, *Optics Letters* **43**, 2260 (2018).
- ²⁵A. L. Yarin, M. Pfaffenlehner, and C. Tropea, *Journal of Fluid Mechanics* **356**, 65 (1998).
- ²⁶D. A. Bohn, *Journal of the Audio Engineering Society* **36**, 223 (1988).